

TECHNISCHE UNIVERSITÄT MÜNCHEN

Lehrstuhl für Biochemische Pflanzenpathologie

Approaches to plant-based production of designed antimicrobial peptides and their immunomodulatory activities

Antonie Sophie Bernhard

Vollständiger Abdruck der von der Fakultät Wissenschaftszentrum Weihenstephan für Ernährung, Landnutzung und Umwelt der Technischen Universität München zur Erlangung des akademischen Grades eines

Doktors der Naturwissenschaften

genehmigten Dissertation.

Vorsitzender: Univ.-Prof. Dr. W. Liebl
Prüfer der Dissertation: 1. Univ.-Prof. Dr. J. Durner
2. Univ.-Prof. Dr. S. Scherer

Die Dissertation wurde am 28.11.2013 bei der Technischen Universität München eingereicht und durch die Fakultät Wissenschaftszentrum Weihenstephan für Ernährung, Landnutzung und Umwelt am 27.03.2014 angenommen.

Table of contents

Table of contents	I
Summary	IV
Abbreviations	V
Index of figures	VII
Index of tables	X
1. Introduction	11
1.1. Antimicrobial peptides	11
1.1.1. Anti-HIV activity of naturally occurring antimicrobial peptides.....	13
1.1.2. Immunomodulatory properties of antimicrobial peptides	15
1.2. De novo design of antimicrobial peptides	16
1.3. Peptide HIV fusion inhibitor T20	17
1.4. Molecular farming	17
1.5. Production of antimicrobial peptides in plants	18
1.5.1. Production in chloroplasts	20
1.5.2. Examples for chloroplast-derived biopharmaceuticals	21
2. Objectives	23
3. Material and Methods	24
3.1. Materials	24
3.1.1. Plant materials.....	24
3.1.1.1. Plant media	24
3.1.1.2. Plant vitamin and salt stocks.....	24
3.1.2. Molecular biology materials.....	25
3.1.2.1. Bacteria strains	25
3.1.2.2. Kits and reaction systems.....	25
3.1.2.3. Buffers, reagents and solutions	25
3.1.2.4. Media	29
3.1.2.5. Chemicals and consumed material	30
3.1.2.6. Antibiotics	30
3.1.2.7. Antibodies	31
3.1.2.8. Enzymes	32
3.1.2.9. Peptides	32
3.1.2.10. Oligonucleotides.....	32
3.1.2.11. Plasmids	35
3.1.3. Disposable materials.....	37
3.1.4. Instruments and accessories	37
3.2. Methods	40
3.2.1. Plant methods.....	40
3.2.1.1. Plant growth on soil	40
3.2.1.2. Seed surface sterilization.....	40
3.2.1.3. Sterile culture on solid medium	40
3.2.1.4. Transferring plants from sterile culture to soil.....	40
3.2.1.5. Infiltration of <i>Nicotiana benthamiana</i> leaves	40
3.2.1.6. Particle gun bombardment.....	41
3.2.1.7. Regeneration and selection	42

3.2.1.8.	Characterization of transplastomic lines	42
3.2.2.	Cell culture methods	43
3.2.2.1.	Isolation of peripheral blood monocytes (PBMCs)	43
3.2.2.2.	Generation of monocyte-derived dendritic cells (MoDC)	43
3.2.2.3.	Stimulation of PBMCs and MoDCs with designed AMP.....	43
3.2.2.4.	PI staining and Flow cytometry.....	44
3.2.2.5.	Analysis of cytokine secretion by enzyme-linked immunosorbent assay	44
3.2.3.	Molecular biology methods.....	44
3.2.3.1.	Preparation of chemically competent bacteria cells	44
3.2.3.2.	Heat shock transformation.....	45
3.2.3.3.	Culture and growth conditions.....	45
3.2.3.4.	Blue-White-Screening	45
3.2.3.5.	Plasmid DNA preparation	45
3.2.3.6.	Determination of nucleic acids concentration	45
3.2.3.7.	Nucleic acid agarose gel electrophoresis	46
3.2.3.8.	Purification of PCR products and DNA reaction mixtures.....	46
3.2.3.9.	PCR (Polymerase Chain Reaction)	46
3.2.3.10.	Colony PCR.....	47
3.2.3.11.	cDNA generation and RT PCR	47
3.2.3.12.	DNA sequencing	48
3.2.3.13.	Digestion by restriction endonucleases and ligation	48
3.2.3.14.	Oligonucleotide annealing	48
3.2.3.15.	Golden Gate Cloning	48
3.2.3.16.	Southern blot.....	50
3.2.4.	Protein biochemical methods.....	52
3.2.4.1.	Extraction of soluble proteins from plant material	52
3.2.4.2.	TSP extraction from plant material for Icon genetics approach	52
3.2.4.3.	Determination of protein concentration.....	52
3.2.4.4.	Acetone precipitation of proteins.....	52
3.2.4.5.	Polyacrylamide gel electrophoresis of proteins	52
3.2.4.6.	Staining methods	53
3.2.4.7.	Western blot analysis	53
4.	Results.....	54
4.1.	Cell-toxic effects of designed peptides	54
4.1.1.	Effects on viability of peripheral blood mononuclear cells	54
4.1.2.	Time-depending effects on peripheral blood mononuclear cells	56
4.1.3.	Effects viability of on monocyte-derived dendritic cells.....	57
4.2.	Immunomodulatory properties	58
4.2.1.	Stimulation and suppression of cytokines.....	59
4.2.2.	Phytohämagglutinin stimulation of peripheral blood mononuclear cells	60
4.2.2.1.	Interleukin 10 response.....	60
4.2.2.2.	Type II interferon response.....	61
4.2.3.	Lipopolysaccharide stimulation of peripheral blood mononuclear cells .	62
4.2.3.1.	Interleukin 10 response.....	63
4.2.4.	Polyinosinic:polycytidylic acid stimulation of monocyte-derived dendritic cells.....	64
4.2.4.1.	Interaction of Polyinosinic:polycytidylic acid and designed peptides	64
4.2.4.2.	Interleukin 12 response.....	66
4.2.4.3.	Interleukin 6 response	68

4.2.4.4.	Interleukin 1 β response.....	69
4.3.	Transplastomic approach for peptide production	70
4.3.1.	Plastid transformation vectors	70
4.3.2.	Golden Gate Cloning	73
4.3.3.	Chloroplast transformation and regeneration	74
4.3.4.	Screening for transplastomic lines.....	77
4.3.5.	Transformation efficiency.....	77
4.3.6.	F0 Generation of transplastomic plants.....	79
4.3.7.	F1 Generation of transplastomic plants.....	80
4.3.8.	Southern Blot analysis of transplastomic plants	81
4.3.9.	Test for translation	82
4.3.10.	Confirmation of transcription.....	83
4.4.	Transient production of designed peptides with expression system magnICON®.....	84
5.	Discussion	86
5.1.	Cell-toxicity of designed peptides.....	86
5.2.	Immunomodulatory features of designed peptides	88
5.2.1.	Pro-inflammatory and anti-inflammatory cytokines	88
5.2.1.1.	Stimulation of PBMCs with peptides triggers release of IL-10	88
5.2.1.2.	Stimulation of PBMCs or MoDCs with designed peptides does not trigger cytokine production of IFN- γ , IL-12, IL-6 or IL-1 β	90
5.2.1.3.	Co-incubation of PBMCs with PHA and peptides influences IFN- γ and IL- 10 production	91
5.2.1.4.	Co-incubation of PBMCs with LPS and peptides influences IL-10 production differently between SP10 and SP13 peptides	93
5.2.1.5.	Incubation of MoDCs with or without Poly I:C influences several cytokine production levels	94
5.2.2.	Conclusion regarding immunomodulatory activities	95
5.3.	Transplastomic plants as production platform.....	96
5.3.1.	Design and construction of the expression cassette	96
5.3.2.	Selection process	97
5.4.	Possible causes of translation inhibition	100
5.4.1.	Degradation in chloroplasts.....	101
5.4.2.	Inhibition of translation initiation	101
5.4.2.1.	Cis-acting elements and trans-acting factors in <i>Nicotiana tabacum</i> psbA mRNA.....	105
5.4.2.2.	Cis-acting elements and trans-acting factors in <i>Chlamydomonas</i> <i>reinhardtii</i> psbA mRNA	106
5.4.3.	Conclusion regarding transplastomic approach.....	108
Outlook.....		109
Bibliography		110
Appendix		120
Acknowledgment		128
Curriculum Vitae.....		129

Summary

The human immunodeficiency virus (HIV) infects vital cells of the immune system and thus causes the acquired immune deficiency syndrome, more commonly known as AIDS. Naturally occurring antimicrobial peptides (AMPs) display antiviral activities, which diminish HIV infection rates either by direct virucidal activity, by inhibition of viral fusion steps or by inducing endogenous antiviral immune defense reaction. In our research group several *de novo* designed peptides were developed based on structural features of naturally occurring AMPs. Four of these designed peptides, namely SP10-11, SP13-3, SP13-11 and SP13-14, show activity against HIV.

In the present work, the immunomodulatory and cell-toxic features of these four HIV active peptides have been characterized. It was found that SP10-11 compared to peptides from the series SP13 exhibit different effects regarding both cell-toxic impact and modulation of cytokine release on human peripheral blood mononuclear cells (PBMCs) and monocyte-derived dendritic cells (MoDCs). While SP10-11 shows no toxic effects on all investigated cell types, SP13-3, SP13-11 and SP13-14 induce significant, concentration-depending cell-toxic effects, although the antiviral active concentrations show no or only low adverse effects. SP10-11 induces a shift of the overall cytokine profile into the anti-inflammatory direction for T-cells and significantly suppresses IFN- γ production *in vitro*, which may have critical implications in HIV pathogenesis. However, SP10-11 does not induce or suppress the other investigated cytokines that are related to viral infections. All SP13 peptides showed similar suppressing impact on cytokine profiles, as these peptides are likely to damage the surviving cells in a way that cytokine production is negatively impacted. SP13 peptides also suppressed anti-inflammatory cytokine IL-10 for antigen-presenting cells but induce this cytokine in T-cells.

As a second part of this work an approach for stable production of designed peptides in chloroplasts of *Nicotiana tabacum* was performed. Chloroplasts were transformed using an biolistic approach by particle gun. Several homoplastomic plant lines were generated and transcription of the inserted transgenes was confirmed. However, translation initiation of the recombinant proteins was inhibited likely due to the non-endogenous 5' untranslated region (5'-UTR), which was derived from *Chlamydomonas reinhardtii psbA* gene and inserted together with the according promoter upstream of the gene of interest.

Taken together, SP10-11 was determined as the most promising peptide candidate for further investigation related to anti-HIV activity *in vivo*. Furthermore, a cloning system especially suited for quick and easy reconstruction of plasmid transformation vectors was established as well as efficient selection and characterization protocols for the development of homoplastomic tobacco plants.

Abbreviations

ACN	Acetonitrile
APC	Antigen presenting cell
AMPs	Antimicrobial peptides
ATP	Adenosine 5'-triphosphat
bp	Base pairs
BSA	Bovine serum albumine
CD14	Cluster of differentiation 14
cDNA	Complementary DNA
cfu	Colony-forming unit
CNBr	Cyanogen bromide
DC	Dendritic cell
DNA	Deoxyribonucleic acid
DMSO	Dimethylsulfoxid
Don1	Donor vector 1 (Golden Gate Cloning)
Don2	Donor vector 2 (Golden Gate Cloning)
DPBS	Dulbeccos modified eagle medium
dpi	Days post infiltration
DTT	Dithiothreitol
EDTA	Ethylendiamintetraacetate
EGTA	Ethylene glycol tetraacetic acid
ELISA	Enzyme linked immuno absorbent assay
FACS	Fluorescent associated cell sorter
FCS	Fetal bovine serum
GFP	Green fluorescent protein
GOI	Gene of interest
h	Hour(s)
AMP	Antimicrobial peptides
HIV	Human immunodeficiency virus
HU-DC	Human dentritic cell medium
kDa	Kilodalton
IFN	Interferon
IL	Interleukin
IPTG	Isopropyl β -D-1-thiogalactopyranoside
IR	Inverted repeat
LB	Luria-Bertani
LPS	Lipopolysaccharide
MACS	Magnetic cell sorting
MES	2-(N-morpholino) ethanesulfonic acid (IUPAC nomenclature)

min	Minute(s)
ml	Milliliter
MoDC	Monocyte-derived dendritic cells
MS	Murashigge & Skoog
nd	Not determined
NK cell	Natural killer cell
nt	Nucleotide
OD	Optical density
oN	Over night
PCR	Polymerase chain reaction
PHA	Phytohämagglutinin
PMSF	Phenylmethanesulfonylfluoride
ptDNA	Plastid DNA
rhGM-CSF	Recombinant human Granulocyte-macrophage colony-stimulating factor
rhIL-4	Recombinant human Interleukin 4
PBMCs	Peripher blood mononuclear cells
PI	Propidium iodide
Poly I:C	Polyinosinic:polycytidylic acid
RdRP	RNA-dependent RNA polymerase
RNA	Ribonucleic acid
rpm	Revolutions per minute
RT	Room temperature
s	Second(s)
SDS-PAGE	Sodium dodecyl sulphate-polyacrylamide electrophoresis
Taq	<i>Thermus aquaticus</i>
TGF- β	Transforming growth factor β
T _h	T helper cell
T _{reg}	CD4+CD25+ regulatory T cell
UTR	Untranslated region
v/v	Volume per volume
w/v	Weight per volume
X-Gal	5-bromo-4-chloro-3-indolyl- β -D-galactopyranoside

Amino acids and nucleotides are expressed according to the IUPAC code (International Union of Pure and Applied Chemistry). All used base units and derived units are conform to the convention of the SI-system (Système International d'unités).

Index of figures

Figure 1: Major structural classes of AMPS.....	12
Figure 2: Anti-HIV activities of defensins and cathelicidins	14
Figure 3: Molecular farming in plants compared to conventional systems.....	18
Figure 4: Southern Blot Unit.....	51
Figure 5: Different effects of SP10-11 peptide and SP13 peptides on PBMC cell viability	55
Figure 6: Cell-toxic effect on PBMCs does not alter over time for all designed peptides	56
Figure 7: Effects of SP13-derived peptides on viability of MoDCs are significantly higher compared to toxic effects on PBMCs.....	57
Figure 8: Schematic overview of all different ELISA assays	59
Figure 9: All designed peptides significantly enhance IL-10 release in PBMCs	61
Figure 10: Designed peptides suppress IFN- γ production in PBMCs when co-incubated with PHA	62
Figure 11: PBMCs were stimulated with different concentration of peptides in the presence or in the absence of LPS	63
Figure 12: Toxic effects of designed peptides on MoDCs differ significantly depending on the presence of Poly I:C	66
Figure 13: Poly I:C in combination with peptides of the SP13 series reduces IL-12 production in human MoDCs, while the presence of SP10-11 does not influence IL-12 levels.....	67
Figure 14: Poly I:C in combination with peptides of the SP13 series significantly diminishes IL-6 secretion in human MoDCs, whereas the present of SP10-11 does not influence IL-6 secretion.....	68
Figure 15: Poly I:C in combination with SP13 peptides suppresses IL-1 β secretion in human MoDCs, whereas the presence of SP10-11 does not alter or even slightly enhances IL-1 β secretion	70
Figure 16: Representation of all constructs for homologous recombination in tobacco chloroplasts.....	71
Figure 17: Schematic assembly of Golden Gate Cloning principle	73

Figure 18: Development of plant tissue cultures derived from PTV 13-3 NH bombardment on RMOP medium containing 500 mg/l spectinomycin (high selection) or 50 mg/l (low selection)	76
Figure 19: Cycling procedure of putative heteroplastomic shoots	77
Figure 22: Germination of F1 generation of transplastomic tobacco plants on B5 medium with 500 mg/l spectinomycin.....	80
Figure 23: Phenotypes of transplastomic plants from the F1 generation and wild-type plants show no differences.	81
Figure 24: Southern Blot analysis of transplastomic plants of the F0 and F1 generation	82
Figure 25: Failure of recombinant protein production in transplastomic plants of the F0 or F1 generation	83
Figure 26: RT-PCR from transformants of the F0 generation shows functional transcription.....	84
Figure 27: Anti gfp western blot with highly sensitive HPO detection	85
Figure 28: Overview of all ELISA results indicating immunomodulatory properties of the designed peptides.....	95
Figure 31: Alignment of <i>C. reinhardtii</i> plastome and <i>psbA</i> promoter with 5'-UTR..	102
Figure 35: Determination of toxic effect of designed peptides in different concentrations on PBMCs over time	121
Figure 36: IFN- γ , PBMC 4, AMP + PHA stimulated.....	122
Figure 37: IFN- γ , PBMC 5, AMP + PHA stimulated.....	122
Figure 38: IL10, PBMC 4, AMP + PHA stimulated	123
Figure 39: IL10, PBMC 5, AMP + PHA stimulated	123
Figure 40: IL10, PBMC 4, AMP + LPS stimulated.....	124
Figure 41: IL10, PBMC 5, AMP + LPS stimulated.....	124
Figure 42: IL6, DC1, AMP + Poly I:C stimulated	125
Figure 43: IL6, DC2, AMP + Poly I:C stimulated	125
Figure 44: Sequence of the <i>psbA</i> gene promoter of <i>Chlamydomonas reinhardtii</i>	126
Figure 45: Sequence of the <i>rps12</i> flank for homologous recombination.....	126
Figure 46: Sequence of the <i>orf131</i> flank for homologous recombination	126

Figure 47: Sequence of the gfp marker gene	126
Figure 48: Sequence of the trpI31 terminator of the recombinant protein expression cassette.....	126
Figure 49: Sequence of the aadA expression cassette, including 16S promotor, aadA marker gene and 3' rbcl terminator	127

Index of tables

Table 1: List of HIV active target peptides of this work.....	16
Table 2: PCR mixes and according thermocycler programs.....	47
Table 3: Workflow for southern blot detection	51
Table 4: Functional units of chloroplast transformation vectors.....	72
Table 5: Inserts provided by Golden Gate Donor vector Don2.....	74
Table 6: Chloroplast transformation by biolistic approach with different plastid transformation vectors.....	75
Table 7: Overview over transplastomic shoots, their tissue culture name and applied plasmid transformation vectors	79
Table 8: Listing of all blood samples that were used in this work	120
Table 9: Applied concentrations of the designed peptides for the toxicity tests	120
Table 10: Applied concentrations of the designed peptides for ELISA.....	120

1. Introduction

Designed antimicrobial peptides are artificial peptides, whose structures are imitating naturally occurring antimicrobial peptides (AMPs), a large and diverse group of peptides that are produced by all types of living organisms as part of their innate immunity to microbial invasion. In this work, we describe the immunomodulatory features of designed, HIV-active peptides and a transplastomic approach towards a plant-production platform suitable for these designed peptides.

1.1. Antimicrobial peptides

Antimicrobial peptides (AMPs) are conserved components of the innate immune system and act as the first line of defense against a wide variety of pathogens prior to the development of an adaptive immune response [8-10]. In April 2013 the APD2 database contains over 2200 AMPs, that have been demonstrated to kill or inhibit a variety of organisms [11]. It was reported that AMPs also act as effector agents within the innate immune system in mammals and thus provide a link between innate and adaptive immune responses [10, 12]. Some AMPs show additionally to their direct antimicrobial features also multiple immunomodulatory activities under physiological conditions. In 2006 Hancock *et al.* referred to these peptides as host defense peptides (HDPs), to describe their broader functions in host innate immunity [13, 14], a term that was acquired by literature. AMPs occur naturally within a large number of different species that include bacteria, plants, insects and vertebrates [12]. However, all AMPs share some common features like short amino acid sequence with approximately 12–50 amino acids and an overall positive net charge of +2 to +9 due to accumulation of basic lysine, arginine and histidine amino acids. Additionally, AMPs display approximately 50% hydrophobic residues, which facilitates folding into an amphiphilic conformation with separated hydrophilic and lipophilic regions [15-17]. Nevertheless, AMPs display an enormous structural diversity and differ from each other by unique size and sequence [10, 18]. Therefore several different approaches exist to categorize AMPs. They were classified on the one hand side regarding the specific toxicity to microorganisms and to mammalian cells [17] and on the other hand side according to secondary structure features. In this second classification, linear, α -helical peptides without cysteine residues, β -sheet AMPs that are stabilized by one to three disulphide bridges, α -helical/ β -sheet mixture AMPs with intermolecular disulfide bonds, cyclic structures and finally extended helices exhibiting flexible loop or hairpin-like structures are distinguished (Figure 1) [13, 16, 17, 19]. Further, alternative classifications draw a distinction between AMPs that are based on conserved sequence segments or subdivide them according to their natural origin [17].

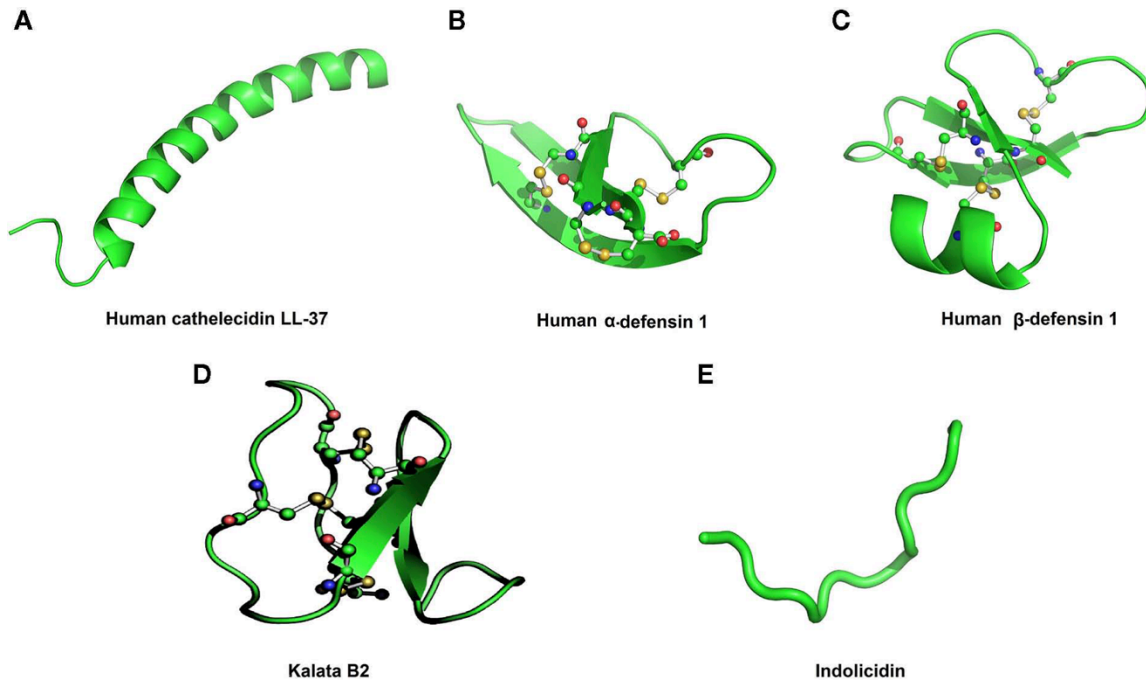


Figure 1: Major structural classes of AMPs differentiated according to their secondary structure features by Silva *et al.* [13]. (A) α -helical AMP (e.g. human cathelicidin LL-37) without cysteine residues, (B) β -sheet AMP (e.g. human α -defensin 1), stabilized by several disulfide bridges (C) AMPs consisting of a mixture of α -helices/ β -sheets structures (e.g. human β -defensin 1). (D) Cyclic AMP (Kalata B2) and (E) AMP with extended helical structures (e.g. Indolicidin). Disulfide bonds are shown as ball and stick.

AMPs display a broad spectrum of activity against a wide variety of organisms including gram-negative and gram-positive bacteria, enveloped viruses, protozoa, parasites, fungi and even cancer cells [17, 20]. Furthermore, in most cases AMPs are active in micromolar concentrations or below, but nevertheless strongly dependent on physiological conditions and are therefore mostly inhibited by high salt concentrations or in the presence of serum [21]. A well-known mechanism of action of positively charged AMPs regarding antimicrobial activity is the selective interaction with the negatively charged phospholipid bilayers of bacterial cell membranes, inducing rapid cell death by membrane disruption or membrane crossing and subsequent interference with metabolic processes or inhibiting of cytoplasmic components [12, 17]. Eukaryotic membranes may not be as susceptible to AMP-induced membrane permeabilization, because their lipid composition differs in charge, fluidity and composition. Mammalian membranes are enriched in zwitterionic phospholipids with neutral net charge like phosphatidylethanolamine, phosphatidylcholine, sphingomyelin and cholesterol. Especially cholesterol is likely to reduce AMP activity by supporting lipid bilayer stabilization, and thus reducing membrane fluidity and flexibility. In contrast, prokaryotic membranes are predominantly composed of phosphatidylglycerol, cardiolipin and phosphatidylserine and display a high negative net charge, which represents a typical AMP target [13, 18, 22]. AMPs do not seem to

raise resistance compared to conventional antimicrobial agents like existing antibiotics [10]. The main reason for this may be the direct, non-specific targeting and destroying of membranes by AMPs, which would require reorganization of the bacterial membrane for establishing resistance mechanisms. Alternatively, certain AMPs can cross membranes and thus are able to act simultaneously on multiple targets [21, 23, 24]. However, induced as well as constitutive resistance in several pathogenic bacteria was described for AMPs [10, 25]. AMPs have attracted the attention of the pharmaceutical industry and some modified AMPs are currently in various stages of clinical development. But so far no AMP-based drug has reached the approval of the FDA [19].

1.1.1. Anti-HIV activity of naturally occurring antimicrobial peptides

Some AMPs display broad-spectrum of antiviral activities against both enveloped and non-enveloped viruses, which includes influenza A, respiratory syncytial virus, herpes simplex viruses types 1 and 2, vesicular stomatitis virus, adenovirus and human immunodeficiency virus (HIV) [23, 26, 27]. Especially naturally occurring, mammalian AMPs are well characterized regarding their antiviral activity. In mammals, two major AMP families are distinguished based on their secondary structural features. Cathelicidins are linear α -helical peptides, whereas defensins are β -strand peptides connected by disulfide bonds [23, 27]. Defensins are sub grouped based on their pattern of cysteine connectivity in α - and β -defensins and furthermore in a circular form called θ -defensin. θ -defensin consists of 18 amino acids and was originally found in macaques. The coding sequence for θ -defensin is also present in the human genome but has been silenced by mutation [12, 27]. Cathelicidins and all defensin subtypes feature activities against HIV (Figure 2).

HIV enters and thus infects susceptible cells by membrane fusion. This entry process requires the viral envelope glycoprotein, whose subunit gp120/ gp41 heterodimers initiate the fusion by interacting with cluster of differentiation 14 (CD14) receptor and C-X-C chemokine receptor type 4 (CXCR4) or type 5 (CXCR5). CXCR4 and CXCR5 are surface proteins on mammal monocytes and macrophages (Figure 2) [28-30]. The antiviral mechanisms of action of cathelicidins and defensins depends on the specific peptide and also on the HI virus strain and ranges from direct adverse effects on the virions, antiviral immunomodulatory properties, inhibition of fusion steps, inhibition of essential signaling pathways to blocking of cellular and viral glycoproteins that are essential for the infection process (Figure 2) [23, 24]. Another, very interesting example is the entry blocking mechanism of θ -defensin retrocyclin 2 and human β -defensin 3 regarding influenza virus by generating a protective network consisting from cross-linked and immobilized surface glycoproteins [31]. It is further known that some AMPs are able integrate into to

outer and inner membranes of bacteria or even to cross lipid membranes and target intracellular components like DNA and RNA, which results in inhibition of DNA -, RNA- or protein synthesis [21]. Similar mechanisms could, regarding anti-HIV mechanisms, stimulate genes or proteins of the host cell and thereby trigger endogenous antiviral mechanisms. Especially in regard to the HI virus, membrane-crossing AMPs could block HIV-1 gene expression by interacting with viral RNA [16].

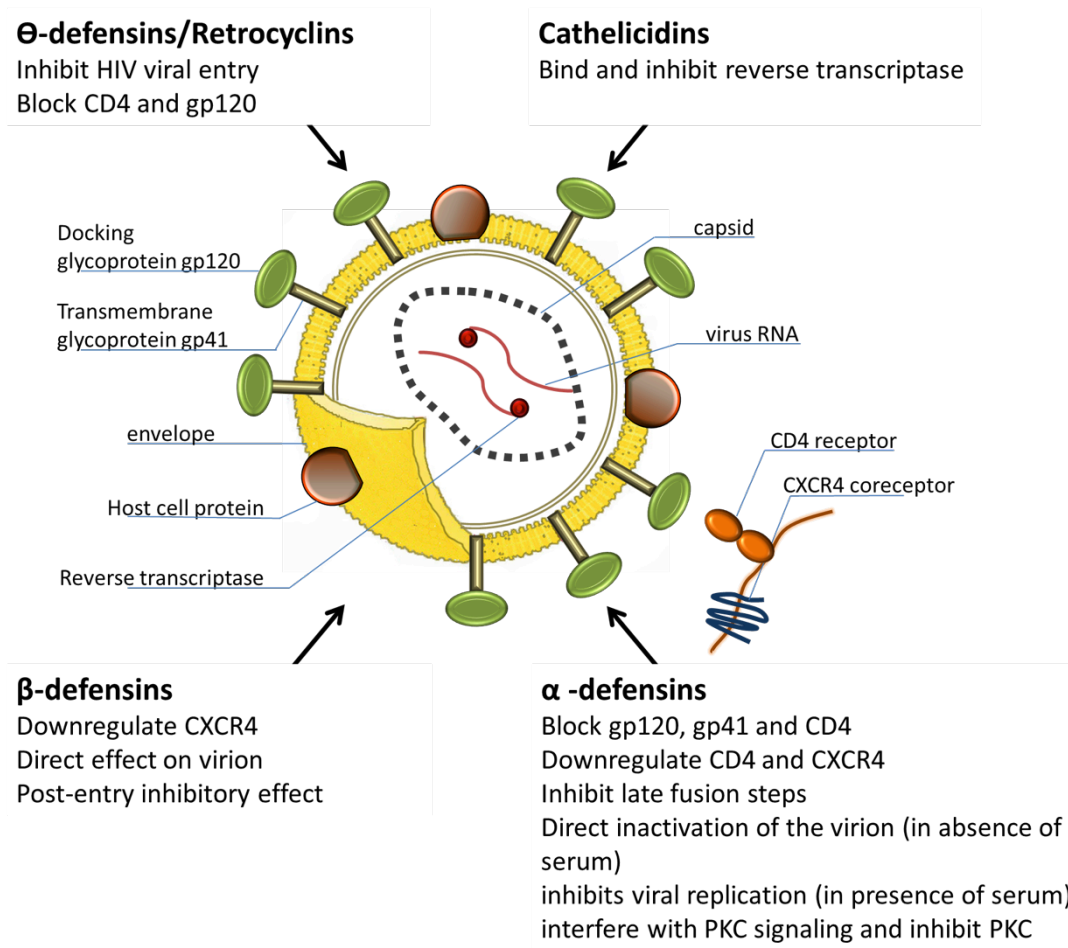


Figure 2: Anti-HIV activities of defensins and cathelicidins [23]. The HI virus is composed of an outer spherical lipid membrane (envelope, marked in yellow), which displays viral glycoproteins composed of gp120 (docking glycoprotein), and gp41 (transmembrane glycoprotein) and additional host cell proteins, which are transmitted when the capsid buds from the host cell. Within the envelope the capsid is located, which encloses two RNA molecules and additional enzymes that are required for HIV replication. Gp120 and gp41 enable attachment and fusion with the chemokine receptor CD4 and CXCR4 present on target cells [28-30].

Generally, defensins are able to inhibit HIV entry by blocking each of the essential steps of infection: The θ -defensin retrocyclin 1 can inhibit HIV-1 mediated fusion by binding gp41 with high affinity in a glycan-independent manner [30]. On the other hand side, human β -defensin 3 (hBD-3) blocks HIV infection by competing with stromal-derived factor 1 (SDF-1), which is a natural ligand for CXCR4 [32]

Furthermore, human β -defensin 2 (hBD-2) and hBD-3 block HIV-1 replication by interacting directly with virions and modulating the CXCR4 [33]. Interestingly, also a single nucleotide polymorphism in a human β -defensin gene correlates with an enhanced risk of HIV-1 infection in newborns, which underlines the importance of AMPs within innate immunity and the antiviral role β -defensins *in vivo* [34]. But also AMPs, which are not classified as cathelicidins or defensins, show anti-HIV activity. The AMP dermaseptin S4, which is isolated from amphibian skin, directly inhibits HIV by disrupting the virion integrity [35]. Nevertheless, also the various antiviral effects are often negated in the presence of serum or high salt concentrations [21].

1.1.2. Immunomodulatory properties of antimicrobial peptides

AMPs are involved in the complex network of immune responses and inflammatory diseases by inducing or modulating cytokines, chemotaxis, angiogenesis, wound repair, adaptive immune induction, apoptosis, T-lymphocyte activation, differentiation of dendritic cells as well as recruitment and stimulation of proliferation of macrophages, neutrophils or eosinophils [12, 13].

Certain AMPs are able to upregulate interferons and chemokines [9, 36, 37] and can thus activate cytokine release from different cell types [38, 39]. For example, inflammatory cells contain - among others - antimicrobial peptide LL-37, which was suggested to regulate the inflammatory process in various inflammatory lung diseases [38]. Some human AMPs possess immunomodulatory activities by displaying chemokine-like activity. This feature is based on similarities of structural motifs to other endogenous chemokines, which allows for example β -defensins to interact with certain chemokine receptors [34, 40]. Also human cathelicidin has been shown to be involved in chemotaxis of mast cells, neutrophils, and CD4 T-cells [38]. Various studies point out, that the release of specific AMPs amplifies inflammation because activation of innate immune mechanisms is related to the pathogenesis of inflammatory diseases [12]. On the other hand, a recently found AMP of the cathelicidin type inhibits the secretion of three inflammatory cytokines, namely tumor necrosis factor (TNF- α), interleukin-6 (IL-6), and monocyte chemoattractant protein-1 (MCP-1) and shows therefore anti-inflammatory activity [24]. A porcine neutrophil AMP modifies IL-1 release [41] and α -defensins block the release of IL-1 β from LPS-activated monocytes, whereas TNF- α expression and release remain unchanged [42]. Furthermore, α -defensins that are released by necrotic neutrophils show a strong anti-inflammatory effect while preserving antimicrobial activity [43]. Still, in clinical studies the deficiency, deregulation, or overproduction of endogenous AMPs is not known to directly cause human disease so far [12].

1.2. De novo design of antimicrobial peptides

Intensive research in the field of AMPs allowed the design of artificial peptides with enhanced antimicrobial activities or improved features for stimulation of the host immune defenses. Some of these designed peptides, when applied in animal models of infection against diverse pathogens, proved to be very effective [25].

The target peptides of this work are designed by following structural features of naturally occurring α -helical cationic AMPs, which is one of the most common types of AMPs in nature [18]: The size of our designed peptides ranges from 12 - 20 amino acids and they present an overall positive charge at pH 7 caused by arginine, lysine, and histidine residues as well as helical features due to strong helix-forming amino acids such as leucine and alanine. Additionally, the peptides display an amphipathic structure, which is provided by clusters of leucine, isoleucine, valine, phenylalanine, alanine, methionine, glycine, serine, and threonine residues. Altogether, several leading structures were designed, differing in charge, hydrophobicity, location and size of the hydrophobic and charged clusters [44-46].

From these peptides, four structures, namely SP10-11, SP13-3, SP13-11 and SP13-14, showed activity against HIV. Exposure of indicator cells to HIV in the presence of these peptides reduced the infection cells but showed no toxic effects on the test cells within the active concentration (Table 1). Preliminary test indicate, that our designed peptides display different modes of anti-HIV activity. In case of SP13-03 and SP13-14, inhibitory effects can only be observed after pre-incubation with the virus or after simultaneous addition of the peptides to the indicator cells, but not when added to already infected cells. Thus the mechanism of action underlying for SP13-03 and SP13-14 may inhibit HIV very early during infection process. Since the inhibitory effect of SP13-03 is much higher after 2h pre-incubation with the virus in comparison to simultaneous addition, a direct virucidal activity for SP13-03 is assumed. SP13-14 might interfere with the fusion process of HIV with host cell membranes or with events involved in cytoplasmic uptake of virus core, since pre-incubation does not significantly increase the activity of this peptide observed after simultaneous addition [47].

Table 1: List of HIV active target peptides of this work [45, 47]. Hydrophobic amino acids are marked in red letters, charged amino acids in blue letters. pI: isoelectric point. MW: molecular weight. IC₅₀: half maximal inhibitory concentration.

Peptide	Amino acid sequence	Charge at pH7	pI	MW	IC ₅₀ [μ M]
SP10-11	LRKAKKI AKK LF-NH ₂	+ 5.76	11.39	1,44 kDa	10,14 \pm 1,11
SP13-3	KRR LILRILRLAIRILV KKR-NH ₂	+ 8.76	12.70	2,53 kDa	3,51 \pm 0,454
SP13-11	KRR LALFRLFRLAL KLVL KK -NH ₂	+ 7.76	12.48	2,48 kDa	3,67 \pm 0,12
SP13-14	KRR KLAFRLFRLFL KLVL KK -NH ₂	+ 8.76	12.49	2,57 kDa	1,44 \pm 0,144

1.3. Peptide HIV fusion inhibitor T20

Despite their promising possibilities, no AMP has been yet approved as a human pharmaceutical [25]. Nevertheless different peptide drugs are already implemented for use in humans such as the HIV fusion inhibitor T-20 (generic name Enfuvirtide), currently marketed by Roche under the brand name Fuzeon®. T-20 is a 36 residue, N-terminal acetylated peptide that inhibits HIV-1 fusion with CD4 cells by targeting gp41 and thus blocking the last step in the viral entry process. There has been no attempt to produce T-20 within plants yet, although production of T-20 as a flagellin fusion protein by *Bacillus halodurans* utilizing a modified flagellin type III secretion system was already shown [48]. Therefore, this medically relevant peptide is aimed to be produced with an analogue transplastomic expression procedure like the designed peptides, to serve as an exploitable control regarding the possibly adverse influences of antimicrobial features to the plant production system.

1.4. Molecular farming

Molecular farming is a special section of plant biotechnology dealing with plant engineering techniques in order to turn plants into production platforms for recombinant pharmaceutical and industrial proteins. Plants have the capabilities to produce complex proteins regarding folding and post-translational modification and it was further demonstrated that plant-derived biopharmaceuticals show functional therapeutic activity in mammals. Therefore plant production platforms are an cost-effective and highly scalable alternative for complex protein production, that is also free from human pathogens, when compared to conventional production systems like in microbial, yeast, or mammalian expression systems [49-51]. Thus plants may supplement in near future these traditional methods also in industrial applications.

So far more than 100 recombinant proteins, which range from subunit vaccines, antibodies, hormones, blood products, cytokines to enzymes have been produced successfully in plants [52, 53]. For these approaches several plant species have been explored, including tobacco, *Arabidopsis thaliana*, alfalfa, spinach, potatoes, duckweed, strawberries, carrots, tomatoes, aloe and single-cell algae. Also expression systems with suspension cell cultures of tobacco and maize, hairy root cultures and in transformed chloroplasts of a variety of plant species have been under investigation [53, 54]. However, clear differences between the various approaches in overall timescales for protein production, host range, possible environmental containment, scalability, downstream processing strategy and last but not least the overall costs have been reported [53, 55]. But also several technical obstacles have been overcome and significant progress has been made regarding production yield, regulation of transcription, enhancing translation, amplifying transgene copy number, suppressing gene silencing, reproducibility or improving

purity of the product. This progress in molecular farming is underlined by increasing interest from investors and biotech- and pharmacy companies as the agreements between Bayer and Icon Genetics and between Pfizer and Protalix demonstrate [51, 53, 55].

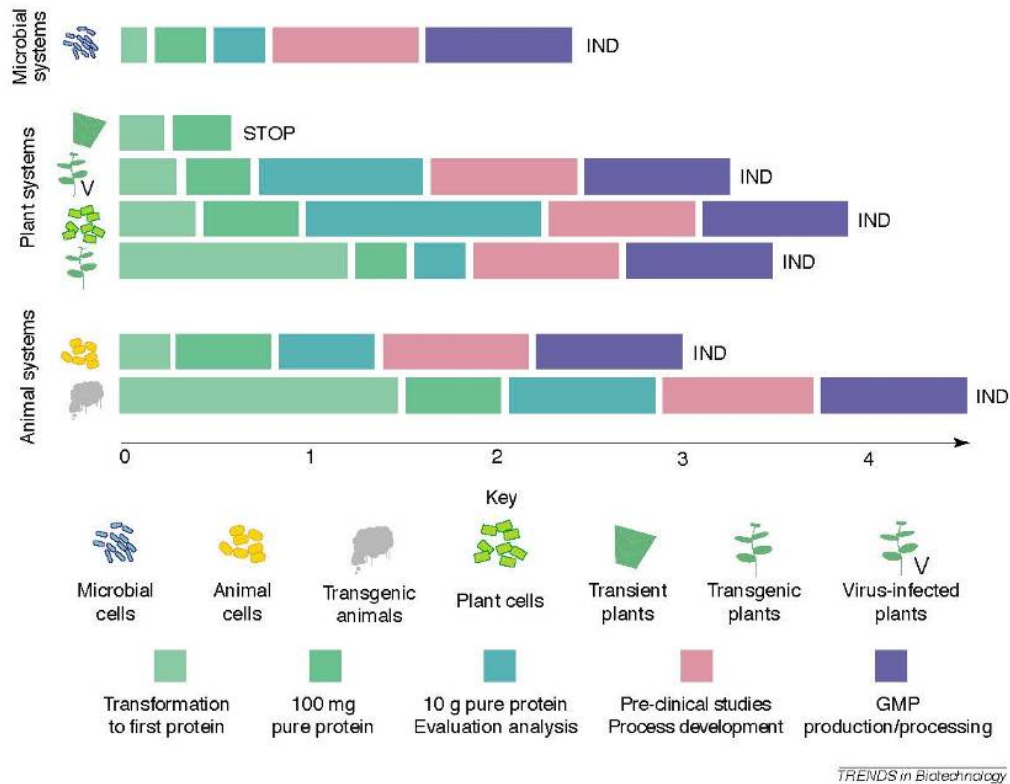


Figure 3: Molecular farming in plants compared to conventional expression systems by Twyman *et al.* [52]. X-axis refers to the time (years) that is required for the different stages of development for each specific production platform, resulting in investigational new drugs (IND).

To date, several different plant transformation strategies have been established. Literature describes either transient transformation of plants or stable integration of transgenes in the case of transgenic or transplastomic plants. Transient expression systems include a broad range of approaches ranging from magnification technology, microprojectile bombardment, agroinfiltration method, virus infection method to plant cell-suspension cultures [49]. Very recently, an inducible, hyperexpressing plant platform for recombinant protein production has been established in tobacco [55].

1.5. Production of antimicrobial peptides in plants

The classical way of chemically synthesizing peptides is by solid phase technique. This step-by-step synthesis in combination with Boc and Fmoc protecting groups is able to provide high quality and quantity of peptides [56]. The synthetic production of peptides is still quite expensive due to expensive precursor components and may

also be difficult, depending on the chemical features of designed peptides [25, 44]. Especially when designed AMPs are compared to conventional antibiotics, which are produced as biopharmaceuticals, the manufacturing costs of synthetic AMPs are in average five to twenty times higher [12, 29, 57, 58]. Next to chemical synthesis, various methods for producing AMPs in bacteria or yeast have been described [59-62]. Also somewhat exotic examples for biotechnological production of functional AMPs are described, including silkworm-baculovirus protein expression system [63] and fungal-based systems [15]. However, even with successful production with an satisfying yield, the downstream and purification processes are always expensive and significantly reduce yield in most cases. Furthermore, difficulties based on toxicity of AMPs for the host organism have been reported and result in problematic scale-up and low yields [25].

In a former project of our group, a transient plant expression system following the 'full virus vector strategy' was used to produce another type of designed peptide named SP1-1, which is highly effective against *Xanthomonas vesicatoria*, *Pseudomonas corrugata* and *Pseudomonas syringae pv syringae*. For this production strategy, SP1-1 was fused to the viral coat protein of tobacco mosaic virus (TMV) and was released by chemical cleavage after extraction of the virions out of *Nicotiana benthamiana* leaves. This approach yielded up to 0,025 mg of peptide per g of infected leaf biomass and the antimicrobial activity of SP1-1 was in the range of the synthetic one [44]. However, transient approaches do not provide identical charges and the ability to scale up biomass with low maintenance and cost is better within stable transformed transgenic plants. Also regarding GMP compliance and regulatory matters, stably transformed plants are preferable to transient systems: the recombinant product is based on a fully defined transgene integration event, and the resulting fully characterized transgenic line can be very well documented and harvested with minimal batch-to-batch variation [55]. For these reasons, a new, stable expression system for our HIV-active peptides should be developed.

The most important economic factor in plant-based protein production is the yield. In case of nuclear transformed plants low production was observed frequently in contrast to chloroplasts, which have the proven potential for high-level production of foreign proteins [64]. Taking account of this high protein production capacity, it seems particularly attractive to exploit plastids for the production of designed peptides, in the form of fusion proteins to stabilize transcript and protein product as well as reduce the likely adverse effects of the peptides on the chloroplast. Therefore, a transplastomic approach was chosen for this project.

1.5.1. Production in chloroplasts

After completion of the chloroplast genome sequencing from tobacco plants, Pal Maliga's group developed the high-frequency chloroplast transformation system in tobacco [65]. This method allows stable integration of foreign DNA at a desired site by homologous recombination, which makes the location of transgene insertion predictable and the gene expression uniform and reproducible among all independently transformed lines [66, 67]. After the first chloroplast transformation in *Chlamydomonas reinhardtii* (*C. reinhardtii*) [68], the first stable plastid transformations were reported soon in higher plants, including rape, *Lesquerella*, rice, potato, lettuce, soybean, cotton, carrot, tomato and poplar [69-71] and also *Nicotiana tabacum* (*N. tabacum*) [71, 72]. However, reproducible generation of higher transplastomic plants with well-established protocols is up to now only available for the *Solanaceae* species tobacco, potato and tomato [73]. Chloroplast transformation became interesting as production system, when it was first reported that genes, which were difficult to express from the plant's nuclear genome, accumulated to extraordinarily high levels in transformed chloroplasts. Ever since this observation, several advantages of the chloroplast production platform compared to nuclear gene transformation have been demonstrated. First, chloroplasts have the potential for synthesizing and accumulating high amounts recombinant proteins that are at least 10–50 times higher than nuclear expressed proteins. For example, transplastomic production of a proteinaceous antibiotic, PlyGBS, in tobacco yielded to the extremely high level of 70% of the plant's total soluble protein content [74]. This capacity is on the one hand side based on the high ploidy level of the plastid. In a single tobacco leaf cell around 100 chloroplasts are present, which contain each up to 100 plastid ptDNA. Thus on average a total of 10,000 genome copies per cell is calculated. On the other hand side the high production capacity relies on the ability of the chloroplast to express multiple proteins from polycistronic mRNAs that are heavily transcribed.

Another relevant point for biotechnology applications is the field management of transplastomic plants, which may be simpler than with nuclear transformants, because the maternal mode of chloroplast inheritance in most crop plants prevents transgene containment from pollen transmission. Further advantages are the absence of epigenetic effects and gene silencing mechanisms in plastids, which is often observed in the nucleus, as well as the high-precision of genetic engineering as the transgenes are exclusively inserted by homologous recombination. Moreover, with chloroplast transformation it is possible to use antibiotic free selectable markers or to excise selectable marker genes within the selection process. The expression of potentially toxic proteins within a cell organelle like chloroplasts prevents possible negative interactions with the cytoplasmic environment, which is especially important

in case of our designed peptides, even when produced as fusion proteins [64, 67, 70, 75-78].

There are two main approaches for stable plastid transformation: on the one hand side PEG-mediated transformation method and on the other hand side the biolistic approach using particle gun bombardment, which is favorable due to higher transformation efficiency [70]. Regarding DNA integration, also two approaches have been made. Firstly, introduction of transforming DNA is possible by independently replicating shuttle vectors. However, these shuttle vectors were not practical because they were rapidly lost in the absence of selection [79, 80]. Secondly, integration of DNA was achieved by homologous recombination. Stable transformation requires that all ptDNA copies in every chloroplast of the transplastomic plant are uniformly converted. Because only a few ptDNA copies are transformed by particle bombardment, homogenous transformation is achieved by gradually diluting plastids carrying non-transformed copies through amplification on a selective medium [67]. All attempts made so far for transient plastid transformation have not been successful [81].

We chose the biolistic approach to transform chloroplasts of *N. tabacum* because tobacco provides one of the best studied and well-established transplastomic transformation platform, which provides additional advantage like high biomass yield, high scale-up capacity and nonfood/ non-feed status [49].

1.5.2. Examples for chloroplast-derived biopharmaceuticals

Examples for chloroplast-derived proteins include several bacterial-derived antigens, which are easy to produce in chloroplasts due to similar mechanisms for folding proteins in bacteria and plastids. Moreover, no glycosylation, which impacts folding, biological activity, solubility and bioavailability is needed for these proteins [54]. Because most therapeutic proteins are based on native human proteins, they need correct synthesizing and processing mechanisms when produced recombinantly, to display correct post-translational modifications. Within chloroplasts, multiple enzymes and chaperones are present, which enable correct folding and furthermore provide the capacity to assemble complex multi-subunits for a recombinant product. Also appropriate disulfide bonds are formed, although no known plastid-encoded protein contains disulfide bonds [67]. However, glycosylation is a problem regarding chloroplast-derived proteins. Generally, glycosylation in plants occurs in the secretory pathway of the ER and the Golgi apparatus whereas extent and nature of glycans are similar to mammalian glycans regarding size and extent of branching. Nevertheless, the predominant mammal terminal residue N-acetyl neuraminic acid is not present in plants [49, 67, 82]. In Chloroplast, glycosylation was thought to be unfeasible, although novel pathways were described that may allow the kind of

protein maturation that occurs in the ER and Golgi compartments also for chloroplasts [83].

Still, functionality of several chloroplast-derived proteins has been confirmed by various means. It was shown that these plant products are effective within macrophage lysis assays, GM1-ganglioside binding assays, protection of HeLA cells or human lung carcinoma cells, systemic immune response, protection against pathogen challenge, and growth or inhibition of cell cultures [78]. For example, one functional chloroplast-derived peptide is the protective 2L21 peptide from virulent canine parvovirus (CPV), an animal vaccine that was expressed in tobacco chloroplasts as a C-terminal translational fusion with the cholera toxin B subunit [84]. Also the severe acute respiratory syndrome coronavirus (SARS-CoV) spike protein—a membrane-associated glycoprotein, has been expressed in chloroplasts but is fully functional for vaccination [85]. Also the LacA lectin fragment of the eukaryote protist pathogen *Entamoeba histolytica*, a putative target for blocking amoebiasis, was produced in tobacco chloroplasts in rates up to 6,3% of total soluble protein (TSP). Subcutaneous immunization with crude extract of transplastomic tobacco leaves resulted in higher immunoglobulin G titres in animal model than in previous reports [86]. The most striking report regarding high-level foreign protein accumulation in plastids is the reported over-expressing of a proteinaceous antibiotic, which accumulated to 70% of the plant's total soluble protein and was furthermore demonstrated to be stable in chloroplasts [74]. The same group reported production of antimicrobial compounds in plastids up to 30% of TSP [87]. The HIV-1 Pr₅₅Gag protein, a candidate for developing a HIV-1 vaccine, that has been expressed at very low level in nuclear transformed plants, was successfully produced in transplastomic tobacco in levels up to 7–8% of TSP and assembled into VLPs similar to those produced in baculovirus/ insect cells and *E. coli* systems [88].

To summarize, all known factors indicate that heterologous genes, which are site-specific inserted into the plastid genome, can be expressed at high levels with correct folding and disulfide bond formation of the recombinant protein, resulting in fully functional biopharmaceuticals [70, 77].

2. Objectives

The BIOP research group designed synthetic peptides based on the physical, chemical and structural features of naturally occurring AMPs. Four of these peptides, namely SP10-11, SP13-3, SP13-11 and SP13-14, display activity against the human immunodeficiency virus (HIV).

In this work, the cell-toxic effects and the immunomodulatory potential of these target peptides should be investigated. Therefore impact on proliferation and cytokine release of different types of human immune cells should be investigated *in vitro*. The results should serve as basis for developing therapeutic strategies for medical applications of the HIV-active peptides that may range from simple administration as topical microbicide on mucous membrane or skin to the possibility of providing the peptide at a suitable tipping point in HIV infection or during specific steps of the viral cycle.

A second part of this work should be the development of a stable plant expression system to produce the designed peptides. Additionally, the HIV fusion inhibiting peptide drug T-20 should be produced analogous. All peptides should be produced in stably transformed chloroplasts of *Nicotiana tabacum* (*N. tabacum*) and in the form of fusion proteins to stabilize transcripts, facilitate purification and reduce the likely adverse impact of the peptides on the chloroplast.

3. Material and Methods

3.1. Materials

3.1.1. Plant materials

3.1.1.1. Plant media

Name	content	
RMOP medium	MS-salts	4,4 g/l
	Myo-Inositol	0,1 g/l
	ThiaminHCK	1 mg/l
	Benzylaminopurin	1,0 mg/l
	NAA	0,1 mg/l
	Sucrose	30,0 g/l
	Plant Agar	8 g/l
	Medium is adjusted to pH 5,8 with	
RMOP selection medium	RMOP medium containing	
	Spectinomycin	500 g/l
B5 Medium	B5-Salze	3,1 g/l
	B5-Vitamine (100fach)	10 ml/l
	MgSO ₄ x 7H ₂ O	0,983 g/l
	Saccharine	20,0 g/l
	Plant Agar	8 g/l
	Medium is adjusted to pH 5, 8 with KOH.	

3.1.1.2. Plant vitamin and salt stocks

Name	composition	
100x B5 Vitamins	Myo Inositol	10 g/l
	Pyrodoxolhydrochlorid	100 mg/l
	Thiaminiumdichlorid	1 g/l
	Nicotinic acid	100 mg/l
B5 salts	EDTA Fe(III) Na-Salt	4g/l
	Potassium iodide	75 mg/l
	H ₃ BO ₃	300 mg/l
	MnSO ₄ x H ₂ O	1 g/l
	ZnSO ₄ x 7 H ₂ O	200 mg/l
	NaMoO ₄ x 2 H ₂ O	25 mg/l

CuSO ₄ x 5 H ₂ O	2,5 mg/l
CoCl ₂ x 6 H ₂ O	2,5 mg/l

3.1.2. Molecular biology materials

3.1.2.1. Bacteria strains

Laboratory strains were available at BIOP.

Strain	Genotype
<i>Escherichia coli</i> DH5a	F- ϕ 80lacZ Δ M15 Δ (lacZYA-argF)U169 recA1 endA1 hsdR17(rk-, mk+) phoA supE44 thi-1 gyrA96 relA1 λ -
<i>Escherichia coli</i> BL21	F-, ompT, hsdSB (rB-, mB-), dcm, gal, λ (DE3), pLysS, Cmr (DE3) pLys

3.1.2.2. Kits and reaction systems

Name/Description	Company
MinElute® PCR Purification Kit, No. 28004	Qiagen GmbH, Hilden
QIAprep® Spin Miniprep Kit, No. 27104	Qiagen GmbH, Hilden
HiSpeed Plasmid Maxi Kit	Qiagen GmbH, Hilden
QIAquick® Gel Extraction Kit, No. 28704	Qiagen GmbH, Hilden
DNeasy Plant Mini Kit	Qiagen GmbH, Hilden
DIG-High Prime DNA Labeling and Detection Starter Kit II	Roche, Mannheim
IL-12 ELISA	BD Biosciences, Heidelberg
IL-10 ELISA	BD Biosciences, Heidelberg
IL-1 β ELISA	BD Biosciences, Heidelberg
IFN- γ ELISA	R&D Systems, Wiesbaden

3.1.2.3. Buffers, reagents and solutions

All buffers and solutions were prepared in double distilled H₂O and if required autoclaved for 10 min at 121 °C on liquid cycle or filter sterilized (0.22 μ m).

for preparation of competent bacteria cells

TFB1	30 mM KOAc (potassium acetate) 100 mM RbCl 10 mM CaCl ₂ 50 mM MnCl ₂ 15% glycerol pH adjusted to 5.8 with acetic acid
TFB2	10 mM MOPS 75 mM CaCl ₂ 10 mM RbCl 15% glycerol pH adjusted to 6.5 with KOH

for Glycine-SDS polyacrylamide gel electrophoresis (according to Lämmli, 1970)

Coomassie R-250 staining solution	0,25% (w/v) Coomassie Brilliant Blue R-250 50% (v/v) methanol 10% (v/v) glacial acetic acid
Coomassie R-250 destaining solution	30% (v/v) methanol 10% (v/v) glacial acetic acid
10x SDS running buffer	250 mM Tris base 2 M glycine 1% (w/v) SDS
Separation gel buffer	1,5 M Tris/ HCl, pH 8.8 0,4% (w/v) SDS
Stacking gel buffer	0,5 M Tris/ HCl, pH 6.8 0,4% (w/v) SDS
2x reducing sample buffer	100 mM Tris/HCl, pH 6.8 4% (w/v) SDS 0.2% (w/v) bromphenol blue 20% (w/v) glycerol 200 mM DTT

for transfer and immunodetection of proteins and peptides

TBS-T buffer	0,5% (w/v) Tween 20 in TBS buffer
--------------	-----------------------------------

TBS buffer	10 mM Tris/HCl, pH 7.4 150 mM NaCl 1 mM MgCl ₂
Blocking buffer	4% (w/v) dry milk 1% (w/v) BSA in TBS-T buffer
Alkaline phosphatase buffer	0,1 M Tris/HCl, pH 9.5 0,1 M NaCl
BCIP solution	5% (w/v) BCIP in 100% DMF
NBT solution	5% (w/v) NBT in 70% DMF

for extraction, transfer and detection of nucleic acids

TE buffer	10 mM Tris/HCl 1 mM EDTA pH 8.0
DNA depurination	250 mM HCl
DNA denaturation	1,5 M NaCl 0,5 M NaOH
DNA neutralization buffer	1,5 M NaCl 0,5 M Tris/HCl pH 7,5
20x SSC transfer buffer	3,0 M NaCl 0,3 M sodium citrate pH 7,5
50x TAE running buffer	2,0 M Tris base 5,71 % (v/v) glacial acetic acid 50 mM EDTA
10x DNA loading buffer	50% (w/v) glycerol 10 mM EDTA, pH 8.0 0,25% (w/v) bromphenol blue 0,25% (w/v) xylene cyanol FF
Transfer buffer	40 mM Tris base 40 mM Tricine 0,04% (w/v) SDS 20% (v/v) methanol

Southern Blot washing buffer	0,1 M Maleic acid, 0,15 M NaCl; pH 7.5; 0,3% (v/v) Tween 20
Southern Blot maleic acid buffer	0,1 M Maleic acid, 0,15 M NaCl; adjust with NaOH (solid) to pH 7.5
Southern Blot detection buffer	0,1 M Tris-HCL, 0.1 M NaCl, pH 9.5
Southern Blot low stringency buffer	2x SSC 0,1% SDS
Southern Blot high stringency buffer	0,5x SSC 0,1% SDS
Southern Blot blocking solution	12 ml 10x blocking solution 108 ml Maleic acid buffer
Southern Blot antibody solution	1:10 000 in blocking solution

for infiltration of *Nicotiana benthamiana* leaves

Infiltration buffer	10 mM MgSO ₄ 10 mM MES, pH 5.7
Ex-His-A Puffer	100 mM NaPO ₄ (pH7,0) 150 mM NaCl 2 mM EDTA 2 mM EGTA 2 mM DTT 5 µl/ml Leurtin 0,5 mM PMSF 5µl/ml Aprotinin Protease Inhibitor Cocktail Sigma P9599 (1:200)
Ex-His-B Puffer	100 mM NaPO ₄ , pH 7,0 150 mM NaCl 5 µl/ml Leurtin 0,5 mM PMSF 5 µl/ml Aprotinin Protease Inhibitor Cocktail Sigma P9599 (1:200)

Cell culture reagents	Company
RPMI	Life Technologies GmbH, Darmstadt, Germany
AIM V Medium	Life Technologies GmbH, Darmstadt, Germany
Aqua ad injectabilia	Laboratori Diaco Biomedicali, Italy
Propidiumiodide (PI)	Sigma-Aldrich, München
PHA (Lectin)	Sigma-Aldrich, München
essential aminoacids	Life Technologies GmbH, Darmstadt, Germany
human serum AB	Lonza, Verviers, Belgum
10x D-PBS w/o Ca/Mg	Life Technologies GmbH, Darmstadt, Germany
Lymphoprep	Axis Shield
Heparin	Merck, Darmstadt
Streptavidin-horseradish peroxidase	R&D GE Healthcare UK limited, Wiesbaden
Tetramethylbenzidin (TMB)	Fluka, (Sigma-Aldrich) München
Trypanblue 0,4% solution	Gibco, Paisley, Scotland

3.1.2.4. Media

Media for bacteria

All media were prepared in double distilled H₂O and autoclaved for 10 min at 121 °C on liquid cycle.

Name	Content
LB medium	1% (w/v) tryptone 0,5% (w/v) yeast extract 0,5% (w/v) NaCl pH 7,0 1,5% (w/v) agar for solid media
SOC medium	2% (w/v) tryptone 0.5% (w/v) yeast extract 0.05% (w/v) NaCl 2,5 mM KCl

	<i>pH 7.0 and complement before use</i>
	10 mM (final conc.) MgCl ₂
	20 mM (final conc.) glucose
YEP-Medium	1% (v/v) yeast extract
	1% (v/v) peptone
	0,5% (v/v) NaCl

Cell culture media

All media and buffers were sterile filtered, excluding the human serum, and stored at 4°C.

Name	Content
Proliferation medium	5 ml L-Glutamin (200mM) 25 ml Human serum 500 µl 2-Mercaptoethanol 5,6 ml Sodium-Pyruvate 5,6 ml Non-essential Amino Acids 5 ml Penicillin-Streptomycin 450 ml RPMI (+L-Glutamin)
HU-DC medium	50 ml FCS (Fetal Bovine Serum) 2,5 ml Gentamycin (10M) 5 ml L-Glutamin (200mM) 450 ml RPMI (+L-Glutamin)

3.1.2.5. Chemicals and consumed material

All chemicals used were of high purity grade and purchased either from Sigma Aldrich GmbH (Taufkirchen, Germany), Carl Roth GmbH (Karlsruhe, Germany), or other sources as indicated. Handling was performed following standard protocols and the manufacturer's instructions. If any application required chemicals from specific suppliers this is mentioned in the text, otherwise replacement with any chemical of equal purity of any supplier should be possible. Standard laboratory material was used for all experiments and was not restricted to a specific provider.

3.1.2.6. Antibiotics

Working concentrations were 1:1000 of stock solutions. Aqueous stock solutions were sterile filtered through 0.22 µm sterile filters (Millipore, Billerica, MA, United States) and stored as aliquots at -20°C.

	Source	Stock solution (mg/ml)	Dilution reagent	Concentration (μl/ml)
Ampicillin (Amp)	Roche, Mannheim (Germany)	100	ddH ₂ O	100
Kanamycin (Kana)	Sigma, Deisenhofen (Germany)	50	ddH ₂ O	50
Carbenicillin (Carb)	Sigma, Deisenhofen (Germany)	100	20% (v/v) EtOH	100
Spectinomycin (Spec)	Sigma, Deisenhofen (Germany)	50	ddH ₂ O	50
Gentamycin (Spec)	Sigma, Deisenhofen (Germany)	25	ddH ₂ O	25
Rifampicin (Spec)	Sigma, Deisenhofen (Germany)	50	DMF	50

3.1.2.7. Antibodies

Antibody	Immunogen	Working concentration	Source
Primary antibody			
Anti-Histidine-Tagged Protein Mouse mAb	6x His tag	1:3000	Merck KGaA, Darmstadt, Deutschland
Rat monoclonal [3H9] to Green Fluorescent Protein (GFP).	gfp	1:1000	ChromoTek, Planegg-Martinsried, Germany
Secondary antibody			
Anti-Mouse IgG (H&L) AP Conjugate		1:7500	Promega, Mannheim, Germany
goat anti-rat IgGfc (-HRP)		1:2000	available at our institute

3.1.2.8. Enzymes

If not stated elsewhere all restriction endonucleases were purchased from New England Biolabs (Frankfurt, Germany) or MBI Fermentas (St. Leon-Rot, Germany).

Name/Description	Company
Alcaline Phosphatase (CIP)	New England Biolabs, Frankfurt, Germany
Phusion High Fidelity DNA Polymerase	New England Biolabs, Frankfurt, Germany
T4 DNA Ligase	Promega, Mannheim, Germany
Taq DNA Polymerase	Agrobigen, Hilgertshausen, Germany
T4 Polynucleotide Kinase	New England Biolabs, Frankfurt, Germany
BsaI	New England Biolabs, Frankfurt, Germany
SmaI	New England Biolabs, Frankfurt, Germany
AflIII	New England Biolabs, Frankfurt, Germany
EcoRV	New England Biolabs, Frankfurt, Germany

3.1.2.9. Peptides

Synthetic peptides (> 95% purity, lyophilized) were purchased from GenScript, USA. Peptides were dissolved in ddH₂O in stock concentrations of 2 mg/ml and aliquots were stored at -80 °C. The following peptides were used in this study:

Name	Sequence
SP10-11	LRKAKKIAKKLF
SP13-3	KRRLILRLRLAIRILVKKR
SP13-11	KRRLALFRLFRLALKLVLKK
SP13-14	KRRKLAFLFRLFLKLVK
T20	YTSLIHSLIEESQNQQEKNEQELLELDKWASLWNWF

3.1.2.10. Oligonucleotides

Lyophilized oligonucleotides were purchased from Eurofins MWG Operon, Germany. 100 µM stock solutions of deprotected and salt-free oligonucleotides were prepared in sterile ddH₂O and stored at -20 °C.

Sequencing Primer

Rps12	5'-GGCCAATACCGGGTATATAAG-3'
Seq1 rev	5'-GGTCCTAGTTACTCTTCGGG-3'
Seq2 fwd	5'-AAAGTACCATGTGAAATCTTCG-3'
Seq3 fwd	5'-ATGCCC GAAGGCTACGTCCA-3'
Seq4 fwd	5'-CAATACGTAATGGA ACTCGC-3'
Seq5 fwd	5'-TCCAGCGGCGGAGGAACTCTTT-3'
Seq6 fwd	5'-GGAAGAATTTGTCCACTACG-3'
Seq6B rev	5'-TCGCTCATCGCCAGCC-3'
Seq8B fwd	5'-GCGCGCAGATCAGTTGG-3'
M13 uni (-21)	5'- TGTAAAACGACGGCCAGT-3'

Oligonucleotides for creating modified pUC18 donor vector

pUC18 1769T f1	5'-GCTGCAATGATACCGCGAG T CCCACGCTCACCGGCTCCAG
pUC18 1769T rev	5'-CTGGAGCCGGTGAGCGTGGG A CTCGCGGTATCATTGCAGC
pUC18-1769T- f2	5'-GCTGCAATGATACCGCGAG T CCCACGCTCACCGGCTCC (38)
pUC18-1769T- r2	5'-GGAGCCGGTGAGCGTGGG A CTCGCGGTATCATTGCAGC (38)
pUC18-1769T- f3	5'-TGCAATGATACCGCGAG T CCCACGCTCACCGGCT (34)
pUC18-1769T- r3	5'-AGCCGGTGAGCGTGGG A CTCGCGGTATCATTGCA (34)

*mutated nucleotides are empathized in bold letters.

Oligonucleotides for creating tagged gfp donor vectors and PpsbA donor vector

gfp N-His fwd	5'-GGTCTCTATGGAACATCACCATCACCATCACGTGAGCAAGGGCGA GGAG-3'
gfp N-His rev	5'-GGTCTCTTTGCCTTGTACAGCTCGTCCATGCCG-3'
gfp C-His fwd	5'- GGTCTCTATGGT GAGCAAGGGCGAGGAGCTG-3'
gfp C-His rev	5'-GGTCTCTTTGCGTGATGGTGATGGTGATGCTTGTACAGCTCGTCC ATGCCG-3'
GFP posK rev	5'-GGTCTCTTTACTTACTTGTACAGCTCGTCCATGCCG-3'
PpsbA korr fwd	5'-GGTCTCTGCCAAAGAAAAGTGAGC-3'
PpsbA korr rev	5'-GGTCTCTCCATATGTTAATTTTTTAAAGTTTT-3'

Oligonucleotides for Icon Genetics Approach

IG 13-3 fwd	5'-TTTGGTCTCAAGGT ATGAAGAGAAGATTGATTTTGAGAA-3'
IG 13-3 rev	5'-ATCTTCTAGATCATCTTTTCTTAACCAAATTCTAA-3'

IG 13-14 fwd	5'-TTTGGTCTCAAGGT ATGAAAAGAAGAAAATTGGCTTT
IG 13-14 rev	5'-ATCTTCTAGATCACTTTTTCAAACCACTTCA-3'
IG T20 fwd	5'-TTTGGTCTCAAGGTATGTATACTAGTTTAATTCATAGTTTAATTGAA-3'
IG T20 rev	5'-ATCTTCTAGATCAAACCAATTCCATAAACTAGC-3'
IG gfp fwd	5'-TTTGGTCTCAAGGT ATGGTGAGCAAGGGCGA-3'
Sq11599	5'-GCTCATGGTACCTCGAAGC-3'
TMV3'end_rev	5'-TGGGCCCTACCGGGGGTAAC

Oligonucleotides for creating AMP Oligos*

GGCSP10-11s	5'- GGTCTCTGCAATGTTGAGAAAGGCTAAGAAAATTGCTAAGAAATTGT TTTGAGTAAAGAGACC-3'
GGCSP10-11as	5'- GGTCTCTTTACTCAAACAATTTCTTAGCAATTTTCTTAGCCTTTCTCA ACATTGCAGAGACC-3'
GGCSP13-3s	5'-GGTCTCTGCAATGAAGAGAAGATTGATTTTGAGAATTTTGAGATTGGC TATTAGAATTTTGGTTAAGAAAAGATGAGTAAAGAGACC-3'
GGCSP13-3as	5'-GGTCTCTTTACTCATCTTTTCTTAACCAAATTCTAATAGCCAATCTCAA AATTCTCAAATCAATCTTCTTTCATTGCAGAGACC-3'
GGCSP13-14s	5'- GGTCTCTGCAATGAAAAGAAGAAAATTGGCTTTTAGATTGTTTCAGATT GTTTTTGAAGTTGGTTTTGAAAAAGTGAGTAAAGAGACC-3'
GGCSP13-14as	5'-GGTCTCTTTACTCACTTTTTCAAACCACTTCAAACAATCTGAACA ATCTAAAAGCCAATTTTCTTCTTTTCATTGCAGAGACC-3'
GGCSPT20	5'-GAATTCGGTCTCTGCAATGTATACTAGTTTAATTCATAGTTTAATTGAA GAAAGTCAAATCAACAAGAAAAAATGAACAAGAATTATTGGAATTAGA TAAATGGGCTAGTTTATGGAATTGGTTTTGAGTAAAAGAGACCGAATTC- 3'

Oligonucleotides for screening of putative transgenic plants

plantPCR2 f	5'-CCCGACAACCACTACCTGAGCA-3'
plantPCR2 r	5'-TGGATCCCTCCCTACAACCTAGTGA-3'
SiteSpecific PCR f	5'-CGCCCTTGTTGACGATCCTT-3'
SiteSpecific PCR r	5'-TTCAGGGTCAGCTTGCCGTAGG-3'
SiteSpecific PCR2 f	5'-AAATGTAGTGCTTACGTTGTCCCG-3'
SiteSpecific PCR2 r	5'-CCCCTTTGAGACCCCGAAAA-3'
RTPCR T20 f	5'-AGGAGCGCACCATCTTCTTCAA-3'
RTPCR T20 r	5'-CAAACCAATTCCATAAACTAGCCC-3'
RTPCR 13-3 f	5'-AAGCTGACCCTGAAGTTCAT-3'
RTPCR 13-3 r	5'-GCCAATCTCAAATTTCTCAA-3'

RTPCR 13-14 r 5'-CTTCTTTTCATTGCCTTGTACAGCT-3'

RTPCR 13-14 f 5'-AGTTCATCTGCACCACCGGC-3'

Oligonucleotides for generating the Southern Blot probe

sb probe fwd 5'-CTCCCTTTCCTGCTAGGATT-3'

sb probe rev 5'-TGTCGGAGTAAAGGATCGTC-3'

3.1.2.11. Plasmids

Plasmid DNA was extracted from *E. coli* cells as described in 3.2.3.5 and stored in ddH₂O at -20 °C.

Name	Source	Selection	Description/Use
pICH17388	Bayer – formerly Icon Genetics (Halle, Germany)	Amp/Carb	5' vector with RdRP
pICH14011	Bayer – formerly Icon Genetics (Halle, Germany)	Amp/Carb	Phi C31 Integrase
pICH7410	Bayer – formerly Icon Genetics (Halle, Germany)	Amp/Carb	3' vector with gfp (control)
pICH10990	Bayer – formerly Icon Genetics (Halle, Germany)	Amp/Carb	Plant Transfection magnICON® 3'-module
pICH10990- gfp::13-14	BIOP	Amp/Carb	Plant Transfection magnICON® 3'-module: gfp::SP13-14 fusion protein
pICH10990- gfp::T20	BIOP	Amp/Carb	Plant Transfection magnICON® 3'-module: gfp::T20 fusion protein
pUC18	Proteome facility Helmholtz Zentrum München	Amp/Carb	Precursor vector for GG Don1
pB7FWG2	Gateway (Life Technologies)		GFP from Gateway vector pB7FWG2

	GmbH, Darmstadt)		
pJET1.2 blunt	MBI Fermentas, St Leon-Rot, Germany	Amp/Carb	
pDrive receptor	Cooperation AG Koop, LMU	Kana	
Don1	This work	Amp/Carb	PUC18 with silent mutation in BsaI cleavage site
Don2	Cooperation AG Koop, LMU	Spec	pJET1.2 blunt with replacement of <i>bla</i> gene with <i>aadA</i> gene
Don1 PpsbA	This work	Amp/Carb	Don1 with Golden Gate compatible PpsbA gene insert
Don1 SP13-3	This work	Amp/Carb	Don1 with Golden Gate compatible SP13-3 gene insert
Don1 SP13-14	This work	Amp/Carb	Don1 with Golden Gate compatible SP13-14 gene insert
Don1 T20	This work	Amp/Carb	Don1 with Golden Gate compatible T20 gene insert
Don1 gfpNH	This work	Amp/Carb	Don1 with Golden Gate compatible gfp gene insert with an N-terminal 6xhistidin-tag
Don1 gfpPK	This work	Amp/Carb	Don1 with Golden Gate compatible gfp gene insert with an N-terminal 6xhistidin-tag
Don2 rps12	This work	Spec	Don2 with Golden Gate compatible <i>rps12</i> insert
Don2 trpIHA	This work	Spec	Don2 with Golden Gate compatible <i>trpIHA</i> insert
Don2 aadA	This work	Spec	Don2 with Golden Gate compatible <i>aadA</i> gene insert
PTV 13-3 NH	This work	Kana/Spec	Plasmid transformation vector with GOI consisting from 6xHistidin tag:: <i>gfp</i> ::SP13-3
PTV 13-14 NH	This work	Kana/Spec	Plasmid transformation vector with GOI consisting from

			6xHistidin tag:: <gfp>::SP13-14</gfp>
PTV T20 NH	This work	Kana/Spec	Plasmid transformation vector with GOI consisting from 6xHistidin tag:: <gfp>::T20</gfp>
PTV gfp PK	This work	Kana/Spec	Plasmid transformation vector with GOI consisting from 6xHistidin tag:: <gfp></gfp>

3.1.3. Disposable materials

Material	Company
Heat-sealing paper	Perkin Elmer, Rodgau-Rüdesheim
Maxi sorp plates (96 well)	Nunc, Roskilde, Denmark
Petri Dish	Greiner bio-one, Frickenhausen
Pipettes (1, 5, 10, and 25 ml)	Greiner bio-one, Frickenhausen
Sterile filter (0.22; 0.45 µm)	Millipore express, Cork, Ireland
Sterile filter device (250ml, 500ml)	Millipore, Billerica, USA
Tissue culture flask (175 cm ² , 650ml)	Greiner bio-one, Frickenhausen
Tissue culture plates (96 well; 24 well, 6well) flat/U-bottom	Sarstedt, Nümbrecht
Gold 0,6 µ	Bio-Rad Laboratories GmbH, Munich
Rupture Disc 900 PSI	Bio-Rad Laboratories GmbH, Munich
Stopping screens	Bio-Rad Laboratories GmbH, Munich
Macrocarrier	Bio-Rad Laboratories GmbH, Munich

3.1.4. Instruments and accessories

Name/Description	Type	Company
Autoclave	D-150	Systec
Balance	LC 620 S	Sartorius
	A 210 P	Sartorius
	L 2200 P	Sartorius
Camera	Powershot G2	Canon
Centrifuge	Beckman J2-21	Beckmann Coulter

	Centrifuge 5415 D	Eppendorf
	Centrifuge 5810 R	Eppendorf
	Biofuge 28 RS	Heraeus
Electrophoresis systems	Mini-vertical electrophoresis unit SE250	Hoefer
Electroporator	Gene Pulser Electroporation system	Bio-Rad
Flow Hood	Gelaire BSB 4A	Flow Laboratories
Fume Hood	CAPT AIR Filter system 804N	Captair
Gel Caster	Multiple gel caster SE215	Hoefer
Gel Documentation	Benchtop 2UV Transilluminator & PhotoDocIt Imaging System	UVP
Magnetic stirrer	IKA-Combimag Ret	Jahnke & Kunke
pH measurement	pH Meter pH 523 pH electrode SenTix 21	WTW
Particle gun	PDS/1000/He	Bio-Rad
Power supply	Electrophoresis power supply EPS 601	GE Healthcare
Rotors	JA-10, JA-20 F45-24-11	Beckman Coulter Eppendorf
Shaker	UniTherm HB Reax 2	UniEquip Heidolph
Spectrophotometer	NanoDrop ND-1000 Ultrospec 3100 pro	NanoDrop Technologies Amersham
Temperature thermostat	RW 6	Lauda
Thermal Cycler	Hybaid PCR express	Thermo Life Sciences
Thermoblock	Thermomix Comfort	Eppendorf
Ultra-pure water system	Ultra Clear Direct	SG
Ultra sonic bath	Sonorex Super 10 P	Bandelin
UV lamp	B-100 AP	UVP
Vacuum concentrator	Univapo 150W	UniEquip

Vortexer	Vortex-Genie 2	Scientific Industries
Centrifuge	Centrifuge	Thermo Scientific
Centrifuge	Centrifuge Megafuge 1.0R	Heraeus
ELISA-Reader	ELISA-Reader Mrx tc revelation	Thermo Labsystems
Flow Cytometer	FACSCalibur	Becton Dickinson
Incubator	Incubator	Heraeus
Microscope	Microscope Axiovert	Zeiss
Precision balance	Precision balance	Eppendorf
Water bath	Water quench Typ1003	GFL

3.2. Methods

3.2.1. Plant methods

3.2.1.1. Plant growth on soil

Nicotiana tabacum (*N. tabacum*) and *Nicotiana benthamiana* seeds were loosely sown in homogenized soil Type T (NPK 310, 300, 420 mg/l) mixed with perlite in a ratio of 1:5 to improve root aeration and water supply. Three weeks after germination when the seedlings reached a height of about three cm they were repotted in 11x11x12 cm pots (Teku Tainer, Pöppelmann). Controlled climate conditions were assured by cultivation in a growth chamber (14h day light, intensity 100 μ E/ms at 25 °C, 10h dark at 20°C, humidity ~ 70%) [47].

3.2.1.2. Seed surface sterilization

For surface sterilization, seeds were placed in a clean bench on filter paper and submerged in 70% ethanol. Seeds were allowed to dry in the clean bench until complete dryness and the process was repeated a second time.

3.2.1.3. Sterile culture on solid medium

Sterile seeds were sown on petri dishes with B5 plant medium with or without selection marker spectinomycin, respectively. After germination, seedlings were grown under controlled conditions in growth chamber (16 h/day light, intensity 100 μ E/ms at 25°C, humidity ~ 56%). After approximately 12 weeks, young, healthy and fully expanded leaves from sterile propagated plants were used for transformation experiments [89].

3.2.1.4. Transferring plants from sterile culture to soil

Sterile propagated *N. tabacum* shoots were transferred on B5 medium w/o spectinomycin under sterile conditions and cultured for approximately 12 weeks until development of roots under controlled conditions in a growth chamber (16 h/day light, intensity 100 μ E/ms at 25°C). Rooted shoots were recovered from sterile culture and remaining medium was carefully washed from the roots with warm water. Plants were repotted into homogenized soil Type T (NPK 310, 300, 420 mg/l) mixed with perlite in a ratio of 1:5. Transferred lines were cultivated for 1 week under foil to increase air humidity and under controlled conditions (14h day light, intensity 100 μ E/ms at 25°C, 10 h darkness at 20°C, humidity ~ 70%).

3.2.1.5. Infiltration of *Nicotiana benthamiana* leaves

The transient transformation approach was realized as a part of a master's thesis [90]. Approximately six week old plants of the tobacco cultivar *Nicotiana*

benthamiana were infiltrated with *Agrobacterium tumefaciens* (*A. tumefaciens*) for expression performance regarding the fusion protein of the transplastomic approach. Here, three different *A. tumefaciens* strains were used carrying the vectors pICH14011 (phage C31 integrase), pICH17388 (5'-provector module) and pICH11599 or pICH10990 carrying the 3'-provector module with GFP::peptide fusion. Additionally, pICH7410 carrying the 3'-provector module with only GFP as positive control was applied. 5 ml cultures of *Agrobacterium tumefaciens* GV3101 pMP90 carrying the different plasmids were grown for 24 h at 28 °C and 200 rpm in YEP medium. When the cultures reached a sufficient optical density, they were transferred into 50 ml YEP medium and again incubated at 28°C for 24 h with 200 rpm. Cultures were harvested by centrifugation (3,000 g, 20 min, 4 °C). Bacteria were washed three times 15 ml infiltration buffer to remove cell fragments and remaining medium and subsequently resuspended in infiltration buffer with an OD_{600nm} of 0.01 for each culture. Subsequently, the cultures were mixed in equal ratio in a way that pICH14011, pICH17388 and one of the vectors containing the 3'-provector module with specific gene of interest were combined to an infiltration mixture. One day before infiltration, plants were fertilized and watered. Single, minimum palm-sized leaves of healthy *Nicotiana benthamiana* plants were sprayed on the abaxial side with ddH₂O one hour before infiltration to help opening the stomata which helps with manual infiltration. Leaves were scratched slightly and infiltrated with a syringe without a needle from the abaxial side with approximately 30 ml infiltration mixture per plant. After infiltration plants were kept under standard growth conditions and from day 5 after infiltration, GFP expression was monitored under fluorescent light [47].

3.2.1.6. Particle gun bombardment

Chloroplast transformation vectors were transferred into plastids of sterile cultivated *N. tabacum* leaves with a particle gun. The particle gun device PDS/1000/He (Bio-Rad, Munich) was provided by AG Koop, LMU. Sterilization of particle gun chamber, microcarrier launch assembly, rupture disc holder, target shelf, macrocarrier holder, macrocarriers and stopping screens was performed with 70% EtOH. Rupture discs were sterilized individually by submersion in 75% isopropanol for 5-10 s. All components were air dried under sterile conditions. Stock solution of gold nanoparticles consisted from 60 mg/ml in 100% Ethanol absolute. 35 µl of the gold stock suspension were spun down (13 000 rpm, 1 min) and the supernatant was carefully removed. All subsequent protocol steps were performed on ice. 230 µl sterile dH₂O, 250 µl of 2.5M CaCl₂ and 25 µl of plasmid preparation (1.0 µg/µl dissolved in ddH₂O) were mixed with the gold particles. 50 µl of 0.1 M spermidine were added and the mixture was incubated for 10 min and mixed thoroughly every 2

min. The coated particles were spun down (13 000 rpm/ 1 min,) and the supernatant was discarded. The pellet was washed twice in 100% Ethanol absolute and resuspended in 72 µl of 100% Ethanol absolute. 5,4 µl of the suspension was transferred on a macro projectile (Bio-Rad, USA) and air-dried completely. The rupture disc, the stopping screen and the macrocarrier holder were fitted into the vacuum chamber according to the manufactures instructions. The particles were accelerated with air pressure and shot into *N. tabacum* tissue on a petri plate with the following shooting parameters:

Pressure of helium:	1100 psi (7584.17 Kilopascal)
Rupture discs:	900 psi (6205.2 Kilopascal)
Distance rupture disc-macrocarrier:	8-10 mm
Distance macrocarrier-stopping screen:	10 mm
Distance stopping plate-leaf:	7 cm
Vacuum:	27 -28 inches Hg (91.4-94.8 Kilopascal)

A perforated screen was used to stop the macro projectile, while allowing the micro projectiles to pass through to the plant cells on the other side. After bombardment, plant material was transferred on RMOP medium without Spectinomycin and regenerated under controlled conditions (3.2.1.2) for two days [89].

3.2.1.7. Regeneration and selection

Spectinomycin-resistant lines were selected on RMOP medium containing 500 mg/l respectively 50 mg/l spectinomycin dihydrochloride. Bombarded leaves were chopped into small sections and placed on selection medium. Within a week, leaf tissue bleached out and developed callus tissue. After eight to twelve weeks, spectinomycin resistant, green shoots emerged from the callus. As a control, wild-type *N. tabacum* leaf sections were accordingly cultivated on RMOP medium without Spectinomycin.

3.2.1.8. Characterization of transplastomic lines

Putative heteroplastomic transformants were isolated and subjected to three rounds of regeneration on selection medium to obtain homoplastomic lines. Therefore leaves of regenerated shoots were chopped and sub-cloned into fresh selection medium for development of new shoots. Total DNA from both wild-type and putative transplastomic shoots was extracted using DNeasy Mini Kit (Qiagen, USA) and screened via PCR to verify integration of transgenes in the chloroplast genome.

3.2.2. Cell culture methods

3.2.2.1. Isolation of peripheral blood monocytes (PBMCs)

PBMCs from healthy volunteers were isolated from heparinized peripheral blood by density gradient centrifugation using lymphoprep (density: 1.077 g/ml). 25 ml heparinized blood was diluted in 25 ml D-PBS w/o $\text{Ca}^{2+}/\text{Mg}^{2+}$ and 25 ml of this dilution was layered slowly over 10 ml lymphoprep and centrifuged (15 min, 2000 rpm, without brake). Erythrocytes and granulocytes get collected at the bottom of the column while PBMCs (lymphocytes, monocytes und thrombocytes) build the interphase between lymphoprep and plasma. The PBMC-containing interphase was carefully removed with a pipette tip, washed three times with 5 mM EDTA in D-PBS w/o $\text{Ca}^{2+}/\text{Mg}^{2+}$ and counted with trypanblue staining and Neubauer Cell Counter. PBMCs were suspended in complete medium and placed with a concentration of 300 000 cells/well in a standard 96-well microtiter plate. The cells were incubated at 37°C in a humidified atmosphere with 5% CO_2 [91].

3.2.2.2. Generation of monocyte-derived dendritic cells (MoDC)

Also monocyte-derived dendritic cells (MoDCs) were generated from peripheral blood of allergenic and healthy volunteers. $\text{CD}14^+$ monocytes were purified by magnetic cell sorting (MACS) from formerly isolated PBMCs (3.2.2.1). Therefore, bead-coupled antibodies against the surface molecule CD14 were used. 30 μl anti-CD14 micro beads and 130 μl MACS buffer per 10^8 PBMCs were incubated for 15 min at 4 °C and separated by positive selection through a magnetic column. $\text{CD}14^+$ monocytes were then counted and washed. Subsequently, monocytes were transferred in HU-DC medium and incubated at 37°C in a humidified atmosphere with 5% CO_2 for five days in the presence of 50 U/ml rhGM-CSF and rhIL-4. Cells were fed after three days by removing half of the medium and adding back the same amount of HU-DC medium containing 50 U/ml fresh rhGM-CSF and rhIL-4. On day five, immature MoDCs were harvested, resuspended in complete HU-DC and counted [92].

3.2.2.3. Stimulation of PBMCs and MoDCs with designed AMP

To stimulate PBMCs different concentrations of synthetic peptides with a purity >95% (GeneScript, USA) were applied (100 $\mu\text{g}/\text{ml}$, 75 $\mu\text{g}/\text{ml}$, 50 $\mu\text{g}/\text{ml}$, 25 $\mu\text{g}/\text{ml}$, 15 $\mu\text{g}/\text{ml}$, 10 $\mu\text{g}/\text{ml}$, 5 $\mu\text{g}/\text{ml}$). As a positive control 10 $\mu\text{g}/\text{ml}$ phytohemagglutinin (PHA), 0, 1 $\mu\text{g}/\text{ml}$ lipopolysaccharide (LPS) or 10 $\mu\text{g}/\text{ml}$ Polyinosinic:polycytidylic acid (poly I:C) were used, respectively. Untreated and H_2O -treated cells served as negative controls. Every concentration was measured in two to four technical replicates per biological replicate.

3.2.2.4. PI staining and Flow cytometry

Quantification of apoptosis of simulated cells was measured using the fluorochrome propidium iodide (PI) staining in flow cytometry after different incubation times (1,5h, 26h, 67h). Two to four technical replicates were combined in one FACS tube. Cells were diluted 1:2 in FACS buffer and analyzed using FACS Calibur device (Becton Dickinson, Heidelberg). For the toxicity tests, the following conditions were applied:

- (1) PBMCs in medium without any additives (negative control "medium")
- (2) With addition of 0.01 ml ddH₂O instead of peptides dissolved in ddH₂O (negative control "H₂O")
- (3) Stimulation by PHA, LPS or PolyI:C (positive control "PK"),
- (4) Stimulation by different concentration of each peptide per well (100 µg/ ml, 75 µg/ ml, 50 µg/ ml, 25 µg/ ml, 15 µg/ ml, 10 µg/ ml or 5 µg/ ml) without additional stimulation by PHA, LPS or Poly I:C.
- (5) Stimulation by PHA, LPS or PolyI:C and parallel by different peptide concentration per well (100 µg/ml, 75 µg/ml, 50 µg/ml, 25 µg/ml, 15 µg/ml, 10 µg/ml or 5 µg/ml of each peptide, respectively).

3.2.2.5. Analysis of cytokine secretion by enzyme-linked immunosorbent assay

Concentrations of cytokines IFN- γ , IL-10 and IL-12 in cell-free culture supernatant were quantified using commercially available sandwich enzyme-linked immunosorbent assay (ELISA) kits according to the manufacturer's protocol. Samples for IFN- γ ELISA (R&D Systems) and IL10 ELISA (BD bioscience) were taken from PBMC cultures after 60h incubation. All PBMC supernatants were applied undiluted. Samples for IL-12 ELISA and IL-6 ELISA (BD bioscience) were taken from DC cultures after 24h incubation. For IL-12 ELISA, supernatants were used in 1:100 dilutions and for IL-6 ELISA, supernatants were used undiluted.

3.2.3. Molecular biology methods

3.2.3.1. Preparation of chemically competent bacteria cells

A single colony of *Escherichia coli* DH5 α was inoculated into 2.5 ml of LB medium and cultivated overnight at 37°C and 250 rpm. The culture was then subcultured in 250 ml LB medium containing 20 mM MgSO₄ and grown until an OD₅₉₀ of 0.4 to 0.6. The suspension was centrifuged at 5000 rpm for 5min at 4°C. The supernatant was discarded and the bacterial pellet resuspended carefully in 100 ml of ice-cold TFB1 and kept on ice for 5 min. The bacterial suspension was then centrifuged again and the new pellet was resuspended gently in 10 ml cold TFB2. After incubation on ice for 1h, bacteria were aliquoted (50 µl) in ice-cold Eppendorf tubes, immediately frozen

in liquid nitrogen and stored at -80°C . The expected transformation efficiency with this protocol is around 10^6 cfu/ μg plasmid DNA.

3.2.3.2. Heat shock transformation

For transformation by heat shock an aliquot of 50 μl chemically competent *Escherichia coli* DH5 α cells was thawed on ice for 5 min and then mixed with approximately 20 ng plasmid DNA or 3 μl of an enzymatic reaction mixture and incubated on ice for 30 min. Cells were subsequently transformed by incubation at 42°C for 30 s in an water bath and immediately cooled on ice for 2 min. The cells were suspended in 1 ml LB medium and incubated for one hour (250 rpm, 37°C). Then 20 – 200 μl depending on the reaction mixture were plated on LB plates with appropriate antibiotics and/ or X-Gal and IPTG. The plates were incubated at 37°C oN. Single colonies were selected and used for further experiments.

3.2.3.3. Culture and growth conditions

Escherichia coli (*E. coli*) cell cultures were grown in LB medium with appropriate antibiotics at 37°C . Liquid cultures were incubated with shaking (250 rpm).

3.2.3.4. Blue-White-Screening

For blue-white screening, culture plates were prepared with LB-agar and the appropriate selection markers. After the agar cooled into the solid state, 40 μl of the a 5-bromo-4-chloro-3-indolyl- β -D-galactopyranoside (X-Gal) stock solution (20 mg/ml) and 10 μl of 100 mM Isopropyl β -D-1-thiogalactopyranoside (IPTG) were pipetted onto the plate and spread evenly on with a sterile spatula. After drying the plate at RT for 10 min, bacteria were applied and incubate overnight at 37°C . After colonies are formed, plated were incubated at 4°C for 2 – 4 h for a better distinction.

3.2.3.5. Plasmid DNA preparation

Plasmid DNA from *E. coli* was isolated using the QIAprep Spin Miniprep Kit (Qiagen, Hilden) according to the manufacturer's instructions. For higher amounts (e.g. for the biolistic transformation approach, HiSpeed®Plasmid Maxi Kit (Qiagen, Hilden) was used according to the manufacturer's instructions. For total DNA preparation from plant tissue of small, young plant leaves or callus, plant tissue was disrupted in liquid nitrogen using mortar and pestle. 100 mg grinded plant material was weighed and DNA was extracted using DNeasy Plant Mini Kit (Qiagen, Hilden, Germany) according to the manufactures instructions.

3.2.3.6. Determination of nucleic acids concentration

The concentration and purity of DNA or RNA was analyzed by measuring the absorption at 260 nm and 280 nm using the Nanodrop ND-1000 spectrophotometer

(Kisker-biotech, Germany). Water or buffer, respectively, was used as blank and a volume of 1 μ l was used for each measurement. The A₂₆₀/A₂₈₀ ratio was used to assess the purity of total DNA or RNA and to detect the presence of protein, phenolics or other contaminants that absorb at or near 280nm.

3.2.3.7. Nucleic acid agarose gel electrophoresis

The separation of nucleic acids according to fragment size was done in 1% agarose gels in TAE buffer. After dissolving agarose in TAE buffer by cooking and cooling down to about 50°C, 0.05 μ g/ml ethidium bromide was added and the gel was casted. Samples were mixed with 6x loading dye (MBI Fermentas, St Leon-Rot, Germany) to a final dye concentration of 1x and the gels were run at a voltage of 120 V. After separation, nucleic acids were visualized with UV light (302 nm).

3.2.3.8. Purification of PCR products and DNA reaction mixtures

DNA products from PCR or enzymatic cleavage were cleaned with the QIAquick PCR purification Kit or QIAquick Gel Extraction Kit, according to the manufacturer's instructions (Qiagen, Hilden, Germany).

3.2.3.9. PCR (Polymerase Chain Reaction)

Polymerase Chain Reaction (PCR) is a method that allows exponential amplification of short DNA sequences within a longer double stranded DNA molecule *in vitro* by repeated cycles of denaturation at high temperature, primer annealing and elongation phases. The annealing temperature depends on the length and base pair composition of the primers. PCR mixes were prepared as followed:

Table 2: PCR mixes and according thermocycler programs

Polymerase	PCR mix	Thermocycler program	
Taq DNA Polymerase (Agrobigen)	3 μ l total plant DNA/ 20 ng plasmid DNA	95°C/ 30 – 120 s	1 cycle
	2 μ l 10x reaction buffer	95°C/30 s (denaturation)	
	1,2 μ l 25 mM MgCl ₂	X°C/30 s (annealing)	30 cycles
	0.2 μ l 20 mM dNTPs	72°C/1 min/1kb (extension)	
	1 μ l 10 μ M forward primer	72°C/10 min	1 cycle
	1 μ l 10 μ M reverse primer	Cool down to 10°C	∞
	0,2 μ l (5 U/ μ l) polymerase		
Proofreading Phusion High Fidelity DNA Polymerase (New England Biolabs,	20 ng plasmid DNA	98°C/30 s	1 cycle
	2 μ l 10X reaction buffer	98°C/30 s (denaturation)	
	0.2 μ l 20 mM dNTPs	X°C/30 s (annealing)	30 cycles
	1 μ l 10 μ M forward primer		

Frankfurt)	1 μ l 10 μ M reverse primer	72°C/30 s/1kb (extension)	
	1 μ l (2 U/ μ l) polymerase	72°C/10 min	1 cycle
		Cool down to 10°C	∞

3.2.3.10. Colony PCR

Colonies from oN cultured LB plates were picked with a sterile toothpick and transferred into PCR reaction tubes. Samples were supplied with PCR reaction mixture for *taq* polymerases (3.2.3.9) and PCR was carried out with the following thermocycler program:

95°C/2 min	1 cycle
95°C/30 s (denaturation)	} 30 cycles
X°C/30 s (annealing)	
72°C/1 min/1kb (extension)	
72°C/10 min	1 cycle
Cool down to 10°C	∞

3.2.3.11. cDNA generation and RT PCR

RNA was isolated by RNeasy Plant Mini Kit (Qiagen, Hilden) with DNase digest on filter according to the manufacturer's manual and RNA concentration was determined (3.2.3.6). Generation of complementary DNA (cDNA) was performed using SuperScript™ II Reverse Transcriptase (Life Technologies GmbH, Darmstadt). The following components were added to a nuclease-free microcentrifuge tube:

Oligo(dT)₁₂₋₁₈ (500 μ g/mL)
 5 μ g total RNA
 1 μ L dNTP Mix (10 mM each)
 Sterile, distilled water to 12 μ l

Reaction mixture was heated to 65°C for 5 min and immediately chilled on ice. Following components were added to the mixture:

4 μ L of 5x First-Strand Buffer, 2 μ L of 0.1 M DTT

The reaction was incubated at 42°C for 2 min and 200 units of SuperScript™ II RT were added. Subsequently, mixture was incubated at 42°C for 50 min and finally inactivated by heating to 70°C for 15 min. To remove complementary RNA 2 units of *E. coli* RNase H (Life Technologies GmbH, Darmstadt) were added and incubated at 37°C for 20 min.

3.2.3.12. DNA sequencing

PCR-amplified sequences or plasmid DNA was purified as described in methods 3.2.3.5 and 3.2.3.8, prepared according to the manufacturer's instructions and processed by Eurofins MWG Operon (Martinsried, Germany).

3.2.3.13. Digestion by restriction endonucleases and ligation

Restriction digests were performed with restriction enzymes from New England Biolabs (Frankfurt am Main, Germany) or MBI Fermentas (St Leon-Rot, Germany), using the appropriate buffer and temperature as recommended by the manufacturer. Digest contained about 0.5 to 1 µg plasmid DNA or PCR products, 1x reaction buffer and approx. 5 units of restriction endonuclease(s). ddH₂O was added to a final volume of 20 µl. The mixture was incubated at 37°C for about 2h to oN in an incubator. Afterwards the enzymes were deactivated according to manufacturer's instructions and fragment sizes were checked by agarose gel electrophoresis (3.2.3.7). Ligation of restricted DNA fragments was performed using T4 ligase (Fermentas, St Leon-Rot) overnight at 16°C followed by enzyme inactivation for 10 min at 65°C. A molar ratio for the ligation reaction of 3:1 (insert: vector) was used. For blunt-end ligations, vectors were treated with CIP alkaline phosphatase (New England Biolabs, Frankfurt) prior to the ligation reaction, to inhibit self-ligation.

3.2.3.14. Oligonucleotide annealing

Oligos coding different genes of interest were synthesized as single-stranded DNA (Eurofins MWG Operon, Martinsried). Codon usage was selected according to genetic codes from NCBI for tobacco. Oligonucleotides were annealed to a double stranded construct by heating to 95°C and slow cooling in a Hybaid PCR-Express thermocycler with the following program details:

Step temperature

25°C, 2 min

ramp step: 25°C to 95°C ramp rate: 0.1°C/s

95°C, 10 min

ramp step: 95°C to 4°C ramp rate: 0.1°C/s

(with 30 s incubation steps at: 85, 75, 65, 55, 45, 35, 25, 15°C)

4°C hold

After annealing, the resulting DNA fragments were phosphorylated by T4 Polynucleotide Kinase (New England Biolabs, Frankfurt) and inserted into restricted and dephosphorylated vectors by T4 Ligase (Fermentas, St Leon-Rot). Correct insertion was verified by control digest and sequencing.

3.2.3.15. Golden Gate Cloning

Construction of Golden Gate donor vectors

For the Golden Gate Cloning reaction, it is necessary to provide an empty donor vector, which features no additional BsaI cleavage sites. As a basic frame we used plasmid pUC19 and introduced a silent mutation within the BsaI site by site directed mutagenesis. The pUC18 derived donor vector was obtained by mutagenesis PCR using primers pUC18 2 fwd (5`GCTGCAATGATACCGCG**T**GACCCACGCTCACCGGCTCC 3`) and pUC18 2 rev (5`GGAGCCGGTGAGCGTGGG**TCA**CGCGGTATCATTGCAGC 3`). Bold marked letters label the point of site directed mutagenesis, where the nucleotide triplet TCT was mutated into TCA, which both are codons for serine. Entire, mutated plasmid were amplified in a thermocycling reaction using Proofreading Phusion High Fidelity DNA Polymerase (New England Biolabs, Frankfurt) and 50 ng plasmid template in an 20 µl reaction. Following thermocycler conditions were applied:

98°C/30 sec	1 cycle
98°C/25 s (denaturation)	} 20 cycles
X°C/25 s (annealing)	
72°C/1 min/1kb (extension)	
72°C/10 min	1 cycle
Cool down to 10°C	∞

The template DNA was eliminated by enzymatic digestion with DpnI (Fermentas, St Leon-Rot), according to the manufacturer's instructions. 3 µl of the PCR-digestion mixture were directly used for heat shock transformation (3.2.3.2)

Golden Gate reaction

GGC restriction-ligation reaction was performed according to the following protocol: 50 ng of each plasmid was added to 10 units of BsaI enzyme (New England Biolabs, Frankfurt) and 15 units of T4 DNA ligase (Promega, Mannheim) together with ligation buffer (Promega, Mannheim) in a total volume of 15 µl. The reaction was incubated in a thermocycler (37°C/5 min and 16°C/5 min, 50 repeats), finally digested (50°C/5 min) and heat inactivated (80°C/5 min). The GGC reaction was directly transformed into chemically competent *Escherichia coli* strain DH5α via heat shock transformation (3.2.3.2). Putative positive clones were selected in a first step via blue-white screening (3.2.3.4) with additional use of kanamycin and spectinomycin as the vectors with a correct construct display on the one hand side kanamycin resistance due to the acceptor vector, on the other hand side spectinomycin resistance due to the inserted aadA cassette. Selected clones were further analyzed by colony PCR (3.2.3.10). Plasmids of clones that had the required insert length in colony PCR analysis were extracted (3.2.3.5) and verified by sequencing (3.2.3.12).

3.2.3.16. Southern blot

Integration and homoplasmy in transplastomic plants were assessed by Southern blot analysis. Southern Blots were carried out with the non-radioactive DIG method (DIG High Prime DNA Labeling and Detection Starter Kit II, Roche, Mannheim) according to the manufactures instructions with slight modifications according to Herrera Diaz [89]. Total DNA was extracted from leaves of putative transplastomic plants from the F0- and the F1 generation. Approximately 2 µg DNA were digested with *Bci*IV (New England Biolabs, Frankfurt) at 37 °C for 1h, separated on a 1% agarose gel containing 0,5 mg/ml EtBr and run with 40 V for a minimum of 5h. Specific DNA sequences were detected by hybridization with an *rps7* DNA probe, which was generated by PCR and DIG-labeled according to the manufactures instructions. 1kb DNA ladder (Fermentas, St Leon-Rot) was used to mark the distance on the gel to enable the determination of detected DNA fragment sizes after development of the southern blot. Therefore after electrophoresis, the gel with the separated DNA fragments was documented with a fluorescent 10 cm ruler that was inserted in the gel holding tray. After documentation, the gel was depurinated by constant, gentle shaking (RT, 15 min) in 100 ml 0,5 M HCL. It was further rinsed with ddH₂O and incubated twice in 100 ml denaturing solution (0,5 M NaOH, 1,5 M NaCl) and constant, gentle shaking (RT, 15 min). Afterwards, the gel was neutralized by washing it twice in neutralization solution (0,5 M Tris, 1,5 M NaCl pH 7,5) and constant, gentle shaking (RT, 15 min) and finally equilibrated for 20 minutes in 20 x SSC transfer buffer (3 M NaCl, 0,3 M Natrium Citrate, pH 7,0). For the transfer of DNA from the gel to the membrane, a DNA Blot Unit was prepared (Figure 4) in the following way: Whatman 3 MM paper was cut to large strips, which were arranged in stacks of eight pieces, soaked in 20 x SSC and arranged to a bridge, which joins two reservoirs of 20 x SSC. The agarose gel was placed on the top of the soaked stacks and falcon tube was rolled over the gel to remove air bubbles. Cling film was applied on the paper bridge, surrounding the gel, to avoid short circuit. Hybond-N⁺ nylon membrane (Amersham, Braunschweig) was cut to the size of the gel and shortly incubated in 20 x SSC. The membrane was transferred on the gel and present air bubbles were removed. On top of the membrane three dry sheet of Whatman 3 MM paper and a stack of paper towels were positioned. Finally, 250 g weight was placed on a plastic support on top of the blot unit.

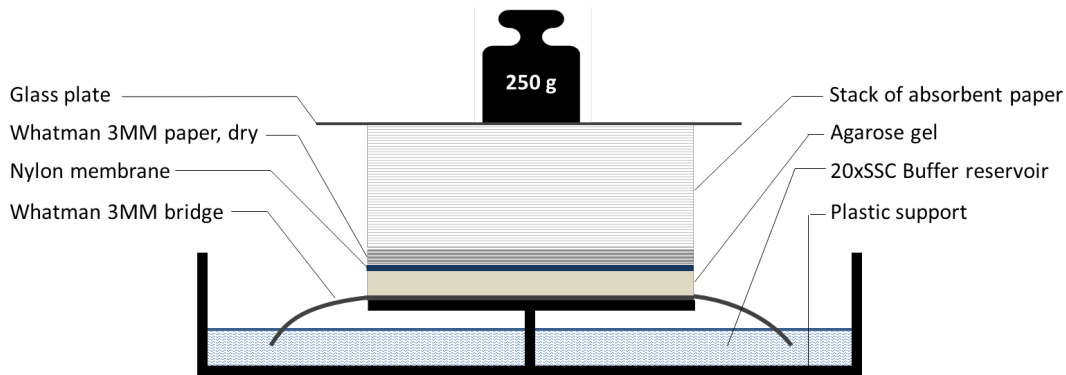


Figure 4: Southern Blot Unit.

After oN transfer (12-18 h) the Hybond-N⁺ nylon membrane was exposed to 1200 microjoules UV light using device UV Stratalinker 1800 (Stratagene, Heidelberg, Germany) for DNA fixation. Pre-hybridization and hybridization were carried out with gentle agitation in a roller bottle at 40 °C for 30 min and oN, respectively. The appropriate hybridization temperature was calculated according to GC content of the probe with the following formula:

$$T_m = 49,82 + (0,41 \cdot P) - (600/L) = 64,712$$

$$T_{opt.} = T_m - 25^\circ\text{C} = 39,712 \approx 40^\circ\text{C}$$

L = 422 = length of hybrid in base pairs.

P = 39,8 = percentage [%] of GC content of the probe.

After hybridization, membranes were washed twice for 5 min at room temperature in ample low stringency buffer (2xSSC, 0.1% SDS) and then twice for 15 min in high stringency buffer (0,5xSSC, 0.1% SDS) at 65°C. After stringency washes, detection was performed after the following workflow (Table 3).

Table 3: Workflow for southern blot detection.

Solution	Volume	Incubation time/ temperature	Repeats
Blocking solution	100 ml	30 min/50°C	1
		↓	
Antibody Anti DIG solution	20 ml	1 h/50°C	1
		↓	
Washing buffer	100 ml	15 min/50°C	2
		↓	
Detection buffer	20 ml	2 – 5 min/RT	1
		↓	
CSPD ready to use	1 ml	15 min/37°C	1
		↓	
X-ray film		~ 20 min/RT	

3.2.4. Protein biochemical methods

3.2.4.1. Extraction of soluble proteins from plant material

Total soluble proteins (TSP) were extracted from leaves by grinding leaf tissue into fine powder with liquid nitrogen. 100 mg of leaf powder were resuspended in CellLytic P Puffer (Sigma-Aldrich, München) with added protease complete inhibitor cocktail (Roche Applied Sciences) according to the manufacturer's instructions and incubated for 10 min on ice followed by centrifugation at 18,000xg for 2x5 min. The supernatant was taken as the TSP fraction.

3.2.4.2. TSP extraction from plant material for Icon genetics approach

Total soluble proteins (TSP) were extracted from infiltrated leaves after approximately 14 days post infiltration. GFP-fluorescent leaf parts were harvested and ground into fine powder with liquid nitrogen. About 1 g of leaf powder was resuspended with 3 ml Ex-His-A Puffer with added EDTA-free protease complete inhibitor cocktail (Roche Applied Sciences) according to the manufacturer's instructions. After centrifugation at 12,000xg for 10 min and 4°C, the supernatant was collected and taken as the TSP fraction.

3.2.4.3. Determination of protein concentration

Determination of protein concentration was done with the Bradford Bio-Rad Protein Assay (Bio-Rad Laboratories GmbH, München, Germany) and carried out as suggested by the manufacturer.

3.2.4.4. Acetone precipitation of proteins

Proteins were precipitated by addition of 4 sample volumes of ice cold acetone p.a. and subsequent incubation for a minimum of 3h at -20 °C. The precipitates were collected by centrifugation (18000xg, 30 min, 4°C) and the supernatant was discarded. The pellet was washed by addition of the same volume of ice cold acetone as in the first step and again centrifuged. After removing the supernatant the protein pellet was air dried at RT and resuspended in an appropriate amount of water or buffer.

3.2.4.5. Polyacrylamide gel electrophoresis of proteins

Separation of proteins on polyacrylamide gels was carried out with a Hoefer SE 250 Mini-Vertical Gel Electrophoresis unit (GE Healthcare, Freiburg, Germany). Proteins were separated according to their molecular weight with 12% or 15% resolving gels and 4% glycine-SDS-polyacrylamide-stacking-gels. Gels were prepared as described by Sambrook and Russell (2001) according to Laemmli (1970). Protein extracts were mixed 1:2 with 2x reducing sample buffer and boiled for 5 min before loading into

the gel pockets. Bacterial cell pellets were dissolved in 20 volumes of culture volume in 2x reducing sample buffer, heated 10 min at 95°C, centrifuged 15 min at 13200 rpm at RT. Supernatant was loaded into the gel pockets. The gels were casted in an 8x7x1 cm Hoefer Mighty Small dual gel caster (GE Healthcare, Freiburg, Germany) according to the manufacturer's handbook. Gels were run at a constant current of 25 mA per gel with an Electrophoresis Power Supply EPS 601 (GE Healthcare, Freiburg, Germany). All gels were run until the bromophenol dye front reached the bottom of the gel.

3.2.4.6. Staining methods

SDS-PAGE gels were stained by incubation and shaking in Coomassie R-250 staining solution for 1h followed by destaining in Coomassie R-250 destaining solution until the background became completely clear.

3.2.4.7. Western blot analysis

Separated proteins in an SDS gel were transferred to Hybond-LFP PVDF membranes with 0.2 µm pore size (GE Healthcare, Freiburg, Germany) by Hoefer SemiPhor semi-dry transfer unit (GE Healthcare, Freiburg, Germany). The membrane was activated by methanol further to transfer. A blotting unit consisted from 3 sheets of Whatman 3 MM paper, the activated membrane, the polyacrylamide gel and again 3 sheets of Whatman 3 MM paper. The blot unit was paper was soaked with transfer buffer. 1,5 mA current per cm² of membrane area were applied for 1h. After transfer, the membrane was stained for 15 min with Ponceau-S, documented and destained by three washing steps of 10 min in water. Afterwards, the membrane was first blocked in freshly prepared blocking buffer (1xTBS buffer, 0.1% Tween-20, 1% milk powder) for 2h at room temperature with gentle shaking and subsequently incubated with the primary antibody in the required dilution in TBST buffer oN at 4°C and gentle shaking. Unbound primary antibodies were removed by washing 3 times with TBST buffer (10 min, RT, gentle shaking), the suitable secondary antibody conjugated with HRP or AP was added in the required dilution in TBST and then incubated for 2 h at room temperature. Subsequently, the membrane was washed twice in TBST and once in TBS buffer. Colorimetric detection of marked proteins was performed by incubating the membrane in 10 ml AP-buffer supplemented with 66 µl NBT solution and 33 µl BCIP solution. In case of HPO-labeling of the secondary antibody, proteins were detected by the substrate Super Signal West Pico Luminol/ Enhancer and Super Signal West Pico Stable Peroxide Solutions (Thermo Scientific) on an X-ray film.

4. Results

The results of this work are divided into the characterization of immunomodulatory properties of synthetic, HIV-active peptides and the transplastomic production approach for the same peptides in *N. tabacum* chloroplasts.

The antiviral response of the human innate immune system consists of enhanced production of cytokines, which orchestrate important responses for virus elimination and thereby produce the typical clinical symptoms of a viral infection [93]. Therefore the potential immunomodulatory properties of the designed peptides regarding cytokine release were studied to determine possible interferences with the human immune response. Furthermore, DNA coding sequences of the designed peptides were derived from their amino acid sequences following codon usage of tobacco chloroplasts. The coding sequences were combined with green fluorescent protein (GFP) coding sequence as N-terminal fusion partner and inserted into *Nicotiana tabacum* (*N. tabacum*) chloroplasts by particle gun. Transplastomic tissue was selected, propagated and rooted and the resulting plants were characterized.

4.1. Cell-toxic effects of designed peptides

Determination of cell viability is critical when evaluating the response to potentially cytotoxic drugs like antimicrobial peptides (AMPs). In this work, peripheral blood mononuclear cells (PBMCs) and monocyte-derived dendritic cells (MoDCs) from healthy and allergenic donors (Appendix, Table 8) were isolated from peripheral blood by density gradient centrifugation and treated with different concentrations of synthetic designed peptides (Appendix, Table 9). Quantitative measurement of cell apoptosis was performed using dye exclusion with the fluorochrome propidium iodide (PI). PI acts as DNA intercalator, which is excluded by healthy cells but can penetrate permeable membranes of non-viable cells. Because PI binds stoichiometrically to DNA, PI-derived signals from a flow cytometer (FACS) are proportional to the DNA content of the measured cell. Apoptotic cells are characterized by DNA fragmentation, which results into loss of nuclear DNA content. Thus, sub-diploid cells are defined as apoptotic and can be distinguished by their broad hypodiploid peak from healthy cells [94].

4.1.1. Effects on viability of peripheral blood mononuclear cells

PBMCs are a heterogeneous cell population consisting mainly from monocytes and lymphocytes [95]. Toxic effects of designed peptides on PBMCs were investigated after 67h incubation time and in defined dilution series (Appendix, Table 9) by PI-staining and flow cytometry. Four biological replicates with two to four technical replicates each were analyzed. Water-treated cells served as negative controls (Figure 5).

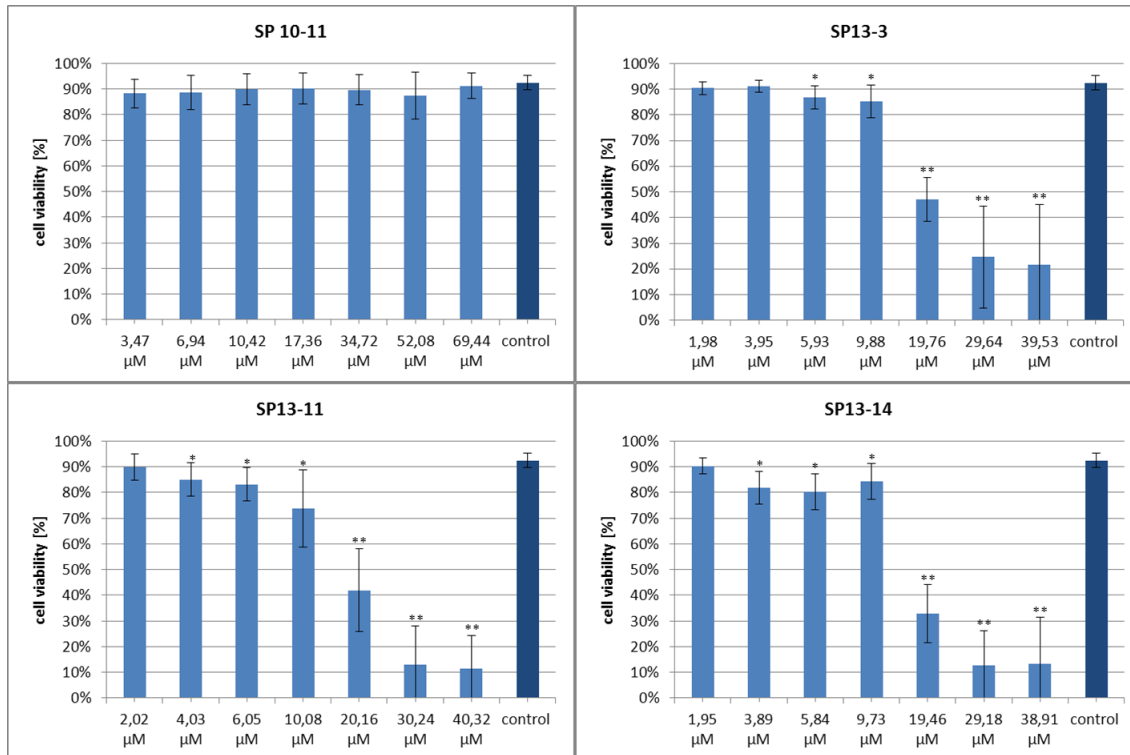


Figure 5: Different effects of SP10-11 peptide and SP13 peptides on PBMC cell viability. PBMCs were incubated with defined dilution series of the designed peptides for 67h in proliferation medium. Quantity of apoptotic cells was determined by PI staining and flow cytometry. Control values consist of measurements from water-treated PBMC in proliferation medium. The values shown here correspond to four biological replicates with two to four technical replicates each. Significance was always calculated by T-test against control values (*: $p < 0,1$; **: $p < 0,01$).

Cell-toxic effects differ clearly between the structural groups of designed peptides. For SP10-11, peptide concentrations of 2,02 μM, 4,03 μM, 6,05 μM, 10,08 μM, 20,16 μM, 30,24 μM and 40,32 μM have been applied, of which none shows toxic effects towards PBMCs (Figure 5). When PBMCs were incubated with peptides from the SP13 group (SP13-3, SP13-11, SP13-14), significant decrease in cell viability was observed at high peptide concentrations. These toxic effects were proportional to the applied concentration (Figure 5). For each SP13 type peptide, there was a clear and reproducible concentration level that delimits the toxicity of more than 50% cell apoptosis. This level was for all three SP13 peptides at a concentration of 50 μg/ml, which corresponds to 19,76 μM for SP13-3, 20,16 μM for SP13-11 and 19,46 μM for SP13-14, respectively. However, SP13-3 induces significant toxic effects on PBMCs from a concentration of 5,39 μM, whereas SP13-11 already decreases cell viability of PBMCs significantly at 4,03 μM as well as SP13-14 at 3,89 μM. Thus, SP13-14 and SP13-11 induce higher adverse effects on PBMCs than SP13-3.

4.1.2. Time-dependent effects on peripheral blood mononuclear cells

To determine how toxic effects on PBMCs change during incubation time, cell viability was determined after different incubation times (1,5h, 18h and 26h) by PI staining and FACS with three biological replicates and two to four technical replicates each (Figure 6). Water-treated cells served as negative control. Incubation periods longer than 67h were not observed because the limited volume of proliferation medium in 96-well plates would result in cell apoptosis independent from peptide treatment for longer time periods.

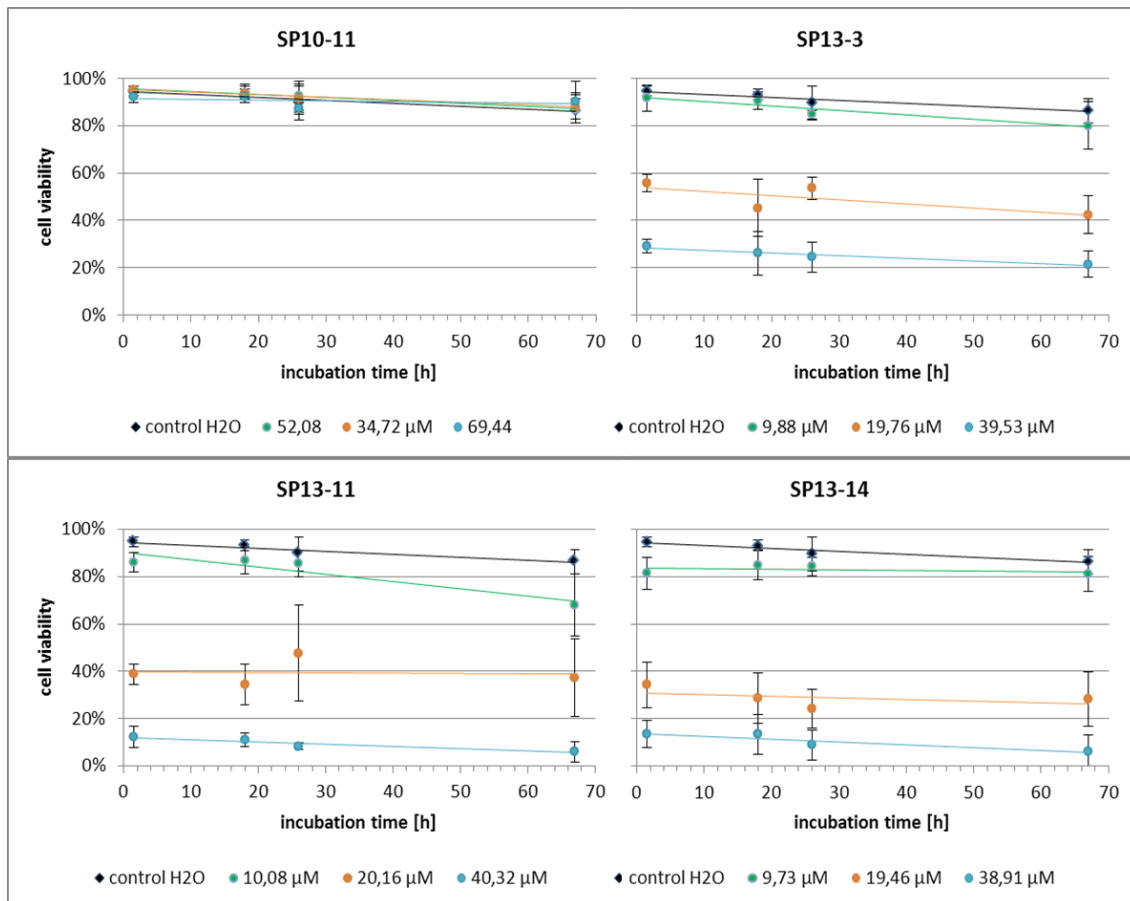


Figure 6: Cell-toxic effect on PBMCs does not alter over time for all designed peptides. Effects on PBMCs were evaluated with four measurement time points (1,5h, 18h, 26h, 67h). Quantity of cell viability was determined by PI staining and flow cytometry. The controls consist of water-treated PBMCs in proliferation medium. The values shown here correspond to three biological replicates with two technical replicates each.

The concentrations of the SP13-derived peptides shown in Figure 6 ranged from 9,88 µM to 39,53 µM (SP13-3), 10,08 µM to 40,32 µM (SP13-11) and from 9,73 µM to 38,91 µM (SP13-14). These concentrations represent the concentration levels delimiting significant toxic effects with more than 50% cell apoptosis, respectively. In case of the non-toxic SP10-11 the three highest applied peptide concentrations are

shown. Data for all other peptide concentrations can be found in the appendix (Appendix, Figure 35). All measurements, including those of control cultures, show a slow decrease in cell viability over incubation time, as expected. Still, for all tested peptide concentrations no deviating, time-dependent change in cell viability was detectable (Figure 6). Therefore we conclude that the length of incubation time seems to play a minor role regarding toxicity of the designed peptides.

4.1.3. Effects viability of on monocyte-derived dendritic cells

CD14⁺ monocytes were purified from isolated PBMCs by magnetic cell sorting with bead-coupled antibodies against the surface molecule CD14. After an incubation time of five days in HU-DC medium with rhIL4 and rhGM-CSF additives, the emerged MoDCs were harvested and stimulated with different peptide concentrations (Appendix, Table 9) in HU-DC medium. Peptide-induced effects on MoDCs were investigated after 24h incubation time and on PBMCs after 26h incubation time. For both PBMCs and MoDCs three biological replicates with two to four technical replicates each were investigated. Water-treated MoDCs, respectively PBMCs, served as negative controls (Figure 7).

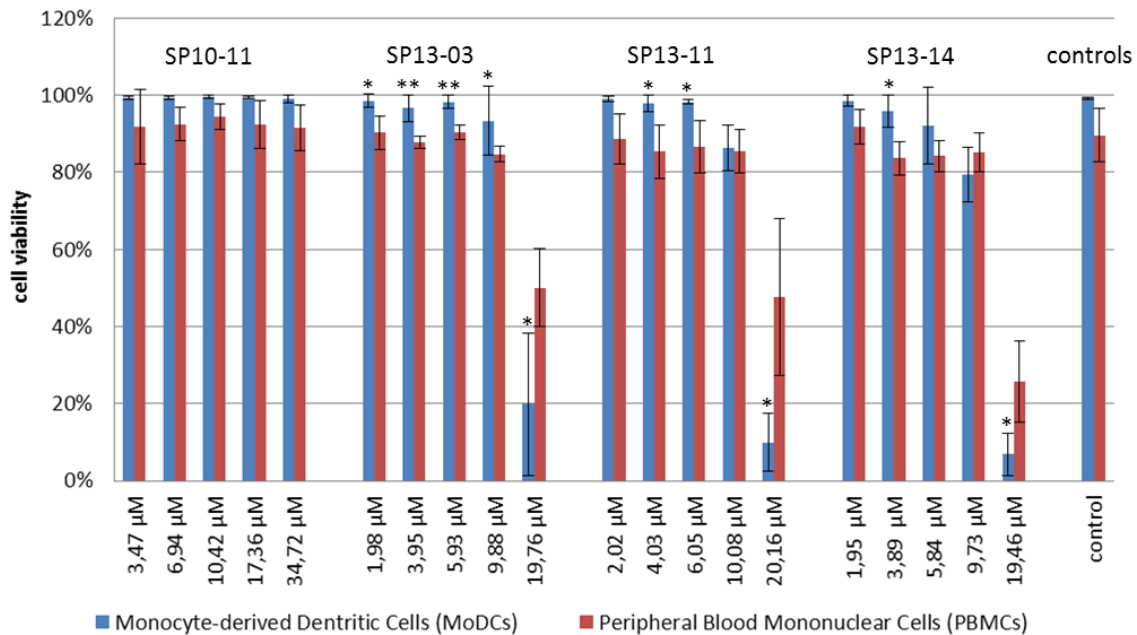


Figure 7: Effects of SP13-derived peptides on viability of MoDCs are significantly higher compared to toxic effects on PBMCs in a peptide-concentration dependent manner, whereas SP10-11 has no adverse effect on both PBMCs and MoDCs. Data shown here consist of three biological replicates with two to four technical replicates, respectively. PBMCs were incubated 26h in proliferation medium with different peptide concentrations, MoDCs were incubated 24h in HU-DC medium with different peptide concentrations. Significance regarding MoDCs was always calculated by T-test against the corresponding incubation conditions of PBMCs (p: * < 0,1, ** < 0,01).

MoDC viability was significantly higher at lower peptide concentrations in case of SP13-3 (1,98 μM – 9,88 μM), SP13-11 (4,03 μM and 6,05 μM) and SP13-14 (3,89 μM). This may be due to better proliferation conditions of MoDCs in HU-DC medium compared to PBMCs in proliferation medium because the controls show the same difference in cell viability. SP10-11 shows no toxic effects in all applied concentrations for both PBMCs and MoDCs. In case of SP13 peptides, MoDCs are more sensitive to the peptide-induced, cell-toxic effect than PBMCs. For SP13-3, the 19,76 μM concentration shows significantly lower cell viability from MoDCs compared to PBMCs. Also 10,08 μM SP13-11 showed the same cell viability of MoDCs and PBMCs, although in all lower SP13-11 concentrations the cell viability of MoDCs is significantly higher compared to PBMCs. This indicates an intensified cell toxic effect of SP13-11 on MoDCs. This observation is supported by the MoDC viability when incubated with 20,16 μM SP13-11. Here, the number of living MoDCs is significantly lower compared to PBMCs. SP13-14 displays for both PBMCs and MoDCs the lowest overall cell viability levels. Also with SP13-14 concentration of 19,46 μM , MoDCs show significantly more cell apoptosis than PBMCs.

Altogether, PI measurements show that peptides from the series SP10 and series SP13 exhibit different effects to humans PBMCs and MoDCs. While SP10-11 shows no toxic effects on both cell types, SP13-3, SP13-11 and SP13-14 induce significant cell-toxic effects on both cell types, which are for all SP 13 peptides concentration-dependent. Concentrations, which induce more than 50% cell apoptosis are similar between the three SP13-derived peptides, but generally show SP13-14 and SP13-11 more cell-toxic impact than SP13-3. Furthermore, measurements indicate that MoDCs are more susceptible for the toxic effect of the SP13 peptides than PBMCs, but in the same, concentration-dependent manner. However, the half maximal inhibitory concentrations (IC_{50}) of the designed peptides, which are necessary to inhibit HIV infection *in vitro*, are in the lower range of the applied concentrations (SP13-03 $\text{IC}_{50} = 3,51 \pm 0,454 \mu\text{M}$), SP13-11 ($\text{IC}_{50} = 3,67 \pm 0,12 \mu\text{M}$) and SP13-14 ($\text{IC}_{50} = 1,44 \pm 0,144 \mu\text{M}$). Thus we can conclude, that the antiviral active concentrations of all tested peptides show no or only low toxic effects towards PBMC or MoDCs.

4.2. Immunomodulatory properties

Supernatants of stimulated PBMC and MoDCs were investigated for secretion of cytokines type II interferon (IFN- γ), Interleukin 6 (IL-6), Interleukin 10 (IL-10), Interleukin 1 β (IL-1 β) and Interleukin 12 (IL-12) by ELISA analysis. Because cell-toxic effects of SP13 peptides on MoDCs are fatal even at 50 $\mu\text{g}/\text{ml}$ (Figure 7), only concentrations equal to and less than 50 $\mu\text{g}/\text{ml}$ were analyzed. However, the concentration of 50 $\mu\text{g}/\text{ml}$ of the SP13 peptides turned out to result in cytokine

measurements, that differ greatly thus also this concentration is not shown in ELISA analysis. In case of the non-toxic SP10-11, all concentrations were applied for ELISA analysis (Appendix, Table 10). The cell viability of all cultures was measured by PI-staining in a flow cytometer directly after the supernatants were taken for ELISA analysis. The resulting cytokine release was calculated according to the measured cell viability. All ELISA assays were repeated with at least two biological replicates and two to four technical replicates each. The complete data sets of all single ELISA assays that were performed in this work are listed in the appendix (Appendix, Figure 36 - Figure 43).

4.2.1. Stimulation and suppression of cytokines

The designed peptides were tested for stimulating or suppressing specific cytokines in PBMCs and MoDCs. Therefore, cells were incubated on the one hand with different peptide dilutions and on the other hand simultaneously with peptides and stimuli for anti-inflammatory and pro-inflammatory cytokine production (Figure 8).

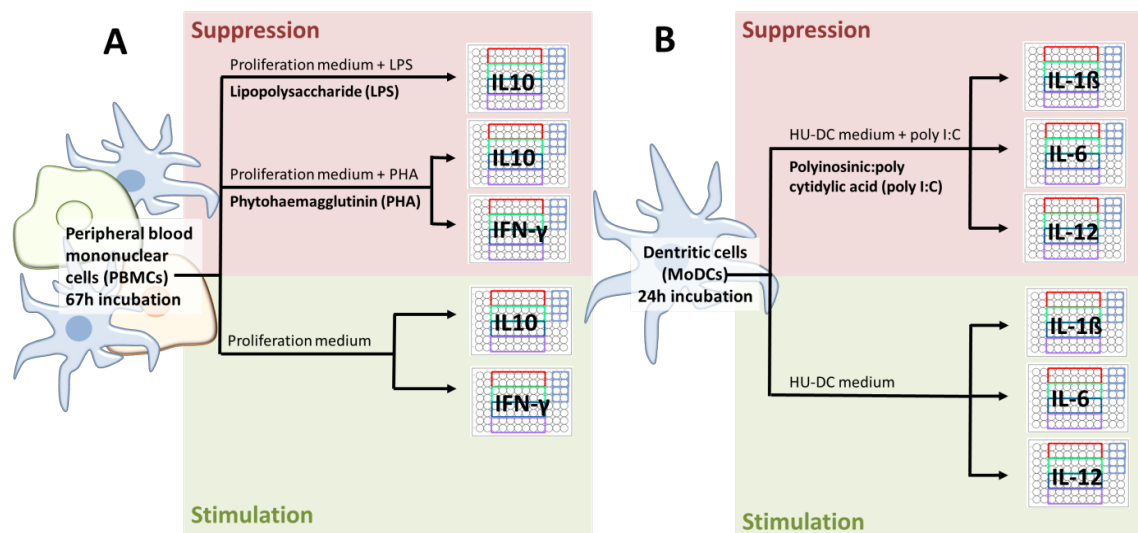


Figure 8: Schematic overview of all different ELISA assays that were performed in this work. Supernatants of cell cultures with or without three different stimuli were analyzed. (A) Peripheral blood mononuclear cells (PBMCs) were incubated with different concentrations of the peptides and with or without stimuli in proliferation medium for 67h. IL-10 ELISA was performed on PBMC supernatants of cultures with and without the addition of LPS, respectively. IFN- γ and IL-10 ELISAs were performed on PBMC supernatants of cultures with or without the addition of PHA. (B) Monocyte-derived dendritic cells (MoDCs) were incubated with different concentrations of the peptides and/or Poly I:C stimulus in HU-DC medium for 24h and analyzed by IL-12, IL-1 β and IL-6 ELISA.

The following stimuli were used: Phytohemagglutinin (PHA) is a mitogen to trigger the activation of T-lymphocytes, which is followed by IFN- γ production. PHA was used for PBMC cell cultures in a concentration of 10 $\mu\text{g/ml}$. Lipopolysaccharide (LPS) is a bacterial endotoxin that binds to the CD14/TLR4 receptor complex, which is followed by the production of pro-inflammatory cytokines in many cell types,

including macrophages and antigen presenting cells. LPS was used for PBMC cell culture at a concentration of 0,1 µg/ml. Finally, MoDCs were stimulated by Polyinosinic:polycytidylic acid (Poly I:C). Poly I:C is a synthetic, double-stranded RNA, which is used in the form of its sodium salt to simulate viral infections *in vivo*. Poly I:C was used for MoDC cell culture at a concentration of 10 µg/ml.

4.2.2. Phytohemagglutinin stimulation of peripheral blood mononuclear cells

First, we were interested, if our designed peptides are able to shift the cytokine profile into the pro-inflammatory or into the anti-inflammatory direction in T-helper cells. To evaluate this question, human PBMCs were stimulated by PHA and analyzed via ELISA for the secretion of IFN-γ and IL-10. Stimulation with PHA triggers response from T_h cells, also known as T-helper cells. Therefore, if IFN-γ is enhanced and simultaneously IL-10 is suppressed by addition of our peptides, the cytokine profile is changed in pro-inflammatory direction and the peptides stimulate Th₁ cells. In contrast, if IL-10 is enhanced and IFN-γ suppressed, peptides have an anti-inflammatory effect and trigger T_{reg} cells.

4.2.2.1. Interleukin 10 response

PBMCs were stimulated by different peptide concentrations and/or 10 µg/ml PHA. After 67h incubation, supernatants were analyzed by IL-10 ELISA (BD Bioscience). All designed peptides trigger a slight but significant IL-10 response in PBMCs when compared to the medium control (Figure 9, left side). These values were determined by two biological replicates and eight technical replicates each, because the stimulated production rates were comparatively low. When PBMCs were incubated with SP10-11 and PHA, significant higher release of IL-10 was measured for the three highest applied SP10-11 concentrations (34,72 µM, 52,08 µM, 69,44 µM). Peptides of the SP13 series did not trigger significantly enhanced IL-10 production. However, in both biological replicates a concentration-dependent increase can be observed (Appendix, Figure 38, Figure 39).

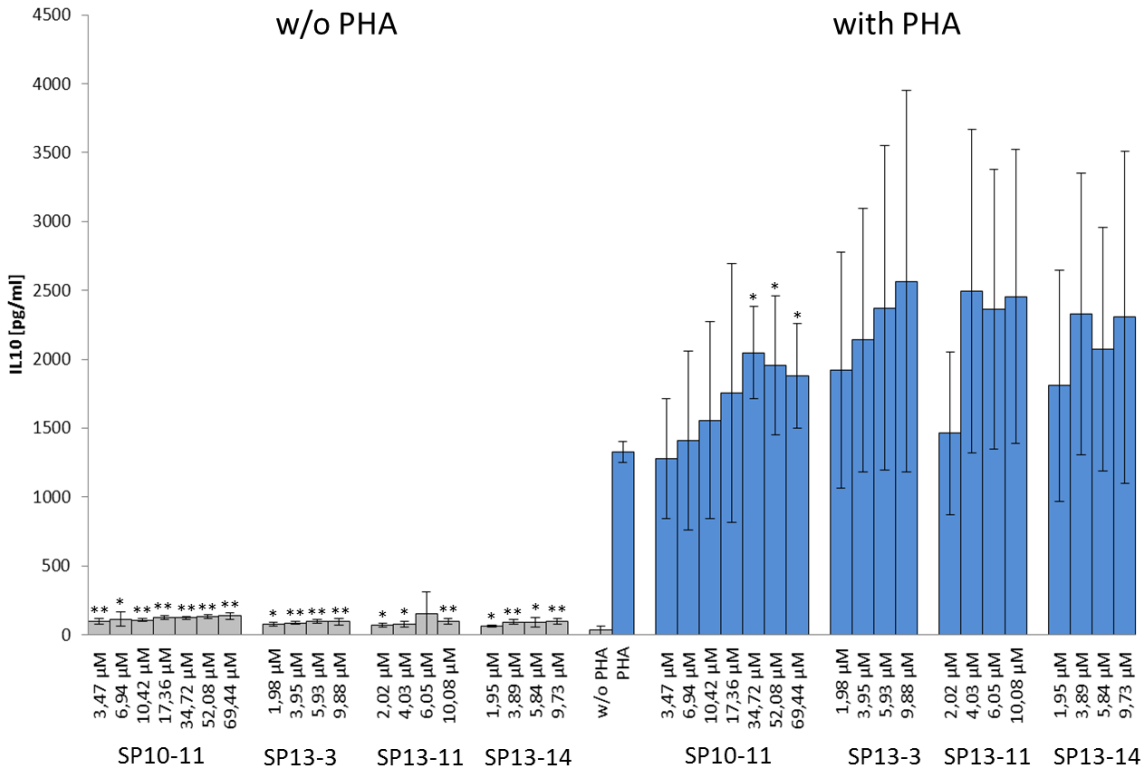


Figure 9: All designed peptides significantly enhance IL-10 release in human PBMCs (left side). PHA in combination with SP10-11 significantly enhances IL-10 secretion in a concentration-dependent manner, whereas the presence of the SP13 peptides in combination of PHA did not show a significant change regarding IL-10 release (right side). Human PBMCs were stimulated with different concentration of peptides in the presence or in the absence of PHA. IL-10 secretion [pg/ml] was analyzed by ELISA after 67h incubation time. Two biological replicates with two to four technical replicates each were measured for simultaneous PHA stimulation and eight technical replicates each were measured for peptide stimulation. Significance was calculated by T-test against the corresponding medium control, respectively (*: $p < 0,1$; **: $p < 0,01$).

4.2.2.2. Type II interferon response

Supernatants of PBMC cultures that were co-incubated with PHA were also investigated for secretion of IFN- γ by ELISA assay (R&D Systems). IFN- γ is a cytokine that is critical for innate and adaptive immunity against viral and intracellular bacterial infections and for tumor control. The importance of IFN- γ in the immune system is partly based on its ability to inhibit viral replication directly [96].

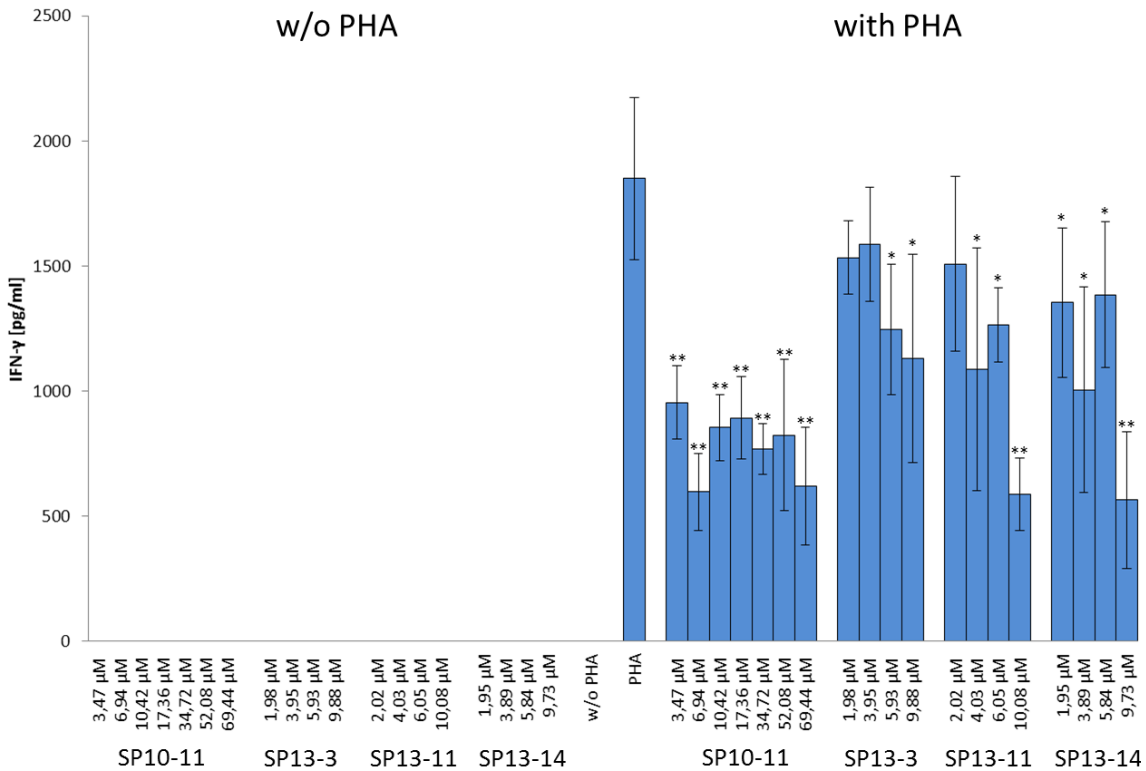


Figure 10: Designed peptides suppress IFN- γ production in human PBMCs when co-incubated with PHA. The strongest suppression was observed with SP10-11 in all concentrations. Also the presence of the SP13 peptides suppresses IFN- γ in a concentration-dependent manner. Human PBMCs were stimulated with different concentration of HIV active peptides in the presence (right side) or in the absence (left side) of PHA. IFN- γ secretion [pg/ml] was analyzed by ELISA after 67h incubation time. Two biological replicates with two to four technical replicates each were measured. Significance was calculated by T-test against the corresponding medium control, respectively (*: $p < 0,1$; **: $p < 0,01$).

IFN- γ ELISA results indicate that all designed antimicrobial peptides have no stimulating effects on the IFN- γ secretion of PBMCs (Figure 10, left side). However, if PBMCs were simultaneously stimulated with PHA and different peptide concentrations, suppressive effects are detectable (Figure 10, right side). In two biological replicates, SP10-11 shows in all concentrations significant suppression of IFN- γ secretion. SP13-3, SP13-11 and SP13-14 show suppressed IFN- γ levels, which increase with higher peptide concentrations. SP13-3 shows lower suppressing effects compared to SP13-11 or SP13-14. SP13-14 shows significant suppression with all applied concentrations. However, suppressive effects of the lower SP13 peptide concentrations are less pronounced compared to the effects of SP10-11.

4.2.3. Lipopolysaccharide stimulation of peripheral blood mononuclear cells

To determine cytokine changes that are induced by our peptides for antigen-presenting cells (APC), PBMCs were also treated with 0,1 $\mu\text{g/ml}$ LPS and investigated for pro- and anti-inflammatory cytokine profiles.

4.2.3.1. Interleukin 10 response

Supernatants of peptide-stimulated PBMCs with or without LPS additives were analyzed by IL-10 ELISA assay (BD Bioscience).

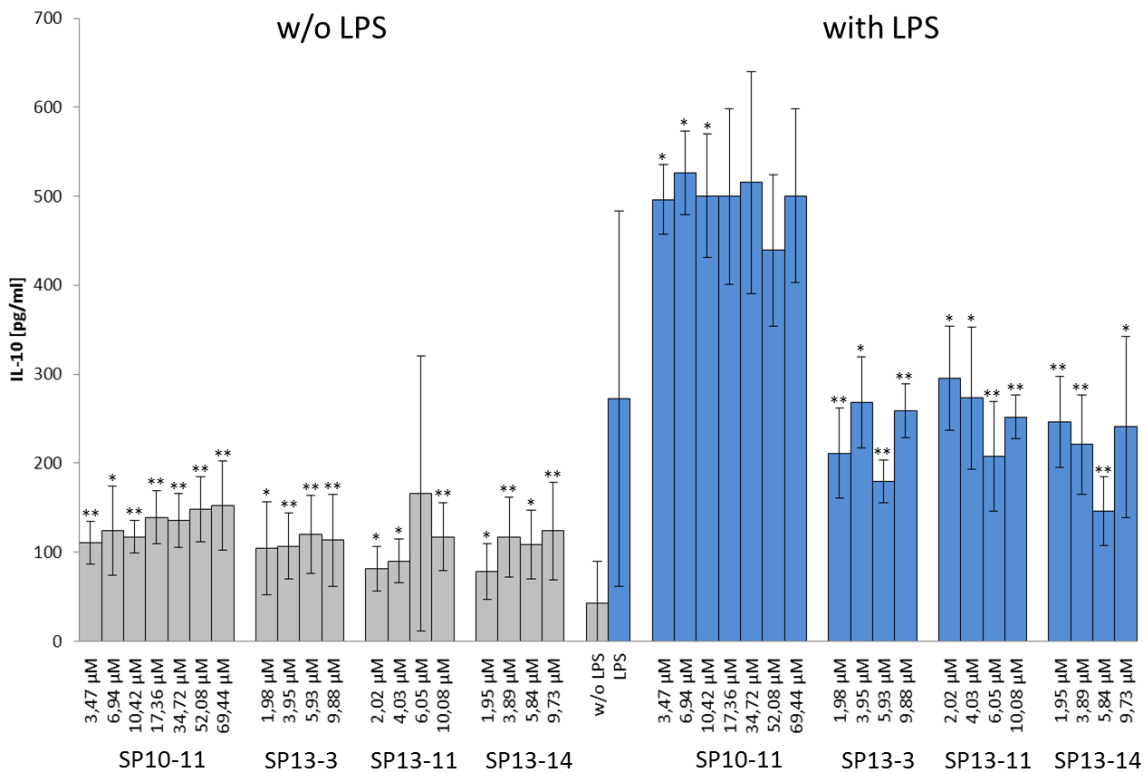


Figure 11: Human PBMCs were stimulated with different concentration of peptides in the presence (right side) or in the absence (left side) of LPS. All tested peptides slightly but significantly enhance IL-10 release in human PBMCs. LPS in combination with SP10-11 significantly enhances IL-10 production in concentrations of 3,47 µM, 6,94 µM and 10,42 µM in PBMCs. LPS in presence of the SP13 peptides suppresses IL-10 secretion significantly in all applied concentrations. IL-10 secretion [pg/ml] was analyzed by ELISA after 67h incubation time. Two biological replicates with two to four technical replicates each were measured. Significance was calculated by T-test against the corresponding medium control, respectively (*: $p < 0,1$; **: $p < 0,01$).

When PBMCs were treated with different peptide concentrations alone, all peptides induced comparable low amounts of IL-10 like described in 4.2.2.1. When PBMCs were stimulated with peptides and LPS together, SP10-11 enhances significantly the LPS-induced IL-10 production at concentrations of 3,47 µM, 6,94 µM and 10,42 µM compared to LPS control. Also the other SP10-11 concentrations showed a trend to enhanced IL-10 production. In contrast to SP10-11 all three SP13 type peptides clearly suppress the LPS-induced IL-10 release in all applied concentrations, which is also clearly shown in both biological replicates (Appendix, Figure 40, Figure 41).

Also IL-12 ELISA (eBioscience) was performed with PBMC and MoDC supernatants after stimulation with peptides and/or LPS. We observed that overall IL-12 cytokine production in PBMCs was too low to result in reliable data. Because both PBMCs and

MoDCs produce IL-12, MoDCs alone were stimulated with LPS. Here, IL-12 was detectable in sufficient amounts, but data varied heavily even within one biological replicate, so that analysis was not possible. However, stimulation of MoDCs with Poly I:C resulted in a sufficient and reproducible IL-12 response as described in 4.2.4.2.

4.2.4. Polyinosinic:polycytidylic acid stimulation of monocyte-derived dendritic cells

Poly I:C is used to simulate viral infections in cell cultures and consists of synthetic double-stranded RNA. As our designed peptides act antiviral, their possible effects on the endogenous, antiviral immune response were thus determined.

4.2.4.1. Interaction of Polyinosinic:polycytidylic acid and designed peptides

Poly I:C is negatively charged in cell culture medium due to its RNA nature, whereas our peptides display an overall positive charge (Table 1). Therefore both molecules may directly react by ionic interactions. Because cell viability of MoDCs was very well reproducible when exposed to different peptide concentrations, the cell viability rates of Poly I:C-treated and control MoDCs were compared by PI staining and flow cytometry (Figure 12). Data show that Poly I:C displays an adverse effect on MoDCs, even in absence of peptides (Figure 12, A). MoDCs incubated in HU-DC medium show significantly higher cell viability than cells that were incubated with Poly I:C additives. The same results are observed for all applied concentrations of SP10-11. In the presence of SP13 peptides, MoDC viability shows significant differences: In case of SP13-3, only with the two lower peptide concentrations of 1,98 μM and 6,94 μM , significantly higher cell viability was measured for MoDCs incubated without Poly I:C and all other concentration show the same or even lower cell viability compared to Poly I:C treated MoDCs. In case of SP13-11, the three lowest concentrations (2,02 μM , 4,03 μM , 6,05 μM) display higher numbers of living MoDCs in medium without Poly I:C. But SP13-11 concentrations of 19,76 μM induces already significantly lower cell viability of medium-incubated MoDCs compared to Poly I:C treated cells. Furthermore, for the two highest SP13-11 concentrations (10,08 μM , 20,16 μM) this pattern is even more pronounced. For the highly toxic SP13-14, only in the lowest applied concentration (1,95 μM) results in a higher viability of the medium-incubated cells compared to the Poly I:C-treated ones. With the following SP13-14 concentrations (3,89 μM , 5,84 μM) no significant differences between living cell number of water-treated and treated MoDCs were detected. In the two highest SP13-14 concentrations (9,73 μM , 19,46 μM), the MoDCs incubated with Poly I:C showed significantly higher viability values (Figure 12, A).

When the cell viability of all peptide-treated and in the presence of Poly I:C incubated MoDCs were compared to the Poly I:C treated control cells significance

regarding toxic effects changes (Figure 12, B). With this data set, a clear decrease in toxicity for Poly I:C treated MoDCs in the presence of SP13 peptides was determined.

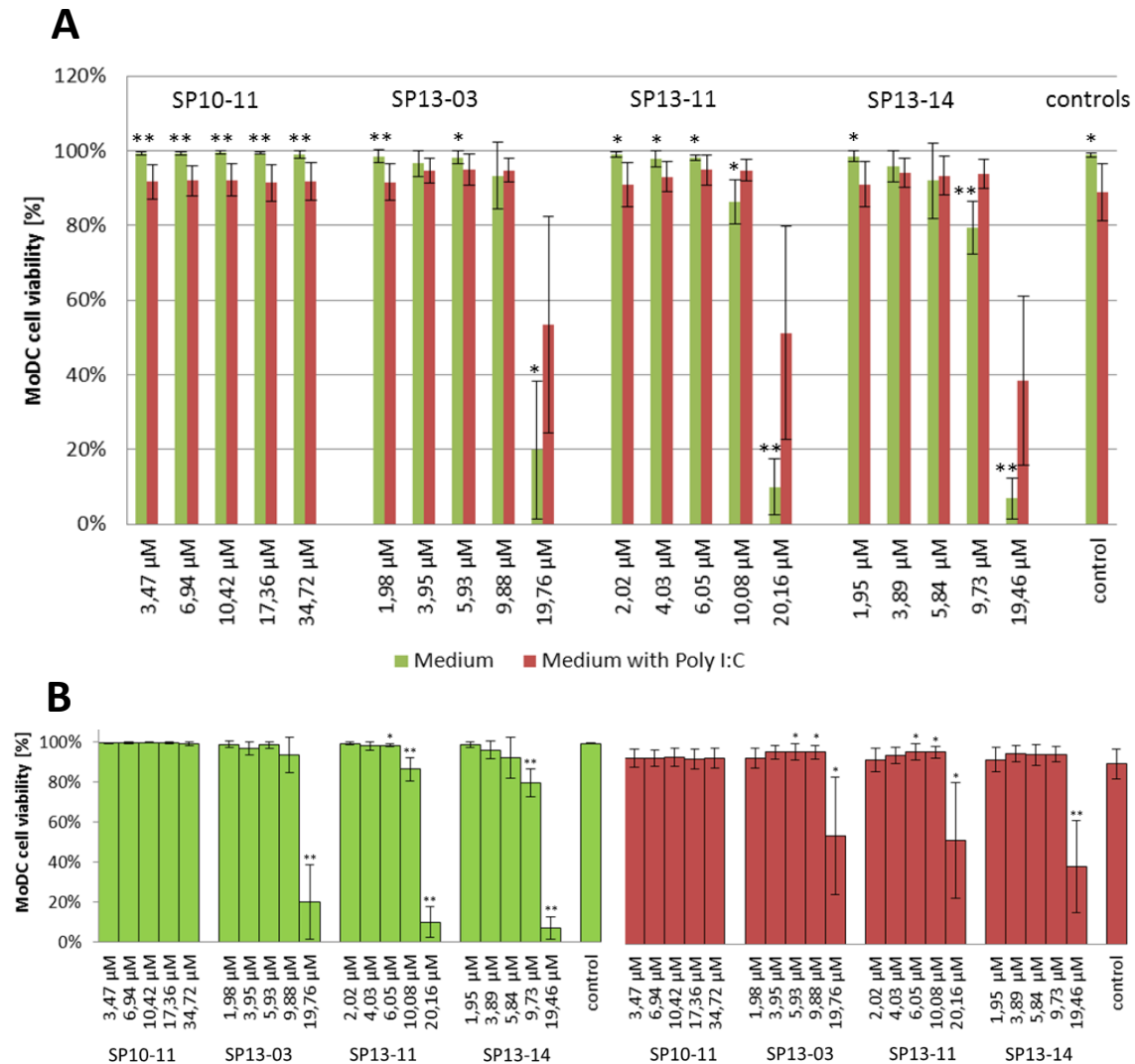


Figure 12: Toxic effects of designed peptides on MoDCs differ significantly depending on the presence of Poly I:C were incubated 24h in HU-DC medium in the presence of different peptide concentrations. (A) MoDC viability measurements were compared between Poly-I:C treated (red bars) and untreated cell cultures (blue bars) after 24h incubation time. Values differ significantly for the major part of all measured peptide concentrations. Also the control values of water-treated MoDCs show a significant difference. (B) Toxic effects of SP13 peptides on MoDCs in the presence of Poly I:C are less pronounced compared with effects on medium without Poly I:C. Cell viability was measured by PI-staining and flow cytometry. Data shown here consist of four biological replicates with two to four technical replicates each. Significance was always calculated by T-test against (A) the corresponding incubation conditions without Poly I:C additives or (B) the control values (p: * < 0,1, ** < 0,01).

When Poly I:C is present, no toxic effects are determined for SP10-11 as expected. In contrast, the concentration of 50 µg/ml for all peptides of the SP13 series results in significant difference in MoDC viability: For SP13-3 and incubation with Poly I:C cell viability of $53,50 \pm 28,93\%$ was determined, whereas without Poly I:C only

19,87 ± 18,47% MoDCs survived. In case of SP13-11, the corresponding values were 51,19 ± 28,50% (with Poly I:C) as well as 9,92 ± 7,51% (w/o Poly I:C) and for SP13-14 38,42 ± 22,68% (with Poly I:C), respectively 6,88 ± 5,50% (w/o Poly I:C) (Figure 12, B). This change in significant cell-toxic effects again underline the possible interaction of Poly I:C and peptides, but also support the previous finding from PBMC experiments, that SP13-14 and SP13-11 induce higher adverse effects than SP13-3 (Figure 5, Figure 7).

To sum up, these results indicate that in the presence of Poly I:C, SP13-derived peptides display lower impact on cell viability. This influence is dependent on the concentration of SP13 peptides. This observation is likely due to interactions of peptides with Poly I:C. Because SP10-11 has no adverse effects on cells, no reliable statements can be made in this case. For all following ELISA results it has to be considered, that the concentrations of the peptides and of Poly I:C are diminished due to inactivation by interaction. However, all ELISA analyses without Poly I:C present in the medium are completely reliable.

4.2.4.2. Interleukin 12 response

MoDCs were stimulated with different peptide concentrations and/or Poly I:C in a concentration of 10 µg/ml. After 24h incubation, supernatants of DC cultures were analyzed by IL-12 ELISA (BD Bioscience). IL-12 release often varies strongly between different blood samples, which is due to the physical condition, the current health condition and also the genetic disposition of each specific donor. Thus, ELISA results of biological replicates regarding IL-12 production in MoDCs are shown individually (Figure 13). If MoDCs were stimulated with peptides alone, no IL12 release was measured in all analyzed samples. Data of MoDCs stimulated simultaneously with Poly I:C and different peptide concentrations show that under these conditions SP13-3 significantly inhibits cytokine release in all analyzed cell cultures. Also in case of SP13-11 and SP13-14, inhibitory effects on IL-12 production were observed, which diminish proportional with decreasing peptide concentrations (Figure 13).

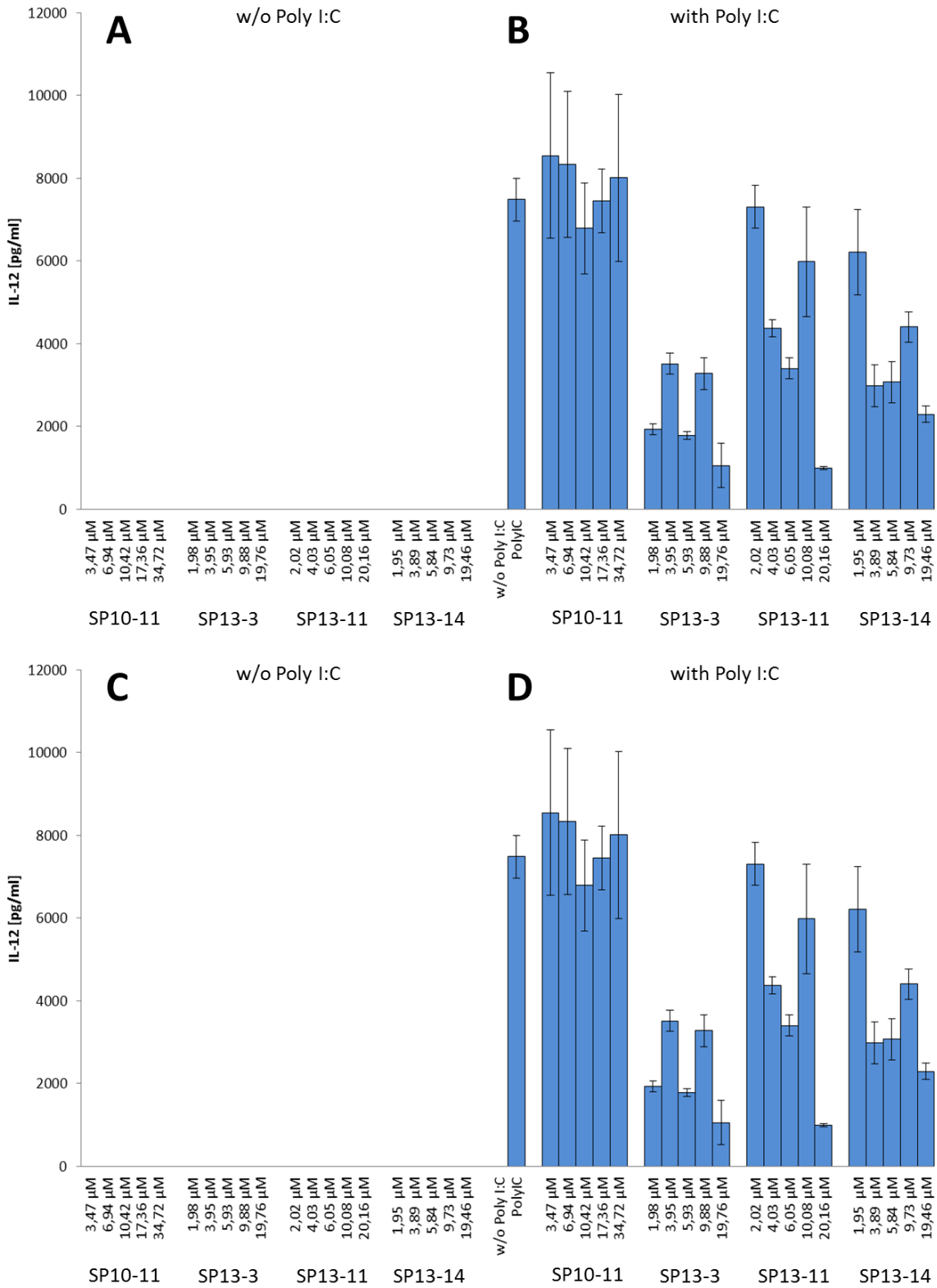


Figure 13: Poly I:C in combination with peptides of the SP13 series reduces IL-12 production in human MoDCs, while the extend of reduction depends on the SP13 peptide type. The presence of SP10-11 does not influence IL-12 levels and stimulation with peptides does not trigger IL-12 production. Two

biological replicates were divided into two graphs (A/B and C/D, respectively), because the donor-dependent variations in IL-12 release varies highly between the first (B, maximal IL-12 production is 3000 pg/ml) and the second biological replicate (D, maximal IL-12 production is 12000 pg/ml). MoDCs were stimulated with different concentration of HIV active peptides in the presence (A/C) or in the absence (B/D) of Poly I:C. IL-12 production [pg/ml] was analyzed by ELISA after 24h incubation time. For each donor, two to four technical replicates each were measured. Significance was calculated by T-test against the corresponding medium control, respectively (*: $p < 0,1$; **: $p < 0,01$).

4.2.4.3. Interleukin 6 response

IL-6 release was analyzed for the supernatants of MoDCs by ELISA assay (eBioscience). MoDCs were incubated with different peptide concentrations (Table 10) with or without addition of Poly I:C.

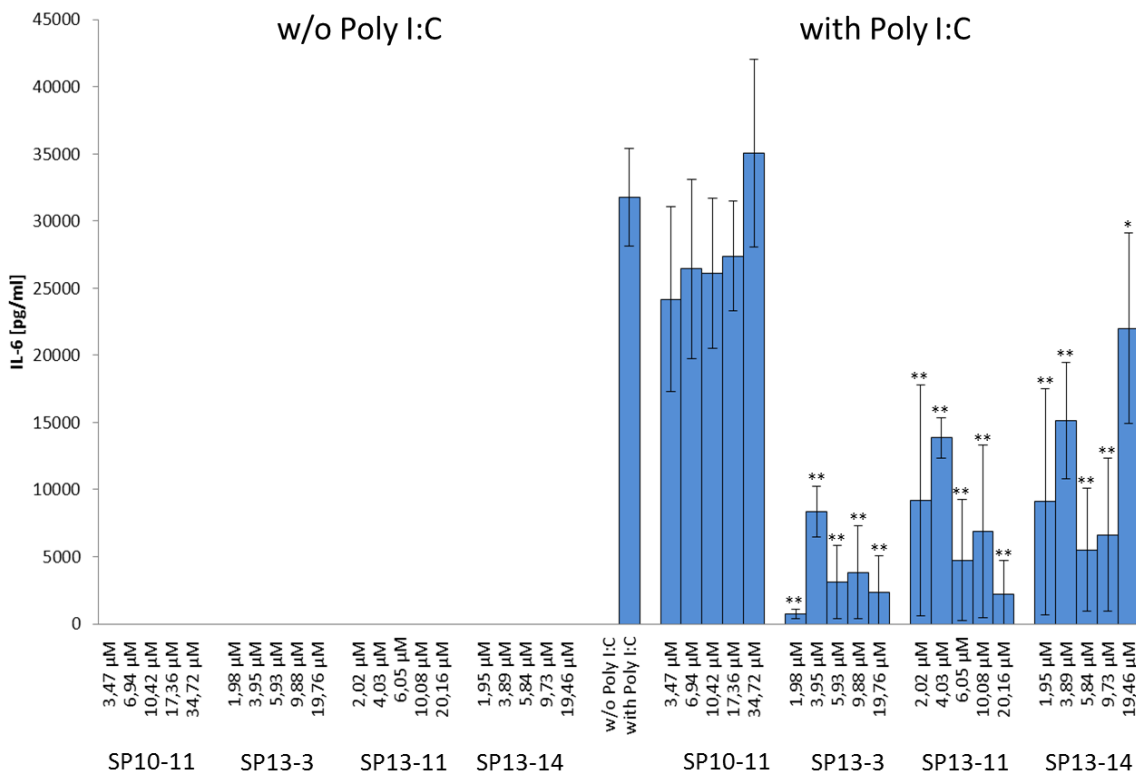


Figure 14: Poly I:C in combination with peptides of the SP13 series significantly diminishes IL-6 secretion in human MoDCs, whereas the presence of SP10-11 does not influence IL-6 secretion. Stimulation with peptides does not trigger IL-12 production. MoDCs were stimulated with different concentrations of HIV active peptides in the presence (right side) or in the absence (left side) of Poly I:C. IL-6 levels [pg/ml] were analyzed by ELISA after 24h incubation time. Two biological replicates with two to four technical replicates each were measured. Significance was calculated by T-test against the corresponding medium control, respectively (*: $p < 0,1$; **: $p < 0,01$).

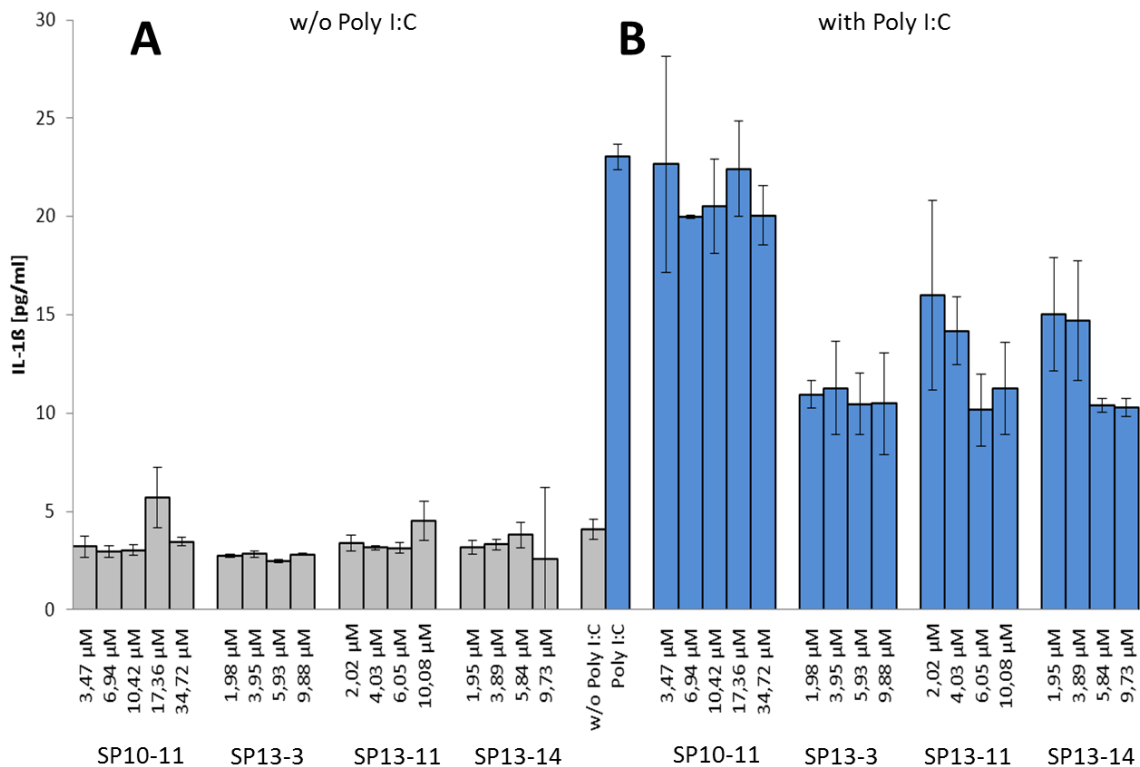
When MoDCs were stimulated with peptides alone, no IL-6 release was detectable in all samples (Figure 14, left side). In case of stimulation of peptides together with Poly I:C, SP10-11 did not show significant differences in IL-6 production compared to the medium control (Figure 14, right side). When MoDCs were incubated with Poly

I:C and SP13-derived peptides, for all measured samples a clear reduction of IL-6 release was detectable, which seems to be independent of the applied concentration (Figure 14, right side). In case of SP13-3 the lowest IL-6 production levels of all SP 13 peptides were observed, whereas SP13-14 showed the highest production levels of the SP13 peptides.

4.2.4.4. Interleukin 1 β response

MoDCs were stimulated with different peptide concentrations and/or Poly I:C in a concentration of 10 $\mu\text{g/ml}$. After 24h incubation, supernatants of DC cultures were analyzed by IL-1 β ELISA (BD Bioscience).

Analogous to IL-12 analysis, IL-1 β overall releases of the blood donors were too diverse to be summarized in one graph and are therefore shown individually (Figure 15). Analysis shows no significant induction of IL-1 β release by incubation of MoDCs with peptides alone. When cells were incubated with Poly I:C and SP10-11, comparable values to the control were observed in the first replicate (Figure 15, B) and slightly higher values compared to the corresponding medium control were observed in the second biological replicate (Figure 15, D). In case of SP 13 peptides, lower IL-1 β production rates were observed in both biological replicates (Figure 15, B/D). Summarized, the profiles of both replicated indicates, that IL-1 β release remains unaffected by simultaneous incubation with SP10-11, whereas the incubation with peptides of the SP13 series shows weak inhibitory effects.



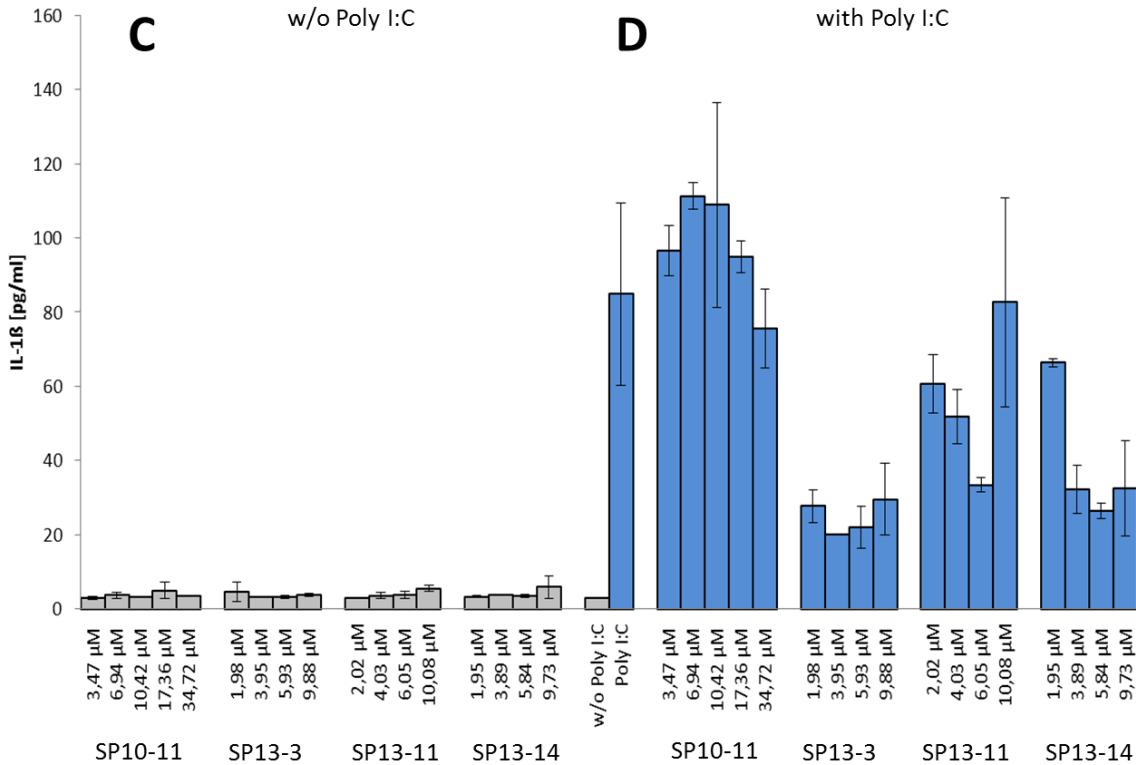


Figure 15: Poly I:C in combination with SP13 peptides suppresses IL-1 β secretion in human MoDCs, whereas the presence of SP10-11 does not alter (B) or even slightly enhances (D) IL-1 β secretion. The overall donor-dependent variations in cytokine release varied highly between first (B, maximal IL-1 β production is 26 pg/ml) and second biological replicate (D, maximal IL-1 β production is 120 pg/ml). MoDCs were stimulated with different peptide concentrations in the presence (A/C) or in the absence (B/D) of Poly I:C. IL-1 β secretion was analyzed by ELISA after 24h incubation time. For each donor, two to four technical replicates were measured. Significance was calculated by T-test against the corresponding medium control (*: $p < 0,1$; **: $p < 0,01$).

4.3. Transplastomic approach for peptide production

To establish a stably transformed, plant-based production platform for production of our designed peptides, a transplastomic approach in chloroplasts of *Nicotiana tabacum* (*N. tabacum*) was chosen. The coding sequences were derived from the amino acid sequences of the designed peptides following tobacco chloroplast codon usage tables and cloned into plasmid transformation vectors (PTV) for insertion via homologous recombination into tobacco chloroplasts.

4.3.1. Plastid transformation vectors

In total, four different transformation vectors (PTV) were cloned (Figure 16), which all share several functional units (Table 4).

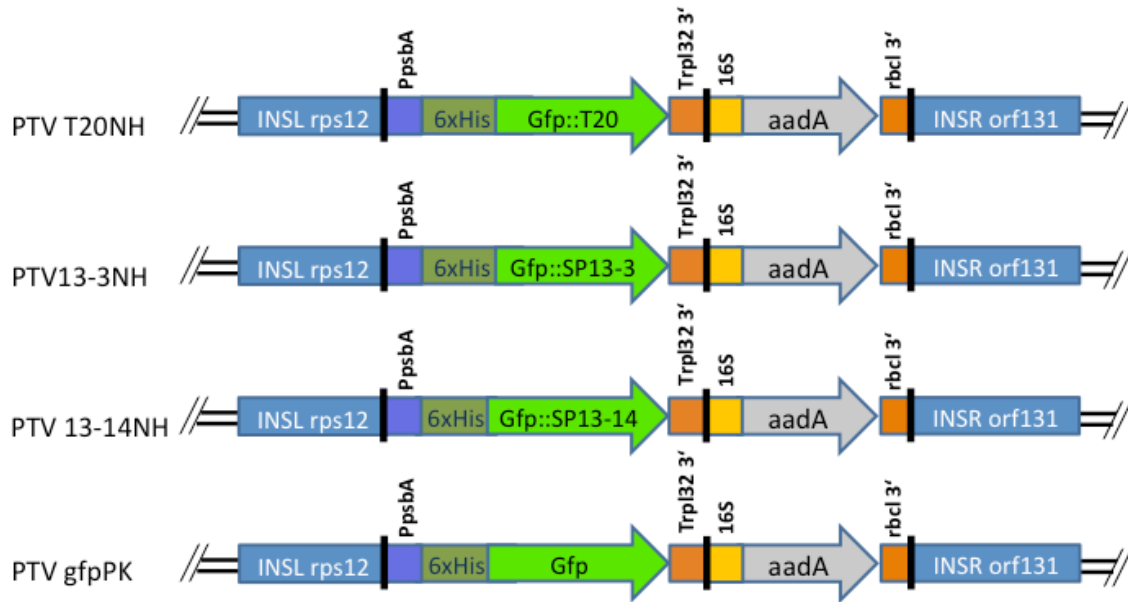


Figure 16: Representation of all constructs for homologous recombination in tobacco chloroplasts. The names of the according plasmid transformation vectors (PTV) are added at the left side next to each insert. All constructs display various functional units: plastome insertion site on the left (INSL rps12), plastome insertion site on the right (INSR orf131), poly-histidine tag (6xHis), two promoters with the according 5' UTR (PpsbA, 16S) for the two expression cassettes (GFP::GOI, aadA) and respectively two terminators (trp132 3', rbc1 3'). The different fusion proteins with the GOI are marked in bright green.

In each PTV used in this work, the promoter and the 5' untranslated region (5'-UTR) of the GOI expression cassette derives from the *Chlamydomonas reinhardtii* (*C. reinhardtii*) plastid and is further called PpsbA. PpsbA naturally facilitates the transcription of the *psbA* genes, whose proteins form the reaction center of the photosystem II complex. The GOI expression cassette is terminated by the endogenous (tobacco) termination sequence for ribosomal protein CS32 gene (trp132). To confer stability and to avoid degradation of the recombinant product that might result from their short size, the peptides were produced as a C-terminal fusion protein with green fluorescent protein (GFP) displaying an N-terminal 6xhistidine tag (Figure 16). His-tagged GFP as fusion partner facilitates purification, serves as reporter for quantification and is expected to inactivate the antimicrobial activity of the designed peptides, which may result in possible toxic effects for the transformed chloroplast. Methionine was introduced upstream of the designed AMP to release the mature peptide from their fusion partners using chemical cleavage with cyanogen bromide (CNBr). CNBr cleaves on the C-terminal side of methionine, thus converting it to a homoserine. Chemical cleavage was chosen to avoid residual amino acids to the mature peptide, which were shown to diminish activity in case of SP1-1 [46]. The second expression cassette provides the *aadA* gene (aadA), conferring resistance to spectinomycin, driven by the constitutive 16S promoter and terminated by the terminator sequence of ribulose-1,5-bisphosphat-carboxylase/-oxygenase (RuBisCo)

large subunit in *C. reinhardtii* (3' *rbcl*). Two different promoter sequences were used to avoid loop structures and mismatching during homologous recombination. The whole construct is flanked by endogenous sequences of *N. tabacum* ptDNA (*rps12*, *orf131*), which serve as targeting regions for direct integration (Table 4).

Table 4: Functional units of chloroplast transformation vectors.

Function	Name	Description
Promoter	PpsbA	Promoter and 5' UTR of the genes encoding the photosystem II protein <i>psbA</i> within the <i>C. reinhardtii</i> plastid.
	16S	Promoter for the <i>aadA</i> expression cassette.
Plastid insertion site	<i>rps12</i>	Part of ribosomal protein CS12 gene within the <i>N. tabacum</i> plastid used as left flank for homologous recombination. (<i>N. tabacum</i> chloroplast genome DNA: 100757 – 101520)
	<i>orf 131</i>	Downstream of <i>rps12</i> gene, used as right flank for homologous recombination. (<i>N. tabacum</i> chloroplast genome DNA: 101518 – 102055)
Terminator	<i>trpI32</i>	3' UTR and terminator for ribosomal protein CS32 gene (<i>rpl32</i>) in the chloroplast in <i>N. tabacum</i> . Here used as terminator for the AMP expression cassette.
	3' <i>rbcl</i>	3' UTR, which belongs to the gene of RuBisCo large subunit (<i>rbcl</i>) in <i>C. reinhardtii</i> . Here used as terminator for the <i>aadA</i> cassette.
Marker	<i>aadA</i> gene	Encodes aminoglycoside-3"-adenylyltransferases (AAD), which confer resistance to streptomycin and spectinomycin by adenylation.
	GFP gene	Marker gene for fluorescence-based detection. The <i>gfp</i> marker used in this work is from gateway plasmid pB7FWG2 and is additionally fused to a 6 x histidine tag (N- or C-terminal)
Variable Units	AMP	SP10-11, SP13-3 or SP13-14
	T-20	36 residue synthetic peptide, an HIV fusion inhibitor

4.3.2. Golden Gate Cloning

To produce PTVs, a technique called Golden Gate Cloning (GGC) was established for this work in our lab (Figure 17). With GGC it is possible to assemble several separate DNA fragments together into one acceptor vector in a particular order and in one single step. The principle of GGC is based on the ability of the type II restriction enzyme *BsaI* to cut outside of its recognition site. Two DNA ends can be designed in a way that they are flanked by *BsaI* restriction site and that *BsaI* digestion of the fragments removes the specific recognition site. Thus, ends with complementary 4 nt overhangs are created, which align to a junction that lacks the *BsaI* restriction site after ligation (Figure 17) [97-99].

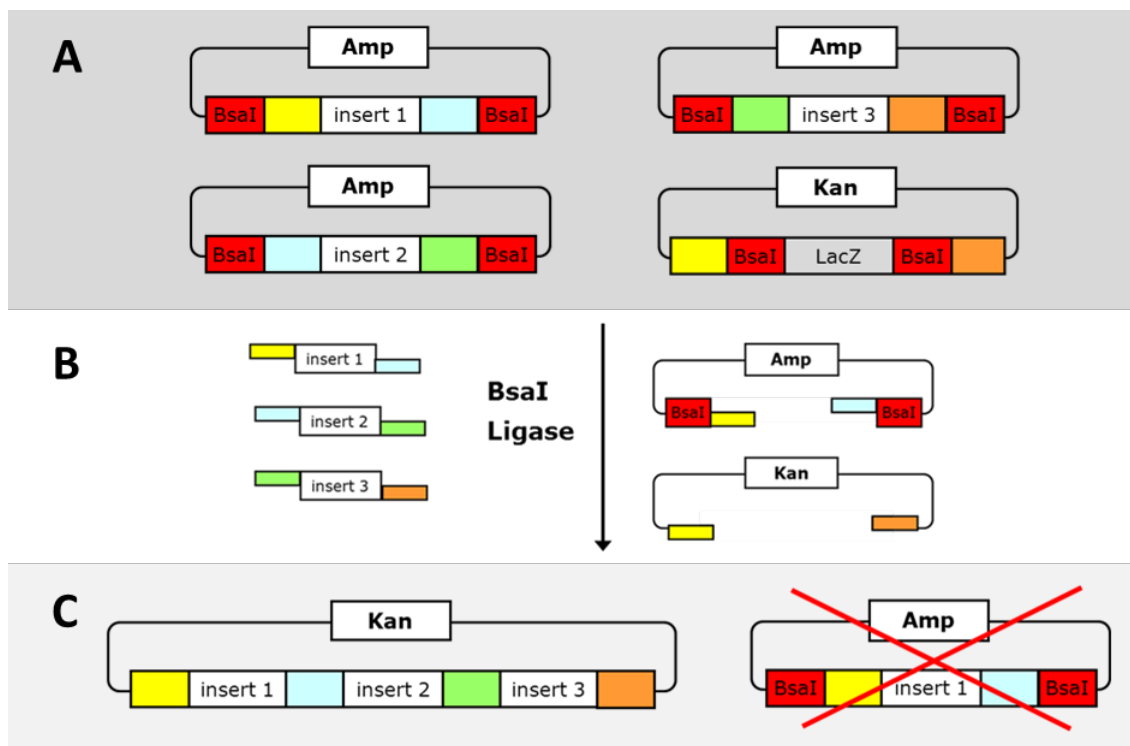


Figure 17: Schematic assembly of Golden Gate Cloning principle. (A) The donor vectors with the ampicillin resistance gene (**Amp**) contain different core regions (**insert 1-3**) that are flanked by *BsaI* restriction sites in opposite orientation composed of a recognition site (*BsaI*, labeled in red) and a 4 nucleotide cleavage site (accordingly color-marked). The acceptor vector features the same structure as the donor vectors, but contains the **LacZ** reporter gene as core region (**LacZ**) and displays the kanamycin resistance gene (**Kan**). **(B)** In restriction-ligation reaction, the donor and the acceptor vector show different 4 nucleotide overhangs, which allow two alignment possibilities. **(C)** The construct with a specific order of **insert 1 - 3** is part of the target vector after restriction-ligation reaction (left side). The realigned donor vector is not stable, because the remaining *BsaI* cleavage sites are permanently cleaved in the restriction-ligation reaction (right side, crossed out). Positive clones with the insert are selected by **Kan** resistance marker and blue-white screening.

In this work, two different plasmids were used as donor vectors for GGC. One donor vector (Don1) was provided by Prof. Koop (Botany department of LMU, Munich). Don1 derives from the commercially available vector pJET2.1/blunt (Thermo Scientific), which contains a lethal restriction enzyme gene that is disrupted by ligation of a DNA insert into the cloning site. pJET2.1/blunt also contains the ampicillin resistance gene *bla* that displays one BsaI cleavage site. For GGC donor vectors it is necessary that no additional BsaI cleavage sites are present. Therefore the *bla* gene of pJET2.1/blunt was replaced by spectinomycin resistance for producing Don1. Different inserts have been provided by the Koop group, including terminator sequences (trpI32, 3'rbcl), the plastid insertion sites (rps12, orf131), the *psbA* promoter and 5' UTR from *C. reinhardtii* (PpsbA) and the selection cassette *aadA*. The second donor vector (Don2) was produced in this work. This second type of donor vector was produced to avoid the repeated process of replacing *bla* gene for pJET2.1/blunt. Don2 derived from the commercial available pUC18 vector, which also contains *bla* gene. For Don2 site-directed mutagenesis was performed to remove the BsaI cleavage site via silent mutation. Subsequently, several inserts were cloned into the multiple cloning site of Don2 by *SmaI* restriction and blunt end ligation. The applied inserts consist of the sequences of our target peptides, of GFP with 6xhistidin tag on the N-terminus and the PpsbA promoter of *C. reinhardtii* (Table 5). Appropriate donor vectors for construction of a specific PTV were assembled in a tube and Golden Gate restriction/ligation reaction was performed with BsaI (New England Biolabs, Frankfurt) and T4 ligase (Promega, Mannheim). GGC preparation was subsequently transformed into *Escherichia coli* DH5 α and resistant clones were verified by colony PCR and subsequent sequencing.

Table 5: Inserts provided by Golden Gate donor vector Don2.

Insert	Description
SP10-11	HIV- active designed peptide
SP13-3	HIV- active designed peptide
SP13-14	HIV- active designed peptide
T-20	HIV- active, 36 residue, N-terminal acetylated synthetic peptide without antimicrobial properties.
GFP NH	GFP with N-terminal 6xhistidin tag
GFP PK	GFP with N-terminal 6xhistidin tag
PpsbA	Promoter and 5'UTR of <i>psbA</i> genes of <i>C. reinhardtii</i>

4.3.3. Chloroplast transformation and regeneration

After propagation in *Escherichia coli* DH5 α , PTVs were purified by HiSpeed Plasmid Maxi Kit (Qiagen GmbH, Hilden) and transferred by biolistic approach into plastids of

N. tabacum leaves. The particle gun device required for this approach was provided by cooperation with the Koop group (Botany department of LMU, Munich). In total, 16 different biolistic approaches for plastid transformation were performed in the present work. For each approach 8 leaves were bombarded with DNA coated micro-projectiles, resulting in 128 different tissue culture lines. Plasmid transformation was newly established for our laboratory therefore only 56 of these lines could be successfully selected due to contaminations and necessary optimization of selection conditions. These seven lines included transformed approaches with four different PTVs that resulted into an overall yield of 14 transplastomic plant lines (Table 6).

Table 6: Chloroplast transformation by biolistic approach with different plastid transformation vectors (PTVs). The number of isolated shoots from bombarded tissue cultures is counted for each applied PTV and is subdivided into bleached shoots, false positives and transplastomic transformants.

PTV name	Tissue culture names	Number of lines	isolated shoots	bleached/false positive	trans-formants
PTV 13-3 NH	GK1/I – VIII GK6/I – VIII	16	47	12/ 31	4
PTV 13-14 NH	GK4/I – VIII GK7/I – VIII	16	56	23/ 27	6
PTV T20 NH	GK2/I – VIII GK3/I – VIII	16	48	24/ 22	2
PTV gfp PK	GK5/I – VIII	8	35	10/ 23	2

After bombardment, leaf segments were transferred on RMOP medium containing 500 mg/l or 50 mg/l spectinomycin dihydrochloride (spec) until resistant shoots emerged after 8 to 12 weeks (Figure 18). The 10-fold lower concentration of spec was tested, because in the first selection process the tissue culture turned brownish within two weeks and only little callus development was observed. Although the bleaching of tobacco tissue with 500 mg/l spec content in the selection medium resembles the one with 50 mg/l (Figure 18), the lower spec concentration leads to around 10 shoots per plate, of which none incorporated the transgene and which bleached out, when put under selection pressure with 500 mg/l spec. Thus we concluded that the low spec conditions did not provide sufficient selection pressure and repeated the process with 500 mg/l spec and additionally lower temperature conditions. These conditions resulted in suitable selection of transplastomic shoots.

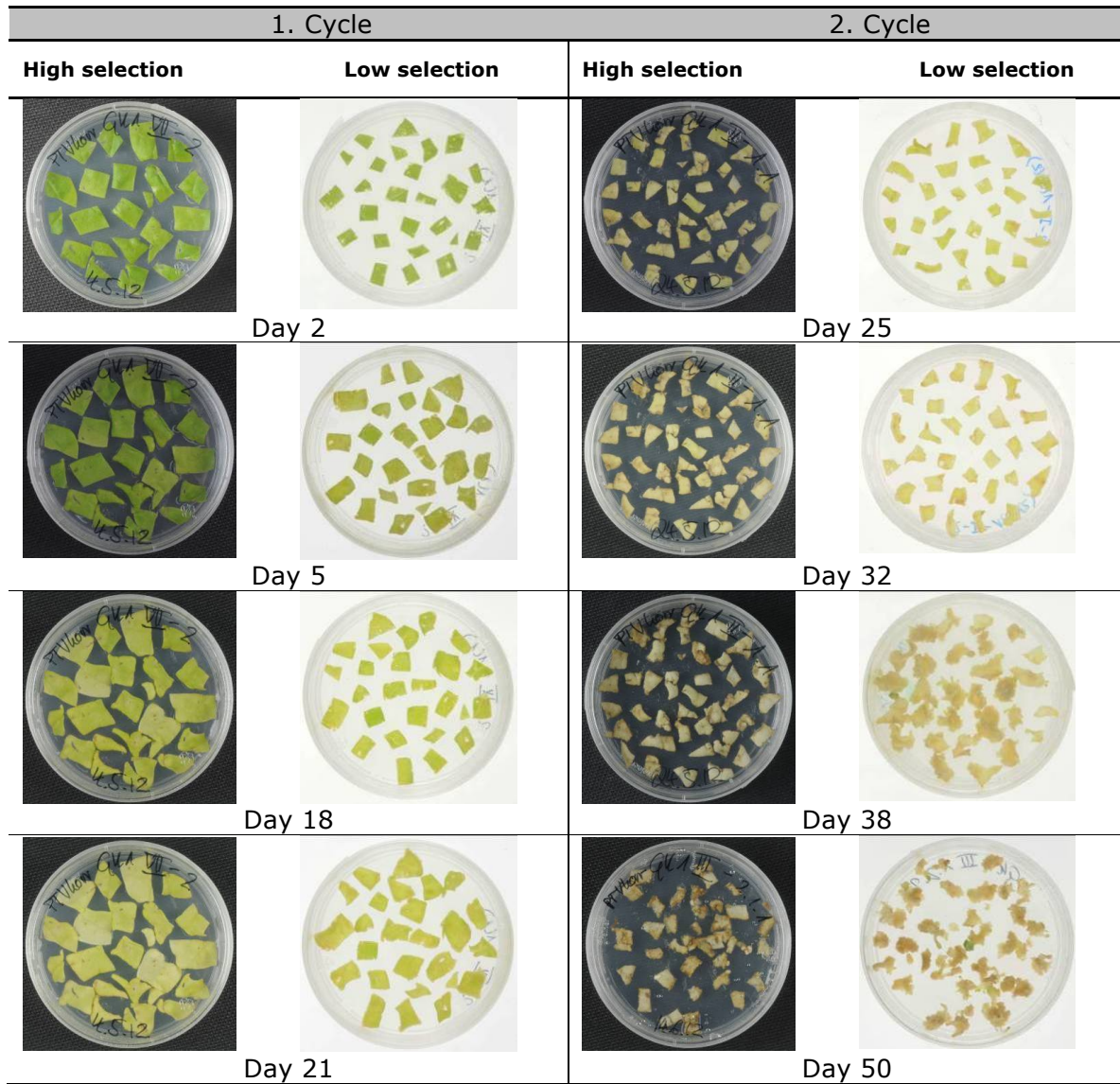


Figure 18: Development of plant tissue cultures derived from PTV 13-3 NH bombardment on RMOP medium containing 500 mg/l spectinomycin (high selection) or 50 mg/l (low selection). Selection periods are indicated by days after particle bombardment.

All putative transgenic shoots were recovered from bleached leaf sections and isolated (Table 7). The shoots were cut in pieces, regenerated on RMOP medium containing 500 mg/l spec and sub-cloned into new plates. This process of cutting and regeneration was repeated for additional 3 months to enhance the overall content of transplastomic ptDNA (Figure 19). Also for the cycling procedures, controlled climate conditions were provided by cultivation in a growth chamber with 14h light (approx. $200 \mu\text{E}\cdot\text{m}^{-2}\cdot\text{s}^{-1}$) at 25°C and 10h dark at 20°C.



Figure 19: Cycling procedure of putative heteroplastomic shoots. Shoots were cut, propagated and further cultivated on a selective medium to gradually diminish non-transformed plastids.

4.3.4. Screening for transplastomic lines

In total, 185 putative transplastomic shoots were isolated, of which 117 shoots did not bleach out when subcultured on fresh selection medium (Figure 21). Total DNA

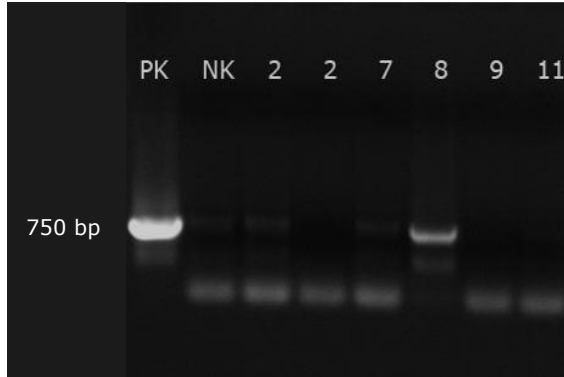


Figure 20: Screening of total DNA from isolated shoots with PCR. Positive control (PK) consists of plasmid PTV 13-3 NH, negative control (NK) consists from total DNA of wild-type *N. tabacum*. Shoots were named in numbers after their appearance.

from these putative transplastomic shoots (after minimum of 4 weeks of selection and regeneration) as well as from wild-type *N. tabacum* leaves was extracted. Integration of the construct was confirmed by PCR using two sets of primers: one primer pair specific to PpsbA and aadA (plantPCR2 fwd/rev) and a second primer pair specific for gfp with n-terminal His-tag (gfp N-his fwd/rev). With one or both of these primer pairs, all spectinomycin-resistant shoots were tested (Figure 20; Figure 26, A). To confirm site-specific

integration of the insert, a second primer set (SiteSpecificPCR2 fwd/rev) was used, where the forward primer is specific to the *N. tabacum* plastome upstream of the integration and the reverse primer anneals within the GFP gene. This primer pair was used to determine site-specific integration of recombinant genes into the chloroplast genome. To check for possible loop outs during homologous recombination, PCR-products were cut out of the gel, purified, cloned into vector pJET1.2/blunt and subsequently sequenced.

4.3.5. Transformation efficiency

For each bombardment the total number of confirmed transplastomic shoots per total number of target plates was counted. An overall efficiency for the chloroplast transformation was 0,175 transplastomic shoots per bombarded plated after 13

weeks of selection (Table 6). Additionally the number of false positive shoots and confirmed plastid transformants was compared in order to determine a period of accumulated occurrence of transplastomic shoots during the selection process (Figure 21).

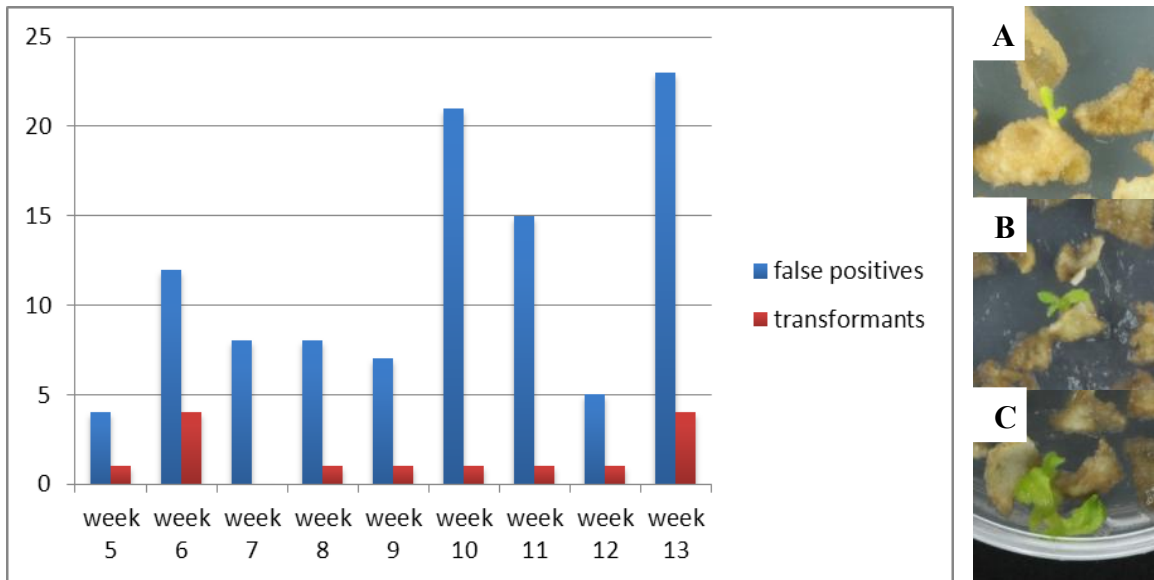


Figure 21: Summary of false positives and plastid transformants of all seven tissue cultures (left side). No distinct time period with accumulated occurrence of transplastomic shoots was detected. Shoots, that bleached out are not shown in this diagram. Examples for isolated shoots (right side). (A) Putative shot that bleached after subculturing. (B) Confirmed transplastomic transformant and (C) a false positive shoot.

The appearance of transplastomic shoots did not show a clear peak within the selection process. Overall, it was noted that a distinctly higher number of false positives was found compared to the number of transformants in all investigated tissue cultures (Table 6; Figure 21). Altogether, 14 transformants were determined and further analyzed (Table 7).

Table 7: Overview over transplastomic shoots, their tissue culture name and applied plasmid transformation vectors.

Shoot ID	Tissue culture name	PTV	Remark
8	GK1	PTV 13-3 NH	PCR positive, Southern Blot negative
10	GK1	PTV 13-3 NH	PCR positive, no fertile seed from F0 generation
16	GK3	PTV T20 NH	PCR positive, Southern Blot positive. homoplastomic F1 generation
26	GK3	PTV T20 NH	PCR positive, Southern Blot positive. heteroplastomic F1 generation
62	GK4	PTV 13-14 NH	PCR positive, Southern Blot positive. homoplastomic F1 generation
73	GK1	PTV 13-3 NH	PCR positive, no fertile seed from F0 generation
77	GK4	PTV 13-14 NH	PCR positive, Southern Blot positive. homoplastomic F1 generation
81	GK4	PTV 13-14 NH	contaminated
82	GK4	PTV 13-14 NH	PCR positive, Southern Blot positive. homoplastomic F1 generation
88	GK5	PTV gfpPK	PCR positive, no fertile seed from F0 generation
109	GK7	PTV 13-14 NH	PCR positive, no fertile seed from F0 generation
136	GK5	PTV gfpPK	PCR positive, Southern Blot positive. homoplastomic F1 generation
146	GK6	PTV 13-3 NH	contaminated
186	GK7	PTV 13-14 NH	contaminated

4.3.6. F0 Generation of transplastomic plants

After 3 month of cycling, transplastomic shoots were subcultured on B5 medium without spectinomycin additives for rooting. After approximately one month of cultivation on B5 medium, rooting was sufficiently advanced to transfer the shoots on soil. For comparison of plant development, which might be influenced by the selection process, unbombarded *N. tabacum* callus was propagated on RMOP without

spectinomycin parallel to the selection of transplastomic plants. Also here, emerging shoots were rooted on B5 medium and later on transferred to soil parallel to the transplastomic lines. Plant size and development speed of the F0 plants were dependent of the size of the transferred shoots and therefore not comparable to each other. Nevertheless, effects of polyploidization, which heavily affects plant fertility, were observed as several of the F0 plant did not produce seed (Table 7).

4.3.7. F1 Generation of transplastomic plants

Seeds from F0 generation plants were harvested, sterilized and transferred on B5 medium with 500 mg/ml spectinomycin to select homoplastomic F1 plants by germination on selection medium (Figure 22).

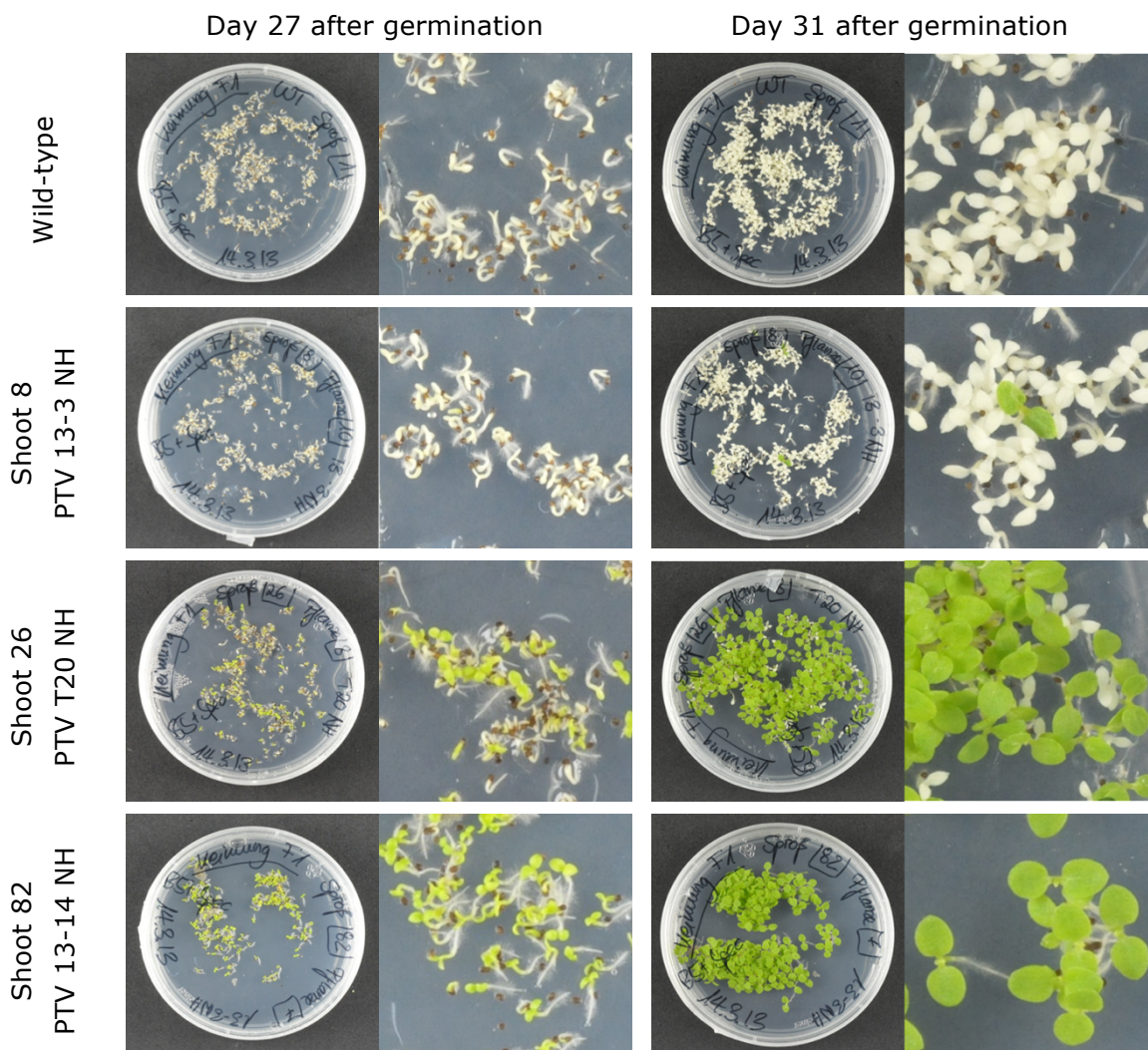


Figure 22: Germination of F1 generation of transplastomic tobacco plants on B5 medium with 500 mg/l spectinomycin. Seed was derived from putative heteroplastomic plants of the F0 generation.

Germination on selection medium results partly in resistant, green seedlings and partly in white, untransformed seedlings. The ratio between transformed and untransformed seedlings varies strongly between the different germination experiments, but the wild-type control seed always show only the white phenotype (Figure 22). Two weeks after germination, green and thus resistant seedlings were transferred into soil. Numerous transplastomic plants with normal phenotype were achieved from these seedlings, which showed normal development and were fertile. Furthermore, no differences in phenotype or development were observed between wild-type control and transplastomic plants (Figure 23).

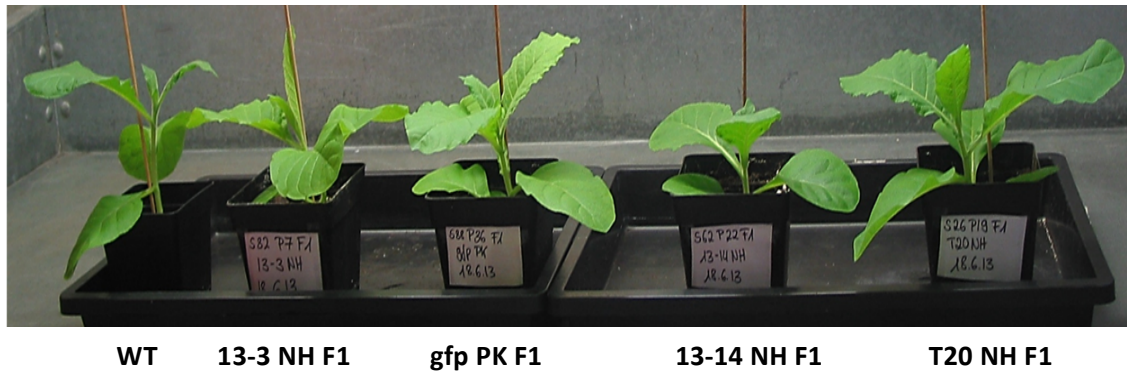


Figure 23: Phenotypes of transplastomic plants from the F1 generation and wild-type plants show no differences. All plants were grown on soil for 4 weeks under controlled conditions. Left side: wild-type plant. Right side: transplastomic plants of the F1 generation.

4.3.8. Southern Blot analysis of transplastomic plants

After 4 weeks, leaves of the putative homoplastomic F1 plants were harvested and total DNA was extracted. Additionally, total DNA of frozen leaf material of parental plants was also extracted. All DNA samples were tested via southern blot for insertion. The southern blot probe was designed to anneal upstream of the *rps12* insertion site on the *N. tabacum* plastome (Figure 24; Table 7). Digestion was performed with restriction enzyme BciVI, which results in a probe-labeled DNA fragment of 2444 bp for the wild-type ptDNA, respectively in a probe-labeled DNA fragment of 5244 bp for transformed ptDNA. Homoplastomic plants were confirmed for shoots 16 (PTV T20 NH), shoot 62 (PTV 13-14 NH), shoot 77 (PTV 13-14 NH) and shoot 136 (PTV *gfpPK*). Heteroplastomic existence was shown for shoot 26 (PTV T20 NH) and loss of insert was documented for shoot 8 (PTV 13-3 NH) and shoot 82 (PTV 13-14 NH) in the F1 generation (Figure 24; Table 7). No homoplastomic existence was observed for plant of the F0 generation (Figure 24).

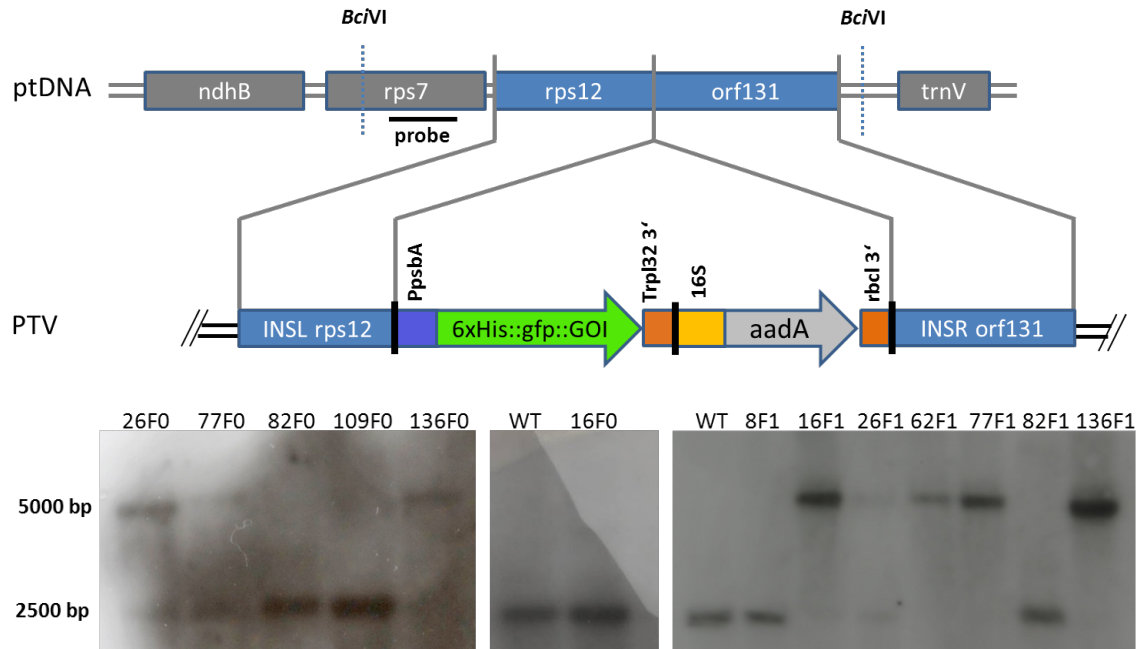


Figure 24: Southern Blot analysis of transplastomic plants of the F0 and F1 generation. Upper figure: Schematic representation of insertion of the PTV construct in the tobacco plastome. The probe used for Southern Blot analysis is indicated. Total plant DNA was digested with *Bci*VI, which results for ptDNA with insert into a probe-labeled fragment of 5244 bp whereas wild-type ptDNA is represented by a 2444 bp fragment. Proportions of the boxes do not match the actual length of DNA functional units. Lower figure: Southern blot analysis shows heteroplasmy nature of F0 generation. The F1 generation was mainly determined as homoplasmy with exceptions of shoot 8 and shoot 82 (8F1, 82F1), which lost the insert during selection and shoot 26 (26F1), which turned out to be heteroplasmy also in F1 generation.

4.3.9. Test for translation

However, all F0 and F1 plants derived from transplastomic shoots showed no GFP fluorescence. Also with western blot analysis using anti-histidine or anti-GFP primary antibody, no recombinant protein was detectable (Figure 25, A/B). Several protein extraction methods were applied for western blot analysis. To test additionally for insoluble fusion proteins, the remaining pellet after total soluble protein (TSP) extraction was also heated (95°C, 10 min) in 50 µl 2xSDS loading dye, separated by SDS-Gel and analyzed via western blot. Additionally, TSP was concentrated by acetone precipitation and 100 µg TSP were loaded on a gel (Figure 25, C/D). In none of these samples, recombinant protein could be detected. Even in TSP fractions, where gfp-fusion proteins were enriched by Epitope-Tag Isolation Kit (Miltenyi Biotec GmbH, Germany) no difference was observed between wild-type and transplastomic tobacco (data not shown). From these data we conclude that there is no translation of the recombinant protein in our transplastomic plants.

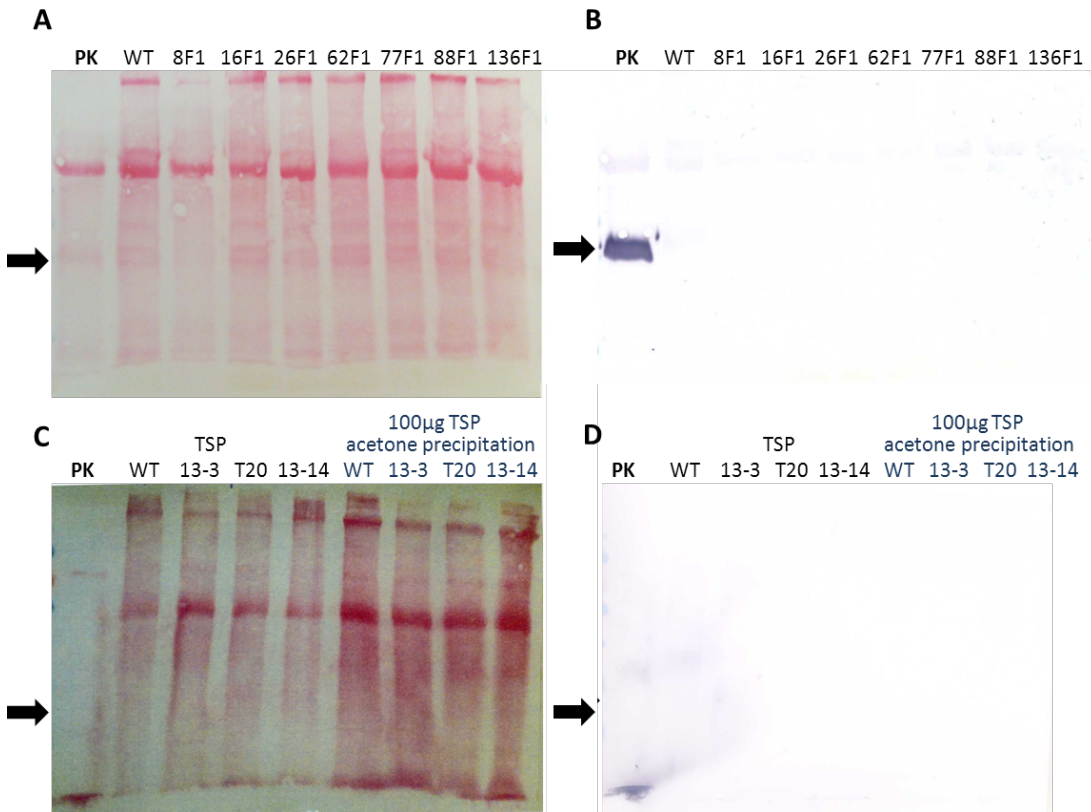


Figure 25: Failure of recombinant protein production in transplastomic plants of the F0 (A/B) or F1 (C/D) generation. Analysis was performed by anti-GFP western blot (A/B) and by anti-histidine western blot (C/D). Positive control (PK) consists of TSP of *Arabidopsis thaliana* expressing *gfp* with the constitutive 35S promoter (A/B) or a purified recombinant protein with an attached His-tag (C/D). (A) Ponceau staining shows sufficient gel loading with protein. (B) Anti-GFP western blot shows no recombinant protein production in all analyzed samples of the F1 generation. (C) Ponceau staining shows enhanced TSP accumulation after acetone precipitation. (D) Anti-histidine western blot shows no recombinant protein production in all analyzed samples.

4.3.10. Confirmation of transcription

RNA from transplastomic plants of the F0 generation was extracted from leaf material. From the RNA templates, cDNA was produced and transcription of the inserted sequence was verified via RT-PCR (Figure 26). To confirm transcription of the homologous insert, primer set specific for *gfp* with an n-terminal His-tag was used (Figure 26, B). A second primer set (PlantPCR2 fwd/rev), specific for *PpsbA* and the S16 promoter of the *aadA* cassette, was applied in a second RT-PCR. This primer was used to test the cDNA for genomic DNA contaminations (Figure 26, C). RT-PCR shows that the inserted DNA is transcribed in all tested plants.

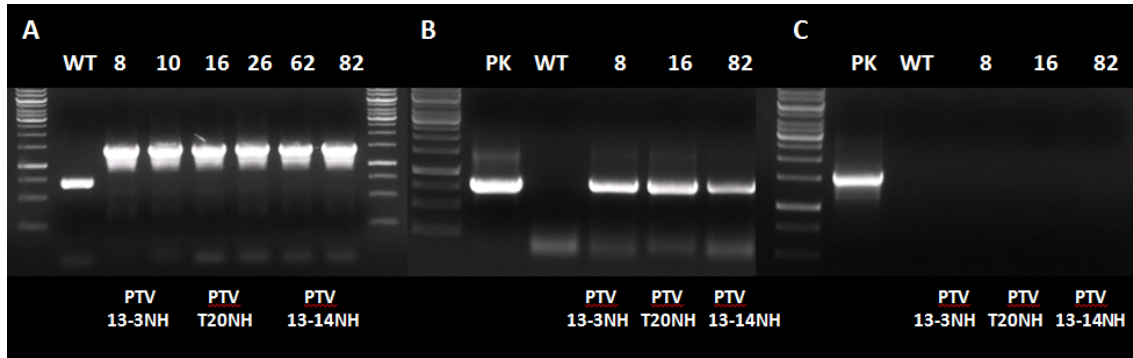


Figure 26: RT-PCR from transformants of the F0 generation shows functional transcription. (A) Primer pair SSSPCR2 was used on total DNA templates from putative shoots, to verify transplastomic existence. (B) RT-PCR from cDNA of transplastomic plants with primers specific for *gfp* was performed to confirm transcription of the GOI sequence. Positive control (PK) consisted from plasmid PTV 13-3 NH. (C) Primer pair PlantPCR2 was used to test cDNA for genomic DNA contaminations. Positive control (PK) consisted from purified plasmid PTV 13-3 NH.

4.4. Transient production of designed peptides with expression system magnICON®

A transient expression system called magnICON®, which is based on a deconstructed Tobacco mosaic virus (TMV), was supplied by Icon Genetics, Munich. This system is built on *in planta* assembly of functional viral vectors from separate pro-vector modules by site-specific recombinase to form a fully functional RNA replicon. Here, *Agrobacterium tumefaciens* is used to deliver the pro-vector modules. The magnICON® production technique results in exceptionally high expression levels up to 80% TSP [100, 101]. As this expression system is not self-made and in addition patent protected it was not the first method of choice. However, the genes for fusion proteins from PTV were re-cloned in magnICON® vectors and used for this approach, which was conducted within a master thesis [90]. Fully grown *Nicotiana benthamiana* plants were infiltrated with a mixture of three diluted agrobacteria suspensions, carrying T-DNAs, which encode the specific prefabricated modules. Experiments with GFP as positive control revealed that *Nicotiana benthamiana* displays high expression levels at the ideal OD_{600nm} 0,01 of the infiltration suspension as it has been previously shown in our lab [47]. Because the expression constructs moves not systemic, syringe infiltration of whole leaves was necessary, which results in varying expression levels that were visible under UV-light. For the constructs *gfp::SP10-11*, *gfp::SP13-3*, *gfp::SP13-11* and *gfp::SP13-14* as well as for positive controls *gfp* and *gfp::T20*, recombinant protein production was shown by western blot [90]. Highly sensitive, HPO based western blot shows that the PTV constructs are expressed with the magnICON® approach, whereas the same constructs remain untranslated in stably transformed transplastomic plants (Figure 27).

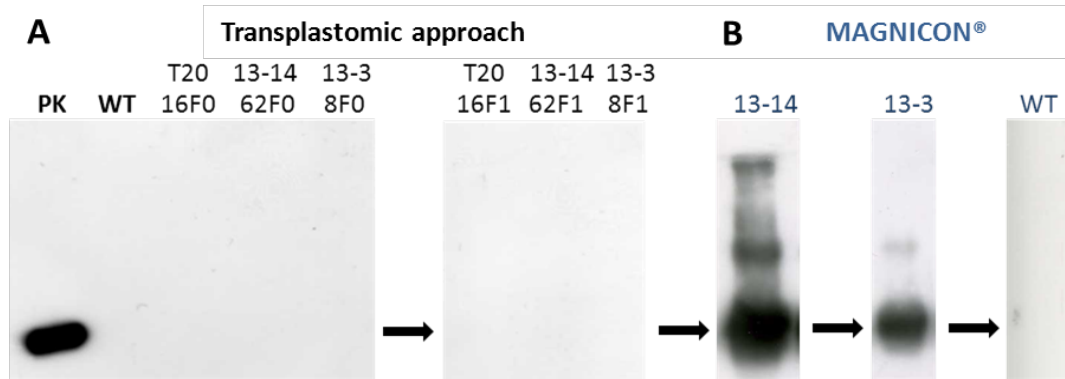


Figure 27: Anti gfp western blot with highly sensitive HPO detection [90]. (A) TSP of transplastomic plants of the F0 and F1 generation. Western blot shows the failure of recombinant protein accumulation. (B) TSP of *Nicotiana benthamiana* leaves after transfection with the magnICON® expression system. Plants are clearly accumulating the peptides SP13-14 and SP13-3 fused to GFP.

5. Discussion

The first defense reaction of our body against infections consists of various responses by our innate immune system. These responses involve secretion of cytokines, which help to mobilize the adaptive immune response and coordinate as well as retain inflammation reactions [29, 102]. One function of endogenous human AMPs within this response is their role as direct antimicrobial agents for example in macrophages. This AMP feature is underlined by the finding, that naturally occurring AMPs changed considerably over evolution, which may be due to the evolutionary pressure of dealing with different pathogens [37]. But on the other hand side AMPs also play an indirect antimicrobial role within immune response by the ability to act as chemokines or by inducing chemokine production by different means [37]. Therefore it is discussed, although quite controversial, that the immunomodulatory properties may be the predominant function of certain AMPs *in vivo*.

5.1. Cell-toxicity of designed peptides

The toxic effect of our designed peptides on peripheral blood mononuclear cells (PBMCs) and monocyte-derived dendritic cells (MoDCs) was investigated to detect possible adverse effects on HIV target cells and additionally to determine suitable concentrations for ELISA analysis.

PBMCs are a heterogeneous cell population consisting of T-cells, B-cells, NK cells, monocytes, thrombocytes and dendritic cells and thus PBMCs represent critical components of the innate and adaptive immune system [95]. Furthermore, PBMCs have been demonstrated to be key players in inflammatory processes and linked to many diseases including HIV [12]. Due to their heterogeneous nature, PBMC populations vary widely across individuals. Therefore, homogeneous MoDCs were tested additionally for possible peptide-induced adverse effects.

Altogether, results from cell-toxicity experiments suggest that peptides from the series SP10 and series SP13 exhibited different effects to humans PBMCs and MoDCs. While SP10-11 displayed no toxic effects, SP13-3, SP13-11 and SP13-14 showed toxicity towards both cell types, which was always depending on the applied concentration. Effects were similar between the three SP13 peptides, but overall, SP13-14 induced the most severe toxic effects of all SP13-derived peptides, followed by SP13-11 and finally SP13-3 (Figure 5; Figure 7). These concentration-dependent cell-toxic effects of peptides from the SP13 series have also been observed with erythrocytes [45].

To further evaluate the mechanisms of action of the SP13-derived peptides regarding cell toxicity, long-term experiments with PBMCs were performed, where the cells were incubated with the previously applied peptide concentrations and cell viability was measured at different time point. Although fluctuations between the biological

replicates were present, the general trend of all graphs showed that the toxic effects influence the cells within the first 90 minutes of incubation and do not induce any long-term effect in the observed time span of 67h (Figure 6). Therefore we conclude that the length of incubation time seems to play a minor role regarding toxicity of the designed peptides. Furthermore, measurements indicate that MoDCs are more susceptible for the toxic effect of the SP13 peptides, but in the same concentration-dependent manner (Figure 7). Still, the overall MoDCs viability was higher than PBMC cell viability, an observation that was also reproducible in the medium control. This may be due to better tolerability of MoDCs for HU-DC medium compared to PBMCs for complete medium.

The peptide-induced differences in cell proliferation may be explained by the different charges of the two groups of designed peptides. The designed peptides from the SP10 group differ from the SP13 group by comparatively short length, a lower overall positive net charge and the distribution of hydrophobic and positively charged amino acids (Table 1). Nevertheless, toxicity problems have not been unexpected as AMPs are likely to act directly on membranes as described in 1.1.1. Interaction between the cationic SP13 peptide and the anionic components on the cell membrane can be critical for cell proliferation, although mammalian cell membranes are enriched in zwitterionic phospholipids, which are neutral in net charge. Still, α -helical peptides were shown to display hemolytic activity, which correlates with high hydrophobicity, high amphipathicity and high helicity [15, 19]. Other possible reasons for the observed cell toxicity may be the possible incorporation of our designed peptides into the cell, where they could interact with RNA, DNA or proteins. For another peptide of the *de novo* designed peptide series in our lab, SP1-1 (RKKRLKLLKRLN-NH₂), strong interaction with a serine kinase was demonstrated, what indicates membrane crossing and intracellular interaction possibilities at least for this peptide [46]. This assumption is however contradicted by the finding that within 67h incubation no peptide-induced changes in cell proliferation were observed (Figure 6). This rather maintains the assumption that the peptides function like detergents on cells by acting directly on the cell membrane via ionic interactions and are consequently inactivated after interaction as shown for co-incubation of the SP13 peptides with Poly I:C (Figure 12). However, the half maximal inhibitory concentrations (IC₅₀) of the designed peptides, which are necessary to inhibit 50% HIV infection *in vitro*, are in the lower range of the applied concentrations of SP13-03 (IC₅₀ = 3,51 ± 0,454 μ M), SP13-11 (IC₅₀ = 3,67 ± 0,12 μ M) or of SP13-14 (IC₅₀ = 1,44 ± 0,144 μ M). Thus we conclude, that the antiviral active concentrations of all tested peptides show no or only little toxic effects towards PBMCs or MoDCs.

5.2. Immunomodulatory features of designed peptides

Early detection of viruses by the innate immune system is critical for successful immune response. Mammalian antiviral immune response is initiated by recognition receptors specific for pathogen-associated molecular patterns such as viral nucleic acids. After recognizing of viral RNA or DNA, pattern-recognition receptors activate signaling pathways that trigger the production of type I interferons and inflammatory cytokines to orchestrate immune responses for virus elimination that are producing the clinical symptoms of a viral infection [93]. Therefore it is necessary to study the potential immunomodulatory properties of our designed peptides in the presence of culture media and thus in the presence of physiologically relevant concentrations of ions and serum proteins. If peptides are neither inducing nor suppressing cytokine secretion under these conditions, they are likely not interfering with the human immune response. In contrary, when the immunomodulatory features of our peptides are distinctive, they may cause adverse effects on the immune system in case of virus infection.

Because of the toxic effects of the SP13 peptides, it was necessary to detect dead cells within the investigated cultures by PI staining and to exclude them from ELISA analysis. However, these dead cells can generate artifacts, which may result in unwanted uptake of fluorescent probes or into nonspecific antibody binding. Therefore we excluded the three highest concentrations of all SP13-derived peptides in the ELISA experiments.

5.2.1. Pro-inflammatory and anti-inflammatory cytokines

Cytokines are a broad and diverse group of small proteins with signaling functions. In humans, they regulate in picomolar concentrations a variety of physiologic functions including inflammation as well as modulating growth and differentiation of different cell types [103, 104]. Cytokines are divided into pro-inflammatory cytokines, which promote inflammation and into anti-inflammatory cytokines, which control the pro-inflammatory cytokine response by suppression mechanisms. Pro- and anti-inflammatory cytokines cooperate in a complex interaction system to regulate the human immune response [102, 105, 106]. In the present work, the impact of our designed peptides on the release of pro-inflammatory cytokines IFN- γ , IL-12, IL-6 and IL-1 β as well as the anti-inflammatory cytokine IL-10 was investigated.

5.2.1.1. Stimulation of PBMCs with peptides triggers release of IL-10

All four HIV-active peptides trigger a comparatively low but significant IL-10 response in PBMCs (Figure 9). IL-10 is categorized as an anti-inflammatory cytokine, that can exert immunosuppressive effects by its ability to suppress genes for pro-

inflammatory cytokines [105, 107]. Moreover, it is also a potent inhibitor of monocyte- and macrophage function [107, 108]. IL-10 is produced by almost every type of cell in the human immune system, including CD4⁺ T-cells, activated CD8⁺ T-cells, and activated B-cells [102, 109].

The enhanced IL-10 production of PBMCs that were treated with the designed peptides indicates a chemokine-like function of our peptides. Chemokines are chemotactic cytokines, a subclass within the cytokine family and function as chemo-attractants, which induce leukocytes migration to the site of infection. Chemokines display two different biological activities: on the one hand side, constitutively expressed, anti-inflammatory chemokines maintain cell homeostasis and on the other hand side pro-inflammatory chemokines induce inflammation as a response to an inflammatory stimulus. When chemokines bind to the corresponding receptor, they trigger, among other reactions, cytokine secretion, apoptosis and cell death [37, 103, 104]. Also naturally occurring human AMPs feature chemotactic and immunomodulatory properties, which play multiple roles in the human immune system [110]. Furthermore, several structural parallels were described between AMPs and chemokines [95, 111]. Regarding human AMPs, there is a controversial debate about whether certain AMPs have evolved from duplication of chemokine genes. However, certain naturally occurring AMPs display chemotactic activities, which function, unlike to the actual chemokines over a wide range of species and only in high peptide concentrations, which correspond approximately to the 100fold or more of the working concentrations that are observed with classical chemokines [37]. Complementary, many chemokines display modest antimicrobial activity [95, 111].

Alternatively, our designed peptides may also be indirectly responsible for the observed effect by inducing an anti-inflammatory cascade via activation of non-chemokine receptors and thus triggering the production of certain cytokines. This is underlined by the immunomodulatory properties of the Cathelicidin-related LL-37, which is an α -helical, cationic human AMP that does not display cysteine residues [13]. Therefore LL-37 resembles the secondary structure and charge of our designed peptides. LL-37 has an impact on pro-inflammatory cytokine levels in various cell types by activating multiple receptors. It is furthermore able to modulate responses to Toll-like receptor (TLR) ligands by forming complexes with LPS [110]. Furthermore, several other naturally occurring AMPs were described to induce the production of cytokines and chemokines from a variety of cell types, including monocytes [37].

5.2.1.2. Stimulation of PBMCs or MoDCs with designed peptides does not trigger cytokine production of IFN- γ , IL-12, IL-6 or IL-1 β

In contrast to IL-10, no enhanced production of IFN- γ , IL-12, IL-6 or IL-1 β production was shown when PBMCs or MoDCs were stimulated with designed peptides (Figure 10; Figure 11; Figure 13; Figure 14; Figure 15). This shows that the designed peptides do not enhance the virus-related immune response, which is associated with these cytokines.

IFN- γ has diverse immunoregulatory effects on various cells, but it is classified as a pro-inflammatory cytokine because it inhibits IL-10 production from monocytes and induces nitric oxide (NO). IFN- γ also promotes cell-mediated cytotoxic responses and makes epithelial, endothelial and other cells capable of antigen presentation [102, 105, 107]. IFN- γ is produced by CD4⁺, CD8⁺, NK cells and T-h₁-cells [102, 107].

IL-6 is described as an inflammatory cytokine because its up-regulation is associated with chronic inflammatory and autoimmune disorders. However, IL-6 also functions pleiotropic, as one of several regulatory effects of IL-6 is inhibition of TNF production, which limits inflammatory cytokine response. Furthermore, IL-6 is categorized as a key growth factor for both malignant and immune cells and is involved in T cell activation and differentiation. A broad range of cells produces IL-6 including mononuclear phagocytes, T cells, and fibroblasts [102, 112].

IL-1 α and IL-1 β are two forms of Interleukin-1, which is a highly pro-inflammatory cytokine especially during viral infection and affects nearly every cell type by increasing proliferation, activating inflammatory responses, and inducing matrix remodeling through the production of neutral proteases. In most studies, the biological activities of the IL-1 α or - β form are indistinguishable. Most cells can both express and respond to IL-1 β in response to some RNA viruses, but synthesis, processing, secretion and activity of IL-1, particularly IL-1 β , are tightly regulated events [93, 113, 114].

IL-12 is also described as important pro-inflammatory cytokine. It triggers cytotoxic T-cells and lymphokine-activated killer (LAK) cell generation and activation, stimulates NK cells and T-cells to produce IFN- γ , increases natural killer (NK) cell cytotoxicity and enhances cell proliferation. IL-12 is produced by activated B-cells, macrophages, and other antigen-presenting cells (APCs), but its production is inhibited by IL-4 and IL-10 [102, 107].

The observation that co-incubation of MoDCs or PBMCs with our designed peptides did not trigger the production of these cytokines indicates good compatibility and no adverse effects of designed peptides on the human immune system, when applied.

5.2.1.3. Co-incubation of PBMCs with PHA and peptides influences IFN- γ and IL-10 production

To test if our designed peptides are suppressing cytokine secretion, supernatants of cells co-incubated with designed peptides and different reagents that act as cytokine stimuli were additionally investigated by ELISA analysis (Figure 8). For determination of the peptide-induced impact on T-cell response, the mitogen Phytohemagglutinin (PHA) was used as stimulus. PHA targets T-cell response and inflammations in mammals, which are naturally induced by immune-activated T helper cells (T_h cells) that initiate the cascade of inflammatory mediators. Normally this cascades are triggered by infection, trauma, ischemia or inflammatory products like endotoxins [105]. A critical role in controlling this inflammation is attributed to regulatory T cells (T_{reg} cells), which display suppressive capacity [115-117].

When PBMCs were co-incubated with SP10-11 and PHA, significant higher release of IL-10 was measured for the three highest applied SP10-11 concentrations (Figure 9). SP13 peptides did not trigger significantly enhanced IL-10 production, although a concentration-dependent increase can be observed in both biological replicates (Appendix, Figure 38; Figure 39).

Additionally, pro-inflammatory cytokine IFN- γ was measured in the supernatants of cells that were simultaneously treated with peptides and PHA. After 24h of PBMC co-culturing with PHA and peptides, IFN- γ production rates were significantly reduced in case of SP10-11 with all applied concentrations (Figure 10). For peptides of the SP13 series also a decrease in the production of IFN- γ was measured, which raises proportionally with increasing peptide concentrations. Still, the suppressive effects observed with low SP13 peptide concentrations are weaker compared to the effects of all applied SP10-11 concentrations. Within the group of SP13 peptides, SP13-14 shows the most prominent suppression (Figure 10).

The suppression of pro-inflammatory IFN- γ in combination with the enhanced anti-inflammatory IL-10 response, like it was observed for SP10-11, clearly indicates a shift of the overall cytokine profile into the anti-inflammatory direction. This is further underlined by the data showing induction of the anti-inflammatory cytokine IL-10 by SP10-11 alone (5.2.1.1). Therefore, we conclude that SP10-11 is inducing an anti-inflammatory cytokine profile in T-cells, and thus shifting the T_h/T_{reg} balance it to T_{reg} side. In regard to patients that are infected with human immunodeficiency virus (HIV), this infection is associated with a progressive depletion of CD4 T-lymphocytes and defective HIV-specific T-cell responses. Especially T_{reg} expansion is observed in case of HIV infection, which is thought to have critical implications in pathogenesis and is further associated with a chronic inflammatory state in progressive HIV disease [118]. Therefore, the clear anti-inflammatory impact of SP10-11 on the cytokine profile of T_h -cells could result in intensifying this negative

inversion of the T_h/T_{reg} balance that is observed in HIV infection. This possible adverse effect of SP10-11 is further underlined by its clear suppression of IFN- γ production. IFN- γ , like IFN- α and IFN- β , was originally identified by its direct anti-viral activity [105]. The secretion of IFNs stimulates up to 300 genes that protect cells from viral infection by retraining viral replication [119]. On the positive side, however, no pro-inflammatory cytokines are induced by SP10-11 (5.2.1.2). Pro-inflammatory cytokines could potentially recruit HIV target cells to the mucosa, when the designed peptides are applied there, which would be a great point of concern [119, 120]. And generally are agents that reduce the production of pro-inflammatory cytokines likely to have an useful impact on clinical medicine [113]. Because our designed peptides are potential candidates for prophylactic surface application on skin and/ or mucous membrane, the aimed application would have no long-term impact on the immune system in contrast to applying the peptides with an injection as an intravenous drug. If the anti-inflammatory features of SP10-11 induce adverse or beneficial effect upon HIV infection in patients cannot be concluded on basis of the available information. This question has to be answered by *in vivo* experiments.

Co-incubation of PHA and SP13-derived peptides with PBMCs results in decreased production levels of IFN- γ as well as slightly increasing IL-10 production (Figure 10). However, with PBMC4 analysis, no clear increase of IL-10 secretion was observed when stimulated with PHA and SP13 peptides (Appendix, Figure 38). Generally, the suppression of IFN- γ is much less pronounced when PHA is co-incubated with the peptides of the SP13 series than with SP10-11. Furthermore, in contrast to SP10-11 the decrease in IFN- γ production was shown to be proportional to increasing SP13 peptide concentrations. Because chemokines are active in picomolar range [103, 104], this concentration-dependent measurements hint, that the cell-toxic effect, which is induced by the SP13 peptides may be responsible for cytokine suppression. The cell toxic features of SP13 peptides are likely to damage the surviving cells in a way that cytokine production is negatively impacted. This is underlined by the finding that the suppression of IFN- γ corresponds to the cell-toxicity of the SP13 peptides: the strongest IFN- γ suppression within all peptides of the SP13 series is induced by SP13-14, the SP13 peptide with the most adverse effects on PBMCs, followed by Sp13-11 and finally SP13-3, which shows the lowest cell-toxicity towards PBMCs (Figure 10). Furthermore, the possibility of interaction of the peptides with PHA cannot be ruled out. This interaction might change concentration level of PHA stimulus and peptide at the same time. This arbitrary assumption is undermined, however, by the cell viability measurements of cells treated with PHA. Here, no differences in cell viability between treated and water-treated cell could be measured. Because the peptide-induced cell-toxic effects are very well reproducible,

this indicates no change in peptide concentration and therefore no interaction of the SP13 peptides with another molecule. Because SP10-11 does not show cell-toxic effects, this conclusion does not, however, apply to SP10-11.

Nevertheless, T-cells proliferate in response to PHA stimulation through activation of the mitogen protein phosphorylation pathway, the alterations in cytokine production induced by SP10-11 and SP13 peptides in combination with PHA stimulation also suggests that the designed peptides may impair T-cell proliferation. Therefore in further experiments, the PBMC proliferation after peptide treatment has to be investigated.

5.2.1.4. Co-incubation of PBMCs with LPS and peptides influences IL-10 production differently between SP10 and SP13 peptides

Gram-negative bacteria or more precisely, the lipopolysaccharide (LPS) component of their outer cell wall, is a very potent activator of macrophages, which induces IL-10 and IL-12 production [109]. Unlike PHA, LPS induces the cytokine response of antigen presenting cells (APCs). Also for APCs the designed peptides may act directly or indirectly as chemokines, as described for T-cell response stimulated by PHA.

When PBMCs were co-stimulated with peptides and LPS, SP10-11 again enhances significantly the LPS-induced IL-10 production. With all SP10-11 concentrations a trend to enhanced IL 10 production was observed in both biological replicates (Appendix, Figure 40; Figure 41). In a clear contrast to SP10-11 all three SP13 type peptides heavily suppress the LPS-induced IL-10 release in all applied concentrations (Figure 11; Appendix, Figure 40; Figure 41).

Reduced IL-10 rates in presence of SP13 peptides might be based on their cell-toxic effect, as previously described (5.2.1.3). However, in case of antigen-presenting cells, the suppression of IL-10 by the SP13 peptides seems to be concentration-independent, which rather hints to function as chemokines. Naturally occurring AMPs have the ability to neutralize endotoxins like LPS by strong binding to LPS aggregates and thus preventing LPS from binding to its receptor, which would result in pro-inflammatory cytokine secretion [12, 121]. Therefore, SP13 peptides may also interact with LPS directly and thus introducing the lower IL-10 production levels. But there is one main objection against this assumption: no differences in cell viability between LPS stimulated and water-treated cell could be measured, which diminishes the possibility of interaction of the peptides with the LPS stimulus, as described in 5.2.1.5.

The pro-inflammatory IL-12 cytokine response when peptides were co-incubated with LPS was neither in MoDCs nor in PBMCS measurable. Thus, no statement can be made at this point regarding APCs on the influence of the pro-inflammatory cytokines by our designed peptides. However, when MoDCs were incubated with Poly I:C, IL-12 response was detectable (Figure 15; 5.2.1.5).

5.2.1.5. Incubation of MoDCs with or without Poly I:C influences several cytokine production levels

Cytokines IL-1 β , IL-6 and IL-12 were analyzed for MoDCs that were stimulated with Poly I:C and designed peptides. Polyinosinic:polycytidylic acid (Poly I:C), a synthetic double-stranded RNA is used to simulate viral infections *in vitro* [122, 123]. Poly I:C induces among others IL-6, IL-1 β and IL-12 cytokine production. Due to its RNA nature, Poly I:C is negatively charged in cell culture medium, whereas our peptides display an overall positive charge. Furthermore, interaction with viral RNA is also a possible mechanism of action regarding antiviral activity of our designed peptides [16, 21]. Therefore both molecules may directly react between each other by ionic interactions.

Comparing cell viability of Poly I:C treated and control cells, it was observed that SP13 peptides display lower, concentration-dependent impact on cell viability in the presence of Poly I:C (Figure 13). This observation is likely due to interactions of peptides with Poly I:C. Because SP10-11 has no adverse effects on cells, no reliable statements can be made in this case. Thus for all ELISA results for cells that were co-incubated with peptides and Poly I:C, it has to be considered, that the concentration of the peptides and Poly I:C may be diminished due to inactivation by interaction.

Data of MoDCs stimulated simultaneously with Poly I:C and different peptide concentrations show that SP13 peptides inhibits IL-12, IL-1 β and IL-6 release in all analyzed cell cultures, whereas SP10-11 did not show any suppressing or stimulating effects (Figure 13; Figure 14; Figure 15). This is consistent with the overall charge differences between the SP13 peptides and SP10-11 (Table 1) and thus supporting the interaction assumption that is responsible for reducing Poly I:C concentration in the SP13 treated cell cultures, which results in lower cytokine release due to diminished Poly I:C concentrations. These considerations are underlined by the finding that in case of IL-12 and IL-1 β measurements, the SP13-11 and SP13-14 induced inhibitory effects are proportional to increasing peptide concentrations. However, in case on ionic interactions of the SP13 peptides with Poly I:C, SP13-3 and SP13-14 would be expected to show the same suppression profile because they display exactly the same charge. In accordance, SP13-11 should feature lower impact as it is slightly less positively charged (Table 1). In contrast to these considerations, SP13-11 did not show a comparatively higher cytokine release rate for all three analyzed cytokines.

Furthermore, in case of IL-6, SP13-3 and SP13-11 induced suppression level seems to be independent of the applied concentration. Here, treatment with SP13-3 displayed the lowest IL-6 production levels, whereas SP13-14 showed the highest production levels of the SP13 peptides. Also the suppression of IL-1 β production

induced by SP13 peptides is clearly not concentration dependent in both biological replicates (Figure 15).

To sum up, the suppressed cytokine release levels for IL-12, IL-6 and IL-1 β that are introduced by co-incubation of SP13 peptides and Poly I:C are likely due to ionic interaction of Poly I:C and the specific peptides. But because not in each analysis concentration-dependent suppression profiles were observed, a direct suppression of these cytokines by SP13 peptides cannot be excluded.

5.2.2. Conclusion regarding immunomodulatory activities

In summary, all peptides that were tested in this work induced low IL-10 secretion but did not trigger IL-6, IL-12, IFN- γ or IL-1 β production. SP10-11 induced a shift of the cytokine profile to the anti-inflammatory direction in T-cells, whereas in APCs only an enhancement of anti-inflammatory IL-10 production was detectable. In MoDCs, no changes are induced for Poly I:C stimulated cytokine production by SP10-11 for IL-6, IL-12 and IL-1 β , whereas for these observation an interaction of SP10-11 with Poly I:C cannot be ruled out.

In case of the peptides from the SP13 series, immunomodulatory effects on T-cells resemble a weaker version of the SP10-11 induced effects but cannot be entirely distinguished from the side-effects of their cell toxicity. In APC, SP13 peptides show clear suppression of IL-10, which is the opposite effect on APCs compared with SP10-11. In MoDCs, which were stimulated with Poly I:C and SP13 peptides, suppressive effects are likely due to interaction of peptides with Poly I:C, which may give a hint for a possible mechanism regarding antiviral activity of SP13 peptides. All trends for peptide-induced impact on cytokine production are summarized in Figure 28.

Cell type	Stimulation	ELISA results	
		SP10-11	SP13 peptides
PBMCs	peptides	IL-10 \uparrow IFN- γ \rightarrow	IL-10 \uparrow IFN- γ \rightarrow
	peptides + PHA (T-cells)	IL-10 \uparrow IFN- γ $\downarrow\downarrow$	IL-10 \uparrow IFN- γ \downarrow
	peptides + LPS (APC)	IL-10 \uparrow	IL-10 \downarrow
MoDCs	peptides	IL-6 \rightarrow IL-12 \rightarrow IL-1 β \rightarrow	IL-6 \rightarrow IL-12 \rightarrow IL-1 β \rightarrow
	peptides + Poly I:C	IL-6 \rightarrow IL-12 \rightarrow IL-1 β \rightarrow	IL-6 \downarrow IL-12 \downarrow IL-1 β \downarrow

Figure 28: Overview of all ELISA results indicating immunomodulatory properties of the designed peptides. Green arrow: enhanced cytokine production. Red arrow: diminished cytokine production. Black arrow: no influence on cytokine production.

It is important to note that in this work only a limited set of soluble immune factors have been evaluated, which were likely to be influenced by our designed peptides.

Other cytokines that play a role in immunomodulation may be influenced accordingly. Therefore, further investigations regarding the mechanism of cytokine production from PBMC, MoDCs and additional specific cell populations stimulated by designed peptides should be conducted.

5.3. Transplastomic plants as production platform

5.3.1. Design and construction of the expression cassette

Plastome transformation in plants and production of heterologous proteins in chloroplasts is a techniques used since two decades. Thus, many publications on this subject describe various chloroplast transformation vectors. The typical plastid transformation vectors consist of gene of interest (GOI) and a selectable marker,

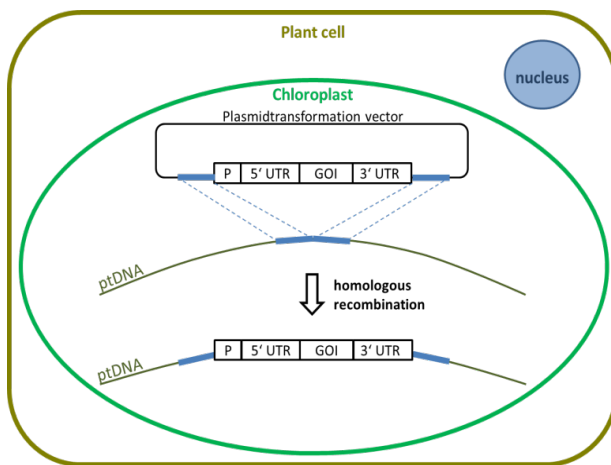


Figure 29: Targeting a transgene expression cassette into the chloroplast genome. The expression cassette consists of a gene of interest (GOI), which coding sequence is downstream of a chloroplast promoter (P) and the according 5'-untranslated region (5'-UTR). A 3'-untranslated region (3'-UTR) is fused to the 3' side of the GOI. The expression cassette is flanked by endogenous chloroplast DNA sequences (indicated by a thick, blue line), that targeting the recombinant expression cassette into the chloroplasts genome. Insertion is accomplished by homologous recombination events.

most commonly the aminoglycoside adenyltransferase (*aadA*) gene conferring resistance to spectinomycin, which enables selection of transplastomic callus. Additionally, specific cis-acting elements containing chloroplast promoter with the according 5'- and 3'-untranslated (UTR) sequences as well as flanking sequences that determine the plastome locus for integration are necessary elements in every chloroplast transformation vector. In this work plasmid transformation vectors (PTV) were designed in cooperation with the AG Koop, LMU. Our locus for homologous integration into the tobacco ptDNA is targeting intergenic spacer region in the inverted repeat (IR) between the *orf131* and *rps12* genes (Figure 16).

This region represents an intron with no read-through transcription and is one of the most commonly used intergenic regions for targeting transplastomic insertions in tobacco [70, 73]. Endogenous promoters of the *psbA*, 16S rRNA (*rrn*) and the *rbcl* genes in combination with their native 5'- and 3'-UTRs, that are derived from plastid genes have been extensively used for constitutive expression of heterologous genes in plastids of higher plants [77]. Therefore we introduced as new feature the heterologous *psbA* promoter with

the respective 5'-UTR as well as the 3'-UTR from *Chlamydomonas reinhardtii* (*C. reinhardtii*), because by reducing the degree of direct homology, unwanted recombination between genomic and introduced sequences is avoided (Table 4). It has been reported that promoters and 5'-, respectively 3'-UTRs were adopted from endogenous as well as heterologous ptDNA and plastid regulatory sequences derived from non-endogenous plastid genomes have also been applied successfully [73, 77]. Even the 5'-UTRs of mitochondrial *atpA* gene, the bacterial *trc* gene and the bacteriophage T7 *tg10* enable translation in higher plant chloroplasts [1, 4, 69]. Furthermore, evidence hints that the *C. reinhardtii* PpsbA with its according 5'-UTR is functional in tobacco [89]. To confer stability and avoid toxic effects of the recombinant peptides, they are fused to green fluorescent protein (GFP) with an n-terminal 6xhistidine tag (Figure 16; Table 4). These fusion partners are expected to aid in purification and to serve as reporter for quantification. Moreover, GFP is reported to be a soluble produced visual marker in plastids [77].

5.3.2. Selection process

In the present work, we aimed to achieve homoplasmy by cultivating putative heteroplasmic callus for altogether 26 weeks on a selective medium and thus gradually diminish non-transformed plastids (Figure 18).

Chloroplast DNA differs in many respects from nuclear DNA, including different melting and renaturation behavior, deviating GC content and the absence from 5-methylcytosine. It also displays numerous prokaryotic features like organization of genes in operons, polycistronic transcripts and a prokaryotic gene expression machinery [124]. The entire complement of genetic material within the chloroplast is generally mapped as a single circular molecule, although as a matter of fact it shows great structural dynamics: Chloroplast DNA consists from a high number of ptDNA copies [64], whose size are in the range of 120 to 160 kb [81, 125]. Due to its eubacterial origin, these multiple

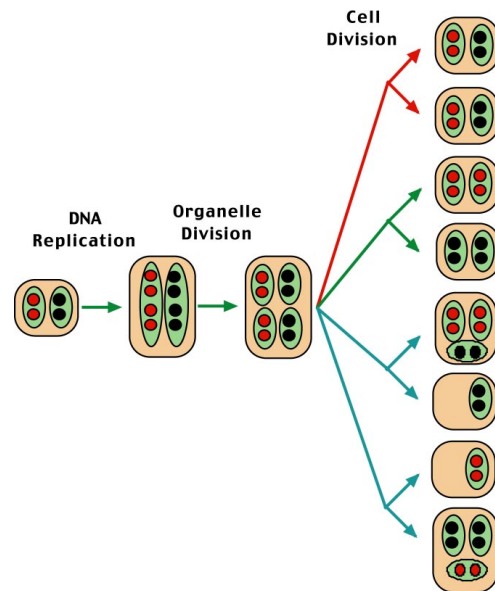


Figure 30: Distribution possibilities of an inserted transgene during organelle division in plastids after Birky Jr et al. Heteroplasmic plant cells display two chloroplasts, one with two wild-type genomes (*black circles*) and one with two mutated genomes (*red circles*). Within organelle division, the genomes are partitioned equally. When the cell divide, several possibilities for organelle distribution are assumed: organelles are partitioned numerically equally (*red and green arrows*) or unequally (*blue arrows*) [6].

copies of the ptDNA are packed in large nucleoprotein bodies, which contain additionally proteins and RNA. Per chloroplast about 5–15 nucleoids are attached in clusters to the intraplasmidial membranes of the chloroplast. Therefore, the ploidy level of the plastome in a single cell can be up to thousands of genome copies [124, 126, 127]. With the biolistic transformation approach, the homologous recombination event only affects one, or in the best case, a few ptDNA within a single chloroplast, which possesses tens to hundreds of ptDNAs. However, it was shown, that a genome with a new mutation increases in frequency under selection pressure to finally achieve homoplasmy [6, 124, 126]. Selection of partly transformed chloroplasts is possible because firstly, plastids can divide as distinct organelles within the cytoplasm of the eukaryotic cell in a similar manner as bacteria. The two resulting daughter cells receive equal or different numbers of chloroplasts and strictly random sample of the chloroplast genotypes (Figure 30) [6, 126]. Secondly, plastid translation has been demonstrated to be essential for cell survival in tobacco and spectinomycin inhibits ribosome translation within chloroplasts [124].

In this work, bombarded tobacco tissue was cultivated for 13 weeks on selection medium (Figure 18), whereas in week 8 to 12 resistant shoots emerged (Figure 22). In total, 185 putative transplastomic shoots were isolated, of which 117 shoots did not bleach out when subcultured on fresh selection medium, but only 14 shoots turned out to be transplastomic transformants (Table 22). Also isolated shoots were cycled for another 13 weeks (Figure 19), because the preferred method to obtain homoplastomic tobacco plants is regenerating new shoots from the transplastomic sectors and thus delaying plant regeneration until plastid segregation is complete [81]. Nevertheless, longer selection periods were avoided because extended propagation of cells in tissue culture results in chromosome rearrangements and polyploidization and it is estimated that after 20 cell divisions the homoplastomic state can be attained [81]. Homoplasmy was not achieved by the above described selection process as demonstrated by southern blot analysis. Instead it was shown, that homoplastomic transformants were only present in the F1 generation (Figure 24). Seed production was not only crucial for maintaining and storage of the stably transformed plant lines, but it is also an alternative way to ensure the homoplastomic nature of the transformants as homoplastomic plants can also be obtained by seed progeny. Transplastomic cells are also present in the cell layer of the maternal germline [81], therefore homoplastomic plant can be distinguished by germination of seeds from F0 plants on selective agar (Figure 22). Still, the effects of polyploidization, which heavily affects plant fertility, were observed in seed production as several of the F0 plant did not produce seed.

When transplastomic cells are selected by the *aadA* gene, plastid transformants rates of one transplastomic shoot (on average) per bombarded leaf are reported [70]. In

this work, a comparatively small overall efficiency of 0,175 transplastomic shoots per bombarded leaf after 13 weeks of selection was observed (Figure 22). This poor transformation rate may be due to a new generation of macro carrier, which was used for particle gun transformation. These carriers show a change in surface tension with the side effect of a greater spreading of the gold-DNA-suspension. Also the unavoidable change light and temperature conditions due to chamber failure during the selection process may be a negative influence. Also the handling of the cycling procedure during selection may have not been ideal as a lot of recovered shoots bleached when cut out and placed in direct contact with the selective medium.

All recovered shoots were putative heteroplastomic chimeras, as spectinomycin resistance is not cell autonomous. Shoots with an resistant (green) phenotype consists mainly from a combination of transformed and non-transformed sectors due to cross-protection [81]. However, transformed and nontransformed sectors are described to be identified by green fluorescent protein (GFP) accumulation, even in the state of heteroplasmy [81]. Still, in all transplastomic plants that were produced in this work no GFP was detectable, although southern blot and PCR analysis confirmed chloroplast insertion (Figure 21; Figure 24) and RT-PCR confirmed transcription (Figure 26). Furthermore, several homoplastomic plants in the F1 generation were confirmed for the constructs in the vectors PTV T20 NH, PTV 13-14 NH and PTV gfp PK. Furthermore, heteroplastomic existence was shown for one plant (PTV T20 NH) in the F1 generation and loss of insert was documented for two plants (Figure 24). Heteroplastomic nature can be explained by the fact that daughter cells do not always receive equal numbers of organelles, and consequently, some plastids may have to divide more often than others to restore equality. Thus, transformed and untransformed plastids together can be inherited from the maternal germline and in the absence of antibiotic selection both plastid types are maintained in heteroplastomic tobacco cells [81]. Loss of the transgene, however, can be explained by internal homologous excision. Plant chloroplasts display the enzymatic machinery required for recombination and therefore intramolecular and intermolecular recombination is possible [6].

However, total soluble protein (TSP) of all transplastomic plant lines was analyzed by SDS page. Here, no enriched protein of the expected size was detectable with Coomassie- or Ponceau staining. Also after immunodetection using anti-histidine antibody or anti-gfp antibody, no recombinant protein was found (Figure 25; Figure 27) even with 100 µg TSP loaded or by enrichment of gfp-fusion proteins by Epitope-Tag Isolation Kit (µMACS, Miltenyi Biotec GmbH, Germany). Because developmental signals and light conditions may play a role regarding control by *psbA* promoter, we additionally tested all plants F1 generation for recombinant protein production, which were germinated and grown on soil in a culture chamber in controlled light conditions

(Figure 27). However, we get the same results as for the plants of the F0 generation. Thus it is virtually certain that there is no translation of the recombinant protein in our transplastomic plants.

5.4. Possible causes of translation inhibition

Regarding recombinant protein production in chloroplasts, highly different yields are described in literature. Reasons for this include various determinants at transcriptional, translational and post-translational levels, which are namely mRNA stability, mRNA-rRNA interactions, appropriate codon usage, efficient processing of polycistronic transcripts, N-terminal amino acid residues and sequences downstream the initial methionine of the nascent polypeptide chain, as well as translation initiation via 5'-UTR [70, 73].

For accessing the reasons for inhibition of recombinant protein production, we first investigated possible loop-outs in consequence of the homologous recombination, because intramolecular and intermolecular recombination is possible in chloroplasts [6]. Therefore we sequenced PCR-Products of total plant DNA of the transplastomic plants (Figure 21; Figure 26) and thus excluded putative loop-out of important elements. Thus we took a closer look at the sequence of our fusion protein. Because the GFP fusion partner was cloned from Gateway-Vector pB7FWG2, which is not designed with the specific tobacco chloroplast codon usage, several codons within our gene of interest are not the ideal choice for high-level production. However, although only 30 tRNAs are encoded in the plastome, it is assumed, that all codons are translated within chloroplasts, which is presumably achieved by extensive four-way-wobble between the third codon position and the 5' nucleotide of the anticodon in the tRNA. [124]. And even if the codon usage is indeed not ideally suited, this would only explain minor changes in production level but not complete inhibition like observed in the this work.

Silencing, which is defined as mRNA interfering gene regulation via antisense RNA (asRNA), is very common in prokaryotes, which express both cis- and trans-encoded antisense transcripts [128]. Although chloroplasts have also the potential to utilize natural asRNAs for gene regulation, it was not demonstrated so far [127, 129-131].

Because transcription was shown in all transplastomic plants (Figure 26), the underlying mechanism for inhibition of recombinant protein production was narrowed down to on the one hand fast degradation of the fusion protein after being translated or on the other hand to malfunction of the translation initiation step.

During evolution, chloroplast gene expression changes from the mostly transcriptional regulation of its prokaryotic ancestor to a mainly posttranscriptional regulation. Therefore for chloroplasts the most important tools for protein

accumulation are the regulation of transcript stability, the translation initiation, protein turnover, and protein activity [3].

5.4.1. Degradation in chloroplasts

De Marcis wrote 2012, that the steady-state level of a recombinant protein, whose gene is inserted into the plastome, cannot be predicted beforehand, which is due to the limited knowledge regarding the maintenance of protein homeostasis, or proteostasis in plastids [132]. Furthermore, next to successful and high-yield production of recombinant protein in chloroplasts, also some examples are reported for low or even undetectable protein accumulation, which is likely the result of degradation processes [133, 134]. Although chloroplast protein degradation mechanisms are known to influence strongly protein accumulation in chloroplasts, most factors, which determine protein stability, are unknown to date. Still, in higher plants the major stability determinants are located in the N-terminus [135].

In this work different developmental stages of the transplastomic plants including very young leaves, seedling, that were just germinated and also callus from tissue cultures were tested for recombinant protein production. All approached showed failure in recombinant protein production at Western Blot detection level. If protein degradation is indeed responsible for inhibition of protein production in our transplastomic plants, this degradation process happens very fast. However, these results rather indicate that degradation is not the reason that prevents recombinant protein accumulation. Furthermore, we added a positive control consisting of PTV gfpPK to our plastid transformation experiments (Figure 16), which only introduces the gene encoding the soluble gfp protein with an n-terminal His-tag into *N. tabacum* chloroplasts. But also the transplastomic plants that were transformed with PTV gfp PK, did not show any GFP production, although it has been demonstrated that GFP and GFP fusion proteins are very well producible as soluble protein within tobacco chloroplasts [77]. Therefore we exclude that the fused peptide respectively the T20 are the reason for inducing fast degradation of the recombinant protein. Moreover, tobacco is able to produce fusion protein consisting from GFP::10-11, GFP::13-3, GFP::13-11 or GFP::13-14, as it was shown by transient production platform Icon Genetics [90] and for designed peptide SP1-1 by a full virus vector strategy approach in our lab [47].

5.4.2. Inhibition of translation initiation

Translation initiation is a key regulatory step and an important control element for *psbA* gene expression, as inhibition of plastid transcription with rifampicin has no effect on protein synthesis for the highly expressed *psbA* gene [136]. The regulation of the translatability of chloroplast transcripts entails the concerted action of RNA

structures and sequence motifs, which are found mostly in the 5'-UTR of the mRNA and of nucleus-encoded transacting proteins [3].

In our constructs the 3' UTR of the GOI, the *psbA* promoter and its according 5'UTR are derived from the green algae *C. reinhardtii* (Table 4) but inserted into chloroplasts of the higher land plant *N. tabacum* (Figure 31).

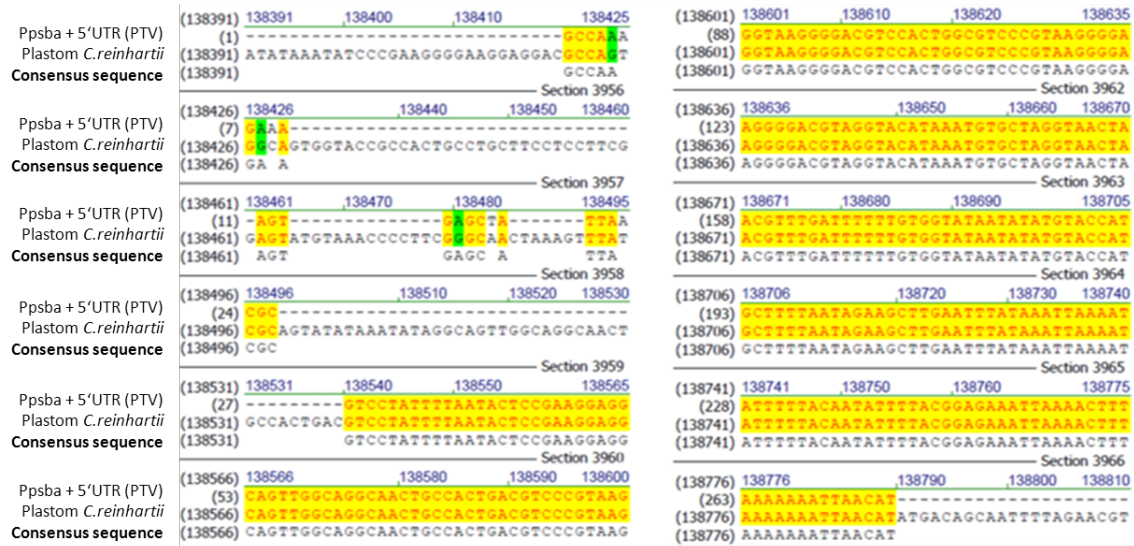


Figure 31: Alignment of *C. reinhardtii* plastome and *psbA* promoter with according 5'-UTR of PTVs. Promoter sequence start at 138540 in *C. reinhardtii* and *PsbA* gene start codon is placed analogously to the gene of interest in all PTVs.

The possibility, that the regulatory mechanisms of the translation have diversified during chloroplast evolution is underlined by the non-conserved position of the Shine-Dalgarno (SD) ribosome binding site in different chloroplast transcripts and the fact that existing SD sequences are not always necessary for translation initiation [3, 137, 138].

Generally, translation in the chloroplast resembles still the prokaryotic translation but became uncoupled to transcription and turned into a highly regulated process [3], which requires a complex interaction with nuclear factors [136]. Chloroplast ribosomes differ from the 80S ribosomes found in the cytosol and appear rather in accordance to bacterial 70S-ribosomes regarding size as well as antibiotic sensitivities, initial fMet-tRNA and associated mRNAs that are lacking the eukaryotic 5'-cap [3, 136]. Although the major part of investigated chloroplast ribosomal subunits resembles similarities to bacteria, some differences have been demonstrated: the small and the large ribosomal subunits in spinach display plastid specific ribosomal proteins (PSRP-1 to PSRP-6) with no homologs in the bacterial ribosome and also in green algae ribosomes, three proteins S2, S3, and S5 that have analogues in prokaryotes, display additional, large domains, which are not found in bacteria [139-143].

Translation initiation of both eukaryotes and prokaryotes begins with two key steps: first step involves the binding of the mRNA by the ribosomal small subunit. The second step is the selection of the proper initiation codon. In eukaryotic translation these steps are separate, while in prokaryotic translation, they are combined [3]. Also within the mechanism of translation initiation in chloroplasts prokaryotic and eukaryotic characteristics are present (Figure 32). The translatability of chloroplast mRNAs depends on sequence motifs of the 5'-UTR and of interaction with nucleus-encoded transacting proteins [3, 70, 144]. Several publications illustrate this important regulation mechanism, as the protein accumulation from the same promoter may vary as much as 10,000-fold depending on the choice of translation control signals within the 5'-UTR [136, 144-147]. Due to the nuclear trans-acting protein factors, translation rates in chloroplasts are influenced by environmental and developmental cues including light and redox poise [3, 148]. Many nucleus-encoded RNA-binding proteins have been identified as essential for the translation of specific chloroplast mRNAs [3, 149, 150] and it has been demonstrated that these proteins bind to different regions of the 5'-UTR [3, 136]. The principle of translation initiation involving stem loop 5'-UTR as well as protein trans-acting factors is known from mammalian cellular mRNAs and also from various RNA viruses where the stem loop RNA motif in the 5'-UTR was designated internal ribosome entry element (IRESes) [151]. IRESes allow the formation of complex secondary structures in the mRNA 5'-UTR, which can associate with the small ribosomal subunit [152]. A crucial difference from chloroplasts to prokaryotic translation initiation is the role of Shine Dalgarno Sequence (SD, 5' AGGAGG 3'), as mentioned above. In chloroplasts, anti-SD sequences are conserved among the 3' end of the highly conserved 16S rRNAs from chloroplast ribosomes of higher plants, green algae and cyanobacteria [3]. Nevertheless the correct distance of SD sequence to the initiation codon, which is crucial in prokaryotes, is variable in most chloroplast mRNAs [137]. Accordingly, the SD sequence turned out to be only essential for some genes, whereas for other genes replacement of SDs had little or no effect [136]. All this indicates that within chloroplasts there might be more than one way for initiating translation. As the positioning mechanism is not fully understood yet, three different model for translation initiation are suggested, depending on the different 5'-UTRs of the individual mRNA (Figure 32) [3]. Firstly, for some mRNAs, translation initiation may occur in the classical prokaryotic way with an essential SD sequence that is in a conserved position within the 5'-UTR (Figure 32, A). Secondly, there might be alternative sequences used for rRNA pairing in absence of SD within the 5'-UTR, which may be complementary to alternative regions of the 16S rRNA [153] (Figure 32, B). And thirdly, SD-like elements might not be necessary for translation in some cases and translation may be initiated only by RNA cis-elements that form the

secondary structures in the 5'-UTRs together with trans-acting factors which would subsequently recruit the ribosome in an eukaryotic-like scanning mechanism which directs the initiation complex to the initiation codon [3, 136, 154, 155] (Figure 32, C). All these ways of initiating translation may require one or more nucleus-encoded trans-acting factors, which is possible species-specific. The absence of these transacting factors from *C. reinhardtii* nucleus in transplastomic tobacco is therefore a likely explanation for the failure of translation initiation in our plants. This makes the *psbA* promoter and the according 5'-UTR of our constructs an obvious candidate for production inhibition.

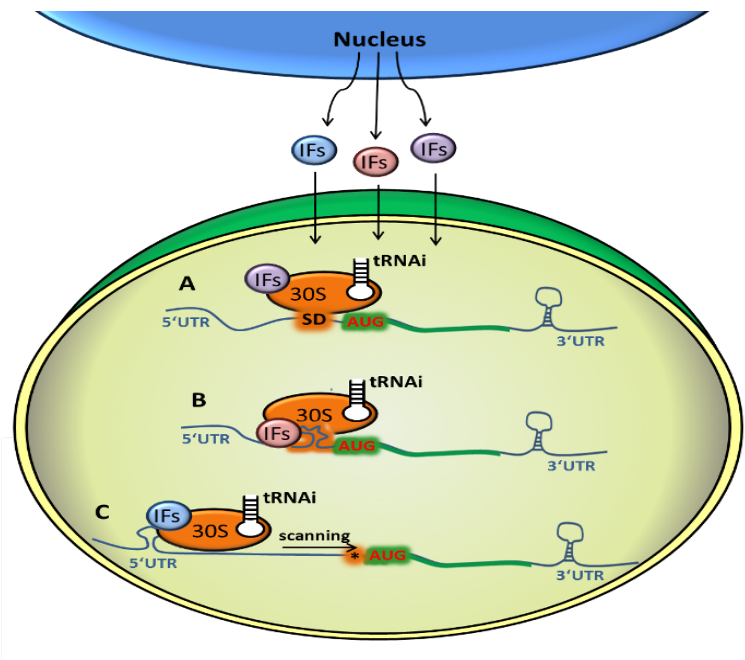


Figure 32: Theoretical models for translation initiation in the chloroplast from Peled-Zehavi *et al.* [3]. Initiation transacting protein factors from the nucleus are labeled IFs. (A) Prokaryotic-like way of translation initiation with two RNA-RNA interactions stabilizing the 30S pre-initiation complex at the proper initiation codon by association of the SD-sequence and the anti-SD of the 16S ribosomal RNA in the small subunit and the codon-anticodon interaction between initiator fMet-tRNA and the initiation codon, possibly supported by IFs (B) In 5'-UTR lacking the SD-sequence, secondary structure elements together with IFs arrange the initiation complex at the correct position. (C) Translation initiation in a similar way as in eukaryotes: Binding of IFs to a cis-acting sequence in the 5' UTR initiates the formation of the initiation complex. A related helicase activity enables the ribosome to scan for the correct initiation codon, though this scanning process is likely to require a functionally analogue to the Kozak sequence.

In chloroplasts, *psbA* promoter regulates the photosynthetic protein D1, which is synthesized on thylakoid membrane bound polyribosomes and assembled co-translationally into the membrane [3, 7]. Thus the overall production of the D1 protein is regulated at the level of translation elongation as *psbA* mRNA is translated through an interaction between specific RNA sequences and RNA-binding proteins.

Like in other chloroplast transcripts also the 5'-UTRs of *psbA* contain an abundance of essential structured and unstructured cis-acting elements for post-transcriptional regulation that interact in a specific manner with trans-acting proteins which may be currently unidentified nuclear-encoded proteins [1, 7]. Translatability of D1 seem to be mainly dependent from these *cis*-elements as it was shown for *psbA* in *C. reinhardtii* chloroplasts as well as in *N. tabacum* chloroplasts [3, 154]. 5'-UTRs of the *psbA* genes in *C. reinhardtii* and *N. tabacum* differ clearly regarding regulatory cis-elements (Figure 33).

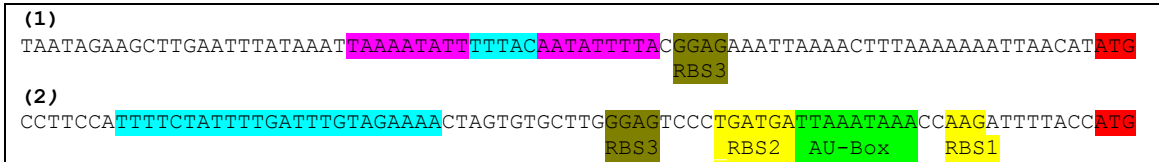


Figure 33: Regulatory regions in *psbA* 5'-UTR of *C. reinhardtii* and *N. tabacum* differ strongly. (1) *PsbA* 5'-UTR of *Chlamydomonas reinhardtii*. Potential Shine Dalgarno-like ribosome binding sequence (RBS3) are marked in dark green. Predicted hairpins are labeled in pink, loop regions in turquoise, start codon of D1 protein in red [1, 2]. (2) *PsbA* 5'-UTR of *Nicotiana tabacum*. RBS1 and RBS2 are marked in yellow, SD-like sequence RBS3 in dark green, stem loop region in turquoise, AU-box in light green, start codon of D1 protein in red [4, 5]

5.4.2.1. Cis-acting elements and trans-acting factors in *Nicotiana tabacum psbA* mRNA

The *psbA* gene in *C. reinhardtii* displays Group I introns, whereas in tobacco *psbA* is an intron-less chloroplast gene [7, 154][19]. High amounts of *psbA* mRNA are present in all green tissues of higher plants even in darkness due to the strong *psbA* promoter and the very stable *psbA* mRNA. Translational regulation is the most prominent step in the regulation of higher plant *psbA* gene expression and it is regulated via *psbA* 5'-UTR [156]. The 5'-UTR of the tobacco *psbA* gene has been analyzed in detail. It consists of a -10 and -35 region interspersed by a single TATA-boxlike element, and the transcription is initiated in a single defined site (Figure 33). In higher plants translation is tissue-specific, light depending and moreover, affected by the developmental stage of the plant [7]. Thus it is indicated that in all higher plant chloroplasts the expression of the *psbA* gene is regulated via a complex interaction with nuclear factors, which are influenced by the above described conditions, to control at the level of translation. Several trans-acting, RNA-binding proteins have been reported to be essential for the translation of chloroplast transcripts, while binding to different regions of the 5'-UTR [7]. Some of these regulatory trans-acting proteins in *N. tabacum* were identified. They are termed HCF173, 47 kDa, 43kDa, 38 kDa and 37 kDa (Figure 34) and were shown to bind to the 5'- and the 3'-UTR of the *psbA* transcript in a light-dependent manner. However, the exact mechanisms how these trans-acting factors influence D1 production, are

unknown to date (Figure 34, B) [7]. Several assumptions were made regarding the thus unleashed mechanisms including possible changes in the tertiary structure of the transcript for positioning the AUG on the small subunit of the ribosome or similarities to the eukaryotic scanning mechanism (Figure 32) [136]. The broad variety of proteins, which are involved in the regulation of *psbA* gene expression hints the various and different initiation mechanisms that are possibly involved [7]. In *N. tabacum*, three elements within the 5'-UTR were described as crucial for translation that are termed RBS1 and RBS2 and an AU Box. All these elements are missing in *psbA* 5'-UTR of *C. reinhardtii* (Figure 33) [5, 144, 157]. Interestingly, SD-like sequence (RBS3), which is located downstream of the RBS1 and RBS2 has comparatively little effect on translation efficiency. RBS1 and RBS2 are complementary to the 3' terminus of chloroplast 16S rRNA and thus binding 16S rRNA cooperatively, as the deletion of both elements has a more severe effect than single deletion of each region. This results in looping out of the AU box, which is located between RBS1 and RBS2 (Figure 33). After looping out, the AU box probably binds various nucleus-encoded trans-acting factors, of which some are critical for the translation initiation. Therefore RBS1 and RBS2 are proposed to constitute a bipartite SD sequence responsible for the ribosome-mRNA association. Furthermore, studies with an *in vitro* chloroplast translation system showed that the position of RBS1 and RBS 2 sequences relative to the initiation codon strongly influence translation initiation [3, 5, 144, 157].

5.4.2.2. Cis-acting elements and trans-acting factors in *Chlamydomonas reinhardtii* *psbA* mRNA

In case of *C. reinhardtii* chloroplasts, a tight correlation between processing of *psbA* transcripts and ribosome association is reported. This main processing event takes place at position -36, within a conserved stem loop, which was identified previously as an important structure for D1 expression and just upstream of a consensus Shine-Dalgarno-like sequence resembling RBS3 in *N. tabacum* (Figure 33). Disruption of RBS3 or sequestration by base pairing with a mutation inhibits *psbA* translation and severely reduces RNA stability in *C. reinhardtii* [155, 158]. Furthermore, in *in vitro* experiments, the elimination of the stem-loop region, which is placed upstream of the RBS3 (Figure 33) does not influence the translation of *psbA* mRNA upon illumination, which indicates that only the SD-like sequence RBS3 is necessary for *psbA* translation and RNA stability in *C. reinhardtii* [3]

However, nucleus encoded transactors were also found in *C. reinhardtii*. They are categorized in four major transacting proteins, which form a translation initiation complex as well as several minor proteins. The major proteins are termed RB38, RB47, RB55 and RB60 and form a complex called *psbA* 5'PC. *psbA* 5'PC enhances translation in dependence of an increased redox potential as well as a lower ADP/ATP

ratio, two parameters that directly correlate to high light and photosynthetic activity. The level of binding of *psbA* 5'PC to the mRNA parallels the level of *psbA* mRNA translation and association with polyribosomes [1, 7, 136, 147, 159-162].

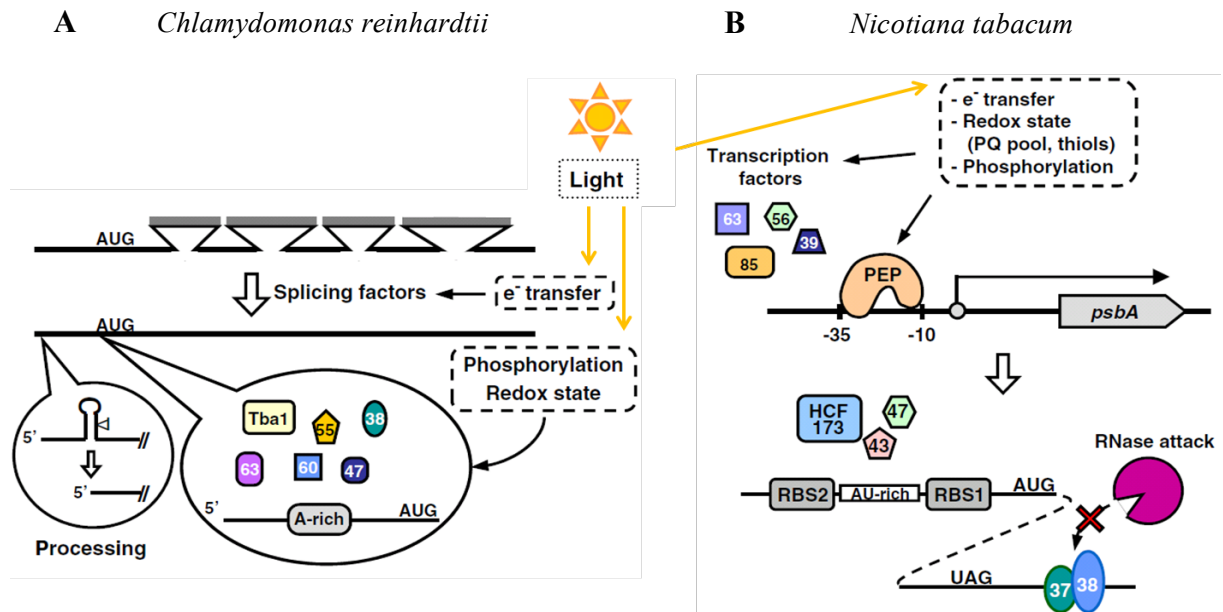


Figure 34: Mechanisms of transcription and translation initiation by nuclear-encoded trans-acting proteins differ in *C. reinhardtii* and in higher plants like *N. tabacum*. (A) In *C. reinhardtii* *psbA* transcript displays introns whereas the splicing efficiency is light dependent. Processing of *psbA* mRNA is probably influenced by stem-loop structures in the 5'-UTR and results in accumulation of two distinct *psbA* transcript forms. Light-dependent changes in phosphorylation and the redox state of trans-acting factors 63 kDa, 60 kDa, 55 kDa, 47 kDa, 38 kDa and Tba1 regulate the efficiency of translation initiation. (B) In *N. tabacum* *psbA* transcript features no introns. Transcription of the *psbA* gene is affected by various transcription factors (39, 56, 63 and 85 kDa) and by light quality and quantity via redox state of chloroplasts and the phosphorylation status of the plastid encoded RNA polymerase (PEP). *PsbA* mRNA translation initiation complexes are formed in a light-dependent manner but protein production is mainly regulated at the level of translation elongation via transacting proteins HCF173, 47 kDa, 43 kDa, 38 kDa and 37 kDa. Modified figure from Mulo *et al.* [7].

Three of these proteins, namely RB47, RB60 and Tba1, have been recombinantly produced and characterized. RB47, also called chloroplast poly(A) binding protein cPAB1, is a member of the eukaryotic poly (A)-binding protein family and enables binding of *PsbA* 5' PC to the 5'-UTR of *psbA* mRNA. RB60 is described as a protein disulfide isomerase, which reacts with high selectivity with the disulfide of RB47 and is hypothesized to modulate its activity by redox and phosphorylation events. [136, 163, 164]. Tba1 is also required for ribosome association and D1 translation by influencing RB47 RNA binding activity, but the underlying mechanisms is still unknown. Interestingly, Tba1 was not found in higher plants [7].

It is unclear whether of light regulated translation of *psbA* mRNA in higher plants displays similar mechanisms like in algae. However, our data suggests that the

regulatory interactions between 5'-UTR elements and nucleus-encoded factors are highly species-specific and very sensitive to sequence changes. Thus the best approach to achieve reliable expression of transgenes in chloroplasts in a follow-on project would be the use of endogenous regulatory elements.

5.4.3. Conclusion regarding transplastomic approach

For both *N. tabacum* and *C. reinhardtii*, translation initiation of *psbA* transcripts is mediated by nuclear-encoded trans-acting proteins that operate ribosome association and translation. Thus translation initiation depends upon the interaction of these trans-acting proteins with the RNA regulatory elements in the 5'-UTR of *psbA* mRNA, whereas these cis-acting regions appear to be very specific and function only from closely related species [1, 2, 155]. Considering the phylogenetic distance between vascular plants like *N. tabacum* and green alga like *C. reinhardtii*, the inhibition of translation in the present work is retrospectively not surprising and the differences in the 5'UTR of *psbA* gene in *N. tabacum* to *C. reinhardtii* are most likely the reason for failure of recombinant protein production in the transplastomic plants that were produced in this work.

Outlook

Challenges remain in optimizing the SP13 peptides either to function at lower concentrations or with diminished cytotoxic effects, which may restore the observed suppression of cytokine release due to minor adverse influence on cells. Moreover, unwanted reactions including aggregation, half-life or further immune-reactivity have to be investigated and, in case of observed severe effects, solved by redesigning the regarding peptides. Engineering of peptides is possible by changing only a few amino acid witch results in more suitable compounds as it was shown in the development of RC101 from RC1, which was performed by changing one single amino acid change resulting in significantly higher anti-HIV-1 activity [23]. Further enhancements may be possible in varying substantially the SP13 peptides by changing peptide hydrophobicity, amphipathicity, charge and degree of α -helicity, whilst in parallel investigating the maintenance or even enhancement of HIV activity. Furthermore, the stability of all designed peptides against protease degradation on skin or mucous membrane and the subsequent loss of antiviral properties [23] as well as the possible generation of resistance have to be determined in further experiments. Although some of our designed peptides were already prove to be most effective when administered after, during or before infection, the exact mechanisms remain to be determined to establish the optimal use as therapeutics, possibly for prophylactic administration in HIV high-risk populations. In this regard, the SP10-11 peptide appears particularly promising as potential topical anti-HIV drug. However, the anti-inflammatory effect of SP10-11 has to be investigated for possible adverse effects *in vivo*.

Transplastomic *N. tabacum* plants are able to produce recombinant protein in extremely high yields, some reaching a massive accumulation of 70% of the total soluble protein (TSP) in the plant leaf tissue [74]. Therefore chloroplasts are favorable to nuclear transformation approaches regarding an efficient stably transformed plant production platform. However, another expression cassette for the GOI has to be designed, preferably using the endogenous 5'-UTR and promoter, although this may be result in incomplete homoplasmy. Alternatively, another insertion site may be targeted in the ptDNA, for example between the *trnI* and *trnA* genes where a transcriptionally active intron is located. Thus endogenous transcriptional activity may be exploited to express foreign genes [77].

Bibliography

1. Gimpel, J.A. and S.P. Mayfield, *Analysis of heterologous regulatory and coding regions in algal chloroplasts*. Appl Microbiol Biotechnol, 2012.
2. Bruick, R.K. and S.P. Mayfield, *Processing of the psbA 5' untranslated region in Chlamydomonas reinhardtii depends upon factors mediating ribosome association*. The Journal of cell biology, 1998. **143**(5): p. 1145-1153.
3. Peled-Zehavi, H. and A. Danon, *Translation and translational regulation in chloroplasts*. 2007.
4. Ruhlman, T., et al., *The role of heterologous chloroplast sequence elements in transgene integration and expression*. Plant Physiol, 2010. **152**(4): p. 2088-104.
5. Hirose, T. and M. Sugiura, *Cis-acting elements and trans-acting factors for accurate translation of chloroplast psbA mRNAs: development of an in vitro translation system from tobacco chloroplasts*. EMBO J, 1996. **15**(7): p. 1687-95.
6. Birky Jr, C.W., *The inheritance of genes in mitochondria and chloroplasts: laws, mechanisms, and models*. Annual review of genetics, 2001. **35**(1): p. 125-148.
7. Mulo, P., I. Sakurai, and E.M. Aro, *Strategies for psbA gene expression in cyanobacteria, green algae and higher plants: from transcription to PSII repair*. Biochim Biophys Acta, 2012. **1817**(1): p. 247-57.
8. Hazlett, L. and M. Wu, *Defensins in innate immunity*. Cell Tissue Res, 2011. **343**(1): p. 175-88.
9. Chang, T.L., et al., *Dual role of α -defensin-1 in anti-HIV-1 innate immunity*. Journal of Clinical Investigation, 2005. **115**(3): p. 765-773.
10. Korting, H.C., et al., *Antimicrobial peptides and skin: a paradigm of translational medicine*. Skin Pharmacol Physiol, 2012. **25**(6): p. 323-34.
11. Wang, G., X. Li, and Z. Wang, *APD2: the updated antimicrobial peptide database and its application in peptide design*. Nucleic acids research, 2009. **37**(suppl 1): p. D933-D937.
12. Zaiou, M., *Multifunctional antimicrobial peptides: therapeutic targets in several human diseases*. Journal of Molecular Medicine, 2007. **85**(4): p. 317-329.
13. Silva, O.N., et al., *Exploring the pharmacological potential of promiscuous host-defense peptides: from natural screenings to biotechnological applications*. Frontiers in microbiology, 2011. **2**.
14. Hancock, R.E. and H.-G. Sahl, *Antimicrobial and host-defense peptides as new anti-infective therapeutic strategies*. Nature biotechnology, 2006. **24**(12): p. 1551-1557.
15. Marr, A.K., W.J. Gooderham, and R.E. Hancock, *Antibacterial peptides for therapeutic use: obstacles and realistic outlook*. Current opinion in pharmacology, 2006. **6**(5): p. 468-472.
16. Jenssen, H., P. Hamill, and R.E. Hancock, *Peptide antimicrobial agents*. Clinical microbiology reviews, 2006. **19**(3): p. 491-511.
17. Splith, K. and I. Neundorff, *Antimicrobial peptides with cell-penetrating peptide properties and vice versa*. European biophysics journal, 2011. **40**(4): p. 387-397.
18. Huang, Y., J. Huang, and Y. Chen, *Alpha-helical cationic antimicrobial peptides: relationships of structure and function*. Protein & cell, 2010. **1**(2): p. 143-152.
19. Kang, S.J., et al., *Antimicrobial peptides: their physicochemical properties and therapeutic application*. Arch Pharm Res, 2012. **35**(3): p. 409-13.

20. Hancock, R.E., *Cationic antimicrobial peptides: towards clinical applications*. Expert Opin Investig Drugs, 2000. **9**(8): p. 1723-9.
21. Haukland, H., et al., *The antimicrobial peptides lactoferricin B and magainin 2 cross over the bacterial cytoplasmic membrane and reside in the cytoplasm*. Febs Letters, 2001. **508**(3): p. 389-393.
22. Matsuzaki, K., *Why and how are peptide-lipid interactions utilized for self-defense? Magainins and tachyplesins as archetypes*. Biochim. Biophys. Acta, 1999. **1462**(1): p. 10.
23. Gwyer Findlay, E., S.M. Currie, and D.J. Davidson, *Cationic Host Defence Peptides: Potential as Antiviral Therapeutics*. BioDrugs, 2013.
24. Wei, L., et al., *Structure and Function of a Potent Lipopolysaccharide-Binding Antimicrobial and Anti-inflammatory Peptide*. J Med Chem, 2013. **56**(9): p. 3546-56.
25. Bommarius, B., et al., *Cost-effective expression and purification of antimicrobial and host defense peptides in *Escherichia coli**. Peptides, 2010. **31**(11): p. 1957-1965.
26. Thakur, N., A. Qureshi, and M. Kumar, *AVPpred: collection and prediction of highly effective antiviral peptides*. Nucleic acids research, 2012. **40**(W1): p. W199-W204.
27. Owen, S.M., et al., *RC-101, a retrocyclin-1 analogue with enhanced activity against primary HIV type 1 isolates*. AIDS Research & Human Retroviruses, 2004. **20**(11): p. 1157-1165.
28. Ramessar, K., et al., *Cost-effective production of a vaginal protein microbicide to prevent HIV transmission*. Proceedings of the National Academy of Sciences, 2008. **105**(10): p. 3727-3732.
29. Yu, F., et al., *Approaches for identification of HIV-1 entry inhibitors targeting gp41 pocket*. Viruses, 2013. **5**(1): p. 127-49.
30. Gallo, S.A., et al., *θ -Defensins prevent HIV-1 Env-mediated fusion by binding gp41 and blocking 6-helix bundle formation*. Journal of Biological Chemistry, 2006. **281**(27): p. 18787-18792.
31. Leikina, E., et al., *Carbohydrate-binding molecules inhibit viral fusion and entry by crosslinking membrane glycoproteins*. Nature immunology, 2005. **6**(10): p. 995-1001.
32. Feng, Z., et al., *Cutting Edge: Human β Defensin 3—A Novel Antagonist of the HIV-1 Coreceptor CXCR4*. The Journal of Immunology, 2006. **177**(2): p. 782-786.
33. Quinones-Mateu, M.E., et al., *Human epithelial beta-defensins 2 and 3 inhibit HIV-1 replication*. AIDS, 2003. **17**(16): p. F39-48.
34. Braida, L., et al., *A single-nucleotide polymorphism in the human beta-defensin 1 gene is associated with HIV-1 infection in Italian children*. Aids, 2004. **18**(11): p. 1598-1600.
35. Lorin, C., et al., *The antimicrobial peptide dermaseptin S4 inhibits HIV-1 infectivity in vitro*. Virology, 2005. **334**(2): p. 264-275.
36. Yang, D., et al., *Multiple Roles of Antimicrobial Defensins, Cathelicidins, and Eosinophil-Derived Neurotoxin in Host Defense**. Annu. Rev. Immunol., 2004. **22**: p. 181-215.

37. Bowdish, D.M., D.J. Davidson, and R.E. Hancock, *Immunomodulatory properties of defensins and cathelicidins*. *Curr Top Microbiol Immunol*, 2006. **306**: p. 27-66.
38. Braff, M.H., et al., *Structure-function relationships among human cathelicidin peptides: dissociation of antimicrobial properties from host immunostimulatory activities*. *The Journal of Immunology*, 2005. **174**(7): p. 4271-4278.
39. Zuyderduyn, S., et al., *The antimicrobial peptide LL-37 enhances IL-8 release by human airway smooth muscle cells*. *Journal of allergy and clinical immunology*, 2006. **117**(6): p. 1328-1335.
40. Hoover, D.M., et al., *The structure of human MIP-3 α /CCL20: linking antimicrobial and CCR6 receptor binding activities with human β -defensins*. *Journal of Biological Chemistry*, 2002.
41. Perregaux, D.G., et al., *Antimicrobial peptides initiate IL-1 β posttranslational processing: a novel role beyond innate immunity*. *The Journal of Immunology*, 2002. **168**(6): p. 3024-3032.
42. Shi, J., et al., *A novel role for defensins in intestinal homeostasis: regulation of IL-1 β secretion*. *The Journal of Immunology*, 2007. **179**(2): p. 1245-1253.
43. Miles, K., et al., *Dying and necrotic neutrophils are anti-inflammatory secondary to the release of alpha-defensins*. *J Immunol*, 2009. **183**(3): p. 2122-32.
44. Zeitler, B., et al., *Production of a de-novo designed antimicrobial peptide in *Nicotiana benthamiana**. *Plant Mol Biol*, 2013. **81**(3): p. 259-72.
45. Zeitler, B., et al., *De-novo design of antimicrobial peptides for plant protection*. *PLoS One*, 2013. **8**(8): p. e71687.
46. Dangel, A., et al., *A de novo-designed antimicrobial peptide with activity against multiresistant *Staphylococcus aureus* acting on RsbW kinase*. *Faseb j*, 2013.
47. Zeitler, B., *Molecular Farming: Production of Antimicrobial Peptides in different *Nicotiana* species*. Technische Universität München, 2011: p. Dissertation.
48. Berger, E., et al., *Extracellular secretion of a recombinant therapeutic peptide by *Bacillus halodurans* utilizing a modified flagellin type III secretion system*. *Microbial cell factories*, 2011. **10**(1): p. 62.
49. Obembe, O.O., et al., *Advances in plant molecular farming*. *Biotechnology advances*, 2011. **29**(2): p. 210-222.
50. Strasser, R., *Challenges in O-glycan engineering of plants*. *Front Plant Sci*, 2012. **3**: p. 218.
51. Yusibov, V., S.J. Streatfield, and N. Kushnir, *Clinical development of plant-produced recombinant pharmaceuticals: vaccines, antibodies and beyond*. *Human vaccines*, 2011. **7**(3): p. 313-321.
52. Twyman, R.M., et al., *Molecular farming in plants: host systems and expression technology*. *TRENDS in Biotechnology*, 2003. **21**(12): p. 570-578.
53. Melnik, S. and E. Stoger, *Green factories for biopharmaceuticals*. *Curr Med Chem*, 2013. **20**(8): p. 1038-46.
54. Rybicki, E.P., *Plant-made vaccines for humans and animals*. *Plant biotechnology journal*, 2010. **8**(5): p. 620-637.
55. Dugdale, B., et al., *In Plant Activation: An Inducible, Hyperexpression Platform for Recombinant Protein Production in Plants*. *The Plant Cell Online*, 2013. **25**(7): p. 2429-2443.

56. Chandrudu, S., P. Simerska, and I. Toth, *Chemical methods for peptide and protein production*. *Molecules*, 2013. **18**(4): p. 4373-88.
57. Hancock, R.E. and M.G. Scott, *The role of antimicrobial peptides in animal defenses*. *Proceedings of the national Academy of Sciences*, 2000. **97**(16): p. 8856-8861.
58. Lu, L., et al., *HIV-1 variants with a single-point mutation in the gp41 pocket region exhibiting different susceptibility to HIV fusion inhibitors with pocket- or membrane-binding domain*. *Biochim Biophys Acta*, 2012. **1818**(12): p. 2950-7.
59. Piers, K.L., M.H. Brown, and R.E. Hancock, *Recombinant DNA procedures for producing small antimicrobial cationic peptides in bacteria*. *Gene*, 1993. **134**(1): p. 7-13.
60. Li, Y., *Carrier proteins for fusion expression of antimicrobial peptides in Escherichia coli*. *Biotechnology and applied biochemistry*, 2009. **54**(1): p. 1-9.
61. Chen, Z., et al., *Recombinant antimicrobial peptide hPAB- β expressed in Pichia pastoris, a potential agent active against methicillin-resistant Staphylococcus aureus*. *Applied microbiology and biotechnology*, 2011. **89**(2): p. 281-291.
62. Wang, A., et al., *High level expression and purification of bioactive human α -defensin 5 mature peptide in Pichia pastoris*. *Applied microbiology and biotechnology*, 2009. **84**(5): p. 877-884.
63. Fukushima, M., et al., *Production of small antibacterial peptides using silkworm-baculovirus protein expression system*. *Prep Biochem Biotechnol*, 2013. **43**(6): p. 565-76.
64. Bock, R., *Plastid biotechnology: prospects for herbicide and insect resistance, metabolic engineering and molecular farming*. *Curr Opin Biotechnol*, 2007. **18**(2): p. 100-6.
65. Svab, Z. and P. Maliga, *High-frequency plastid transformation in tobacco by selection for a chimeric aadA gene*. *Proc Natl Acad Sci U S A*, 1993. **90**(3): p. 913-7.
66. Nakamura, M.S., M., <Selection of synonymous codons for better expression of recombinant proteins in tobacco chloroplasts.pdf>. *Plant Biotechnology*, 2009. **26**: p. 53-56.
67. Staub, J.M., et al., *High-yield production of a human therapeutic protein in tobacco chloroplasts*. *Nat Biotechnol*, 2000. **18**(3): p. 333-8.
68. Boynton, J.E., et al., *Chloroplast transformation in Chlamydomonas with high velocity microprojectiles*. *Science*, 1988. **240**(4858): p. 1534-1538.
69. Verma, D. and H. Daniell, *Chloroplast vector systems for biotechnology applications*. *Plant Physiol*, 2007. **145**(4): p. 1129-43.
70. Wang, H.H., W.B. Yin, and Z.M. Hu, *Advances in chloroplast engineering*. *J Genet Genomics*, 2009. **36**(7): p. 387-98.
71. Svab, Z., P. Hajdukiewicz, and P. Maliga, *Stable transformation of plastids in higher plants*. *Proc Natl Acad Sci U S A*, 1990. **87**(21): p. 8526-30.
72. Daniell, H., et al., *Transient foreign gene expression in chloroplasts of cultured tobacco cells after biolistic delivery of chloroplast vectors*. *Proceedings of the National Academy of Sciences*, 1990. **87**(1): p. 88-92.
73. Kolotilin, I., et al., *Optimization of transplastomic production of hemicellulases in tobacco: effects of expression cassette configuration and tobacco cultivar used as*

- production platform on recombinant protein yields*. Biotechnol Biofuels, 2013. **6**(1): p. 65.
74. Oey, M., et al., *Exhaustion of the chloroplast protein synthesis capacity by massive expression of a highly stable protein antibiotic*. Plant J, 2009. **57**(3): p. 436-45.
75. Nagata, N., et al., *The selective increase or decrease of organellar DNA in generative cells just after pollen mitosis one controls cytoplasmic inheritance*. Planta, 1999. **209**(1): p. 53-65.
76. Smith, S., *Biparental inheritance of organelles and its implications in crop improvement*. Plant Breeding Reviews, Volume 6, 1989: p. 361-393.
77. Heifetz, P.B., *Genetic engineering of the chloroplast*. Biochimie, 2000. **82**(6-7): p. 655-66.
78. Chebolu, S. and H. Daniell, *Chloroplast-derived vaccine antigens and biopharmaceuticals: expression, folding, assembly and functionality*. Curr Top Microbiol Immunol, 2009. **332**: p. 33-54.
79. Staub, J.M. and P. Maliga, *Extrachromosomal elements in tobacco plastids*. Proc Natl Acad Sci U S A, 1994. **91**(16): p. 7468-72.
80. Staub, J.M. and P. Maliga, *Marker rescue from the Nicotiana tabacum plastid genome using a plastid/Escherichia coli shuttle vector*. Molecular and General Genetics MGG, 1995. **249**(1): p. 37-42.
81. Maliga, P., *Plastid transformation in higher plants*. Annu Rev Plant Biol, 2004. **55**: p. 289-313.
82. Zeitlin, L., S.S. Olmsted, and T.R. Moench, *A humanized monoclonal antibody produced in transgenic plants for immunoprotection of the vagina against genital herpes*. Nature biotechnology, 1998. **16**(13): p. 1361-1364.
83. Faye, L. and H. Daniell, *Novel pathways for glycoprotein import into chloroplasts*. Plant biotechnology journal, 2006. **4**(3): p. 275-279.
84. Molina, A., et al., *High-yield expression of a viral peptide animal vaccine in transgenic tobacco chloroplasts*. Plant Biotechnol J, 2004. **2**(2): p. 141-53.
85. Li, H.-Y., S. Ramalingam, and M.-L. Chye, *Accumulation of recombinant SARS-CoV spike protein in plant cytosol and chloroplasts indicate potential for development of plant-derived oral vaccines*. Experimental Biology and Medicine, 2006. **231**(8): p. 1346-1352.
86. Chebolu, S. and H. Daniell, *Stable expression of Gal/GalNAc lectin of Entamoeba histolytica in transgenic chloroplasts and immunogenicity in mice towards vaccine development for amoebiasis*. Plant biotechnology journal, 2007. **5**(2): p. 230-239.
87. Oey, M., et al., *Plastid production of protein antibiotics against pneumonia via a new strategy for high-level expression of antimicrobial proteins*. Proceedings of the National Academy of Sciences, 2009. **106**(16): p. 6579-6584.
88. Scotti, N., et al., *High-level expression of the HIV-1 Pr55gag polyprotein in transgenic tobacco chloroplasts*. Planta, 2009. **229**(5): p. 1109-1122.
89. Herrera Diaz, A., *Regeneration and plastid transformation approaches in Arabidopsis thaliana and Rapic Cycling Brassica rapa*. Ludwig-Maximilians-Universität München, 2011: p. Dissertation.

90. Ageeva, A., *Produktion anti-HIV aktiver Peptide in Nicotiana benthamiana* Technische Universität Dresden - Internationales Hochschulinstitut Zittau: p. Master Thesis.
91. Sallusto, F. and A. Lanzavecchia, *Efficient presentation of soluble antigen by cultured human dendritic cells is maintained by granulocyte/macrophage colony-stimulating factor plus interleukin 4 and downregulated by tumor necrosis factor alpha*. The Journal of experimental medicine, 1994. **179**(4): p. 1109-1118.
92. Traidl-Hoffmann, C., et al., *Pollen-associated phytoprostanes inhibit dendritic cell interleukin-12 production and augment T helper type 2 cell polarization*. The Journal of experimental medicine, 2005. **201**(4): p. 627-636.
93. Poeck, H., et al., *Recognition of RNA virus by RIG-I results in activation of CARD9 and inflammasome signaling for interleukin 1 [beta] production*. Nature immunology, 2009. **11**(1): p. 63-69.
94. Herz, S., et al., *Development of novel types of plastid transformation vectors and evaluation of factors controlling expression*. Transgenic research, 2005. **14**(6): p. 969-982.
95. Maes, E., et al., *Interindividual variation in the proteome of human peripheral blood mononuclear cells*. PLoS One, 2013. **8**(4): p. e61933.
96. Schroder, K., et al., *Interferon-gamma: an overview of signals, mechanisms and functions*. J Leukoc Biol, 2004. **75**(2): p. 163-89.
97. Engler, C., et al., *Golden gate shuffling: a one-pot DNA shuffling method based on type IIs restriction enzymes*. PLoS One, 2009. **4**(5): p. e5553.
98. Engler, C., R. Kandzia, and S. Marillonnet, *A one pot, one step, precision cloning method with high throughput capability*. PLoS One, 2008. **3**(11): p. e3647.
99. Engler, C. and S. Marillonnet, *Generation of families of construct variants using golden gate shuffling*. Methods Mol Biol, 2011. **729**: p. 167-81.
100. Marillonnet, S., et al., *In planta engineering of viral RNA replicons: efficient assembly by recombination of DNA modules delivered by Agrobacterium*. Proc Natl Acad Sci U S A, 2004. **101**(18): p. 6852-7.
101. Marillonnet, S., et al., *In planta engineering of viral RNA replicons: efficient assembly by recombination of DNA modules delivered by Agrobacterium*. Proceedings of the National Academy of Sciences of the United States of America, 2004. **101**(18): p. 6852-6857.
102. Feghali, C.A. and T.M. Wright, *Cytokines in acute and chronic inflammation*. Front Biosci, 1997. **2**(1): p. d12-26.
103. Ramesh, G., A.G. Maclean, and M.T. Philipp, *Cytokines and chemokines at the crossroads of neuroinflammation, neurodegeneration, and neuropathic pain*. Mediators Inflamm, 2013. **2013**: p. 480739.
104. Farina, L. and C. Winkelman, *A review of the role of proinflammatory cytokines in labor and noninfectious preterm labor*. Biological research for nursing, 2005. **6**(3): p. 230-238.
105. Dinarello, C.A., *Proinflammatory cytokines*. CHEST Journal, 2000. **118**(2): p. 503-508.
106. Opal, S.M. and V.A. DePalo, *Anti-inflammatory cytokines*. CHEST Journal, 2000. **117**(4): p. 1162-1172.

107. Chung, F., *Anti-inflammatory cytokines in asthma and allergy: interleukin-10, interleukin-12, interferon- γ* . *Mediators of inflammation*, 2001. **10**(2): p. 51-59.
108. de Waal Malefyt, R., et al., *Interleukin 10 (IL-10) inhibits cytokine synthesis by human monocytes: an autoregulatory role of IL-10 produced by monocytes*. *The Journal of experimental medicine*, 1991. **174**(5): p. 1209-1220.
109. Chanteux, H., et al., *LPS induces IL-10 production by human alveolar macrophages via MAPKinases-and Sp1-dependent mechanisms*. *Respiratory research*, 2007. **8**(1): p. 71.
110. Chen, X., et al., *Human antimicrobial peptide LL-37 modulates proinflammatory responses induced by cytokine milieus and double-stranded RNA in human keratinocytes*. *Biochem Biophys Res Commun*, 2013. **433**(4): p. 532-7.
111. Szoka, P.R., et al., *A general method for retrieving the components of a genetically engineered fusion protein*. *DNA*, 1986. **5**(1): p. 11-20.
112. Mantovani, A., et al., *Cancer-related inflammation*. *Nature*, 2008. **454**(7203): p. 436-444.
113. Dinarello, C.A., *Interleukin-1*. *Cytokine & Growth Factor Reviews*, 1997. **8**(4): p. 253-265.
114. Vincenti, M.P. and C.E. Brinckerhoff, *Early response genes induced in chondrocytes stimulated with the inflammatory cytokine interleukin-1beta*. *Arthritis research*, 2001. **3**(6): p. 381-388.
115. Veldman, C., A. Nagel, and M. Hertl, *Type I regulatory T cells in autoimmunity and inflammatory diseases*. *International archives of allergy and immunology*, 2006. **140**(2): p. 174-183.
116. Clerici, M., et al., *Changes in T-helper cell function in human immunodeficiency virus*. 2011.
117. Kontinen, Y., et al., *PHA stimulation of peripheral blood lymphocytes in oral lichen planus. Abnormality localized between interleukin-2 receptor ligand formation and gamma-interferon secretion*. *Journal of clinical & laboratory immunology*, 1989. **28**(1): p. 33.
118. Chevalier, M.F. and L. Weiss, *The split personality of regulatory T cells in HIV infection*. *Blood*, 2013. **121**(1): p. 29-37.
119. Cunningham, A.L., et al., *Manipulation of dendritic cell function by viruses*. *Current opinion in microbiology*, 2010. **13**(4): p. 524-529.
120. Zeitlin, L., M. Pauly, and K.J. Whaley, *Second-generation HIV microbicides: continued development of griffithsin*. *Proceedings of the National Academy of Sciences*, 2009. **106**(15): p. 6029-6030.
121. Rosenfeld, Y., N. Papo, and Y. Shai, *Endotoxin (Lipopolysaccharide) Neutralization by Innate Immunity Host-Defense Peptides PEPTIDE PROPERTIES AND PLAUSIBLE MODES OF ACTION*. *Journal of Biological Chemistry*, 2006. **281**(3): p. 1636-1643.
122. Fortier, M.-E., et al., *The viral mimic, polyinosinic: polycytidylic acid, induces fever in rats via an interleukin-1-dependent mechanism*. *American Journal of Physiology-Regulatory, Integrative and Comparative Physiology*, 2004. **287**(4): p. R759-R766.
123. Gleba, Y., V. Klimyuk, and S. Marillonnet, *Magniffection—a new platform for expressing recombinant vaccines in plants*. *Vaccine*, 2005. **23**(17): p. 2042-2048.

124. Bock, R., *Structure, function, and inheritance of plastid genomes*, in *Cell and molecular biology of plastids*. 2007, Springer. p. 29-63.
125. Sugiura, M., *The chloroplast genome*. 1992: Springer.
126. Liere, K. and T. Börner, *Transcription and transcriptional regulation in plastids*, in *Cell and molecular biology of plastids*. 2007, Springer. p. 121-174.
127. Nishimura, Y., et al., *Antisense transcript and RNA processing alterations suppress instability of polyadenylated mRNA in Chlamydomonas chloroplasts*. The Plant Cell Online, 2004. **16**(11): p. 2849-2869.
128. Gottesman, S., *The small RNA regulators of Escherichia coli: roles and mechanisms**. Annu. Rev. Microbiol., 2004. **58**: p. 303-328.
129. Lung, B., et al., *Identification of small non-coding RNAs from mitochondria and chloroplasts*. Nucleic acids research, 2006. **34**(14): p. 3842-3852.
130. Hegeman, C.E., et al., *Expression of complementary RNA from chloroplast transgenes affects editing efficiency of transgene and endogenous chloroplast transcripts*. Nucleic acids research, 2005. **33**(5): p. 1454-1464.
131. Hotto, A.M., Z.E. Huston, and D.B. Stern, *Overexpression of a natural chloroplast-encoded antisense RNA in tobacco destabilizes 5S rRNA and retards plant growth*. BMC Plant Biol, 2010. **10**: p. 213.
132. De Marchis, F., A. Pompa, and M. Bellucci, *Plastid proteostasis and heterologous protein accumulation in transplastomic plants*. Plant Physiol, 2012. **160**(2): p. 571-81.
133. Birch-Machin, I., et al., *Accumulation of rotavirus VP6 protein in chloroplasts of transplastomic tobacco is limited by protein stability*. Plant biotechnology journal, 2004. **2**(3): p. 261-270.
134. Bellucci, M., et al., *Cytoplasm and chloroplasts are not suitable subcellular locations for β -zein accumulation in transgenic plants*. Journal of experimental botany, 2005. **56**(414): p. 1205-1212.
135. Apel, W., W.X. Schulze, and R. Bock, *Identification of protein stability determinants in chloroplasts*. Plant J, 2010. **63**(4): p. 636-50.
136. Marín-Navarro, J., et al., *Chloroplast translation regulation*. Photosynthesis Research, 2007. **94**(2-3): p. 359-374.
137. Sugiura, M., T. Hirose, and M. Sugita, *Evolution and mechanism of translation in chloroplasts*. Annual review of genetics, 1998. **32**(1): p. 437-459.
138. Fargo, D., et al., *Shine-Dalgarno-like sequences are not required for translation of chloroplast mRNAs in Chlamydomonas reinhardtii chloroplasts or in Escherichia coli*. Molecular and General Genetics MGG, 1998. **257**(3): p. 271-282.
139. Yamaguchi, K., et al., *Proteomic characterization of the Chlamydomonas reinhardtii chloroplast ribosome. Identification of proteins unique to the e70 S ribosome*. J Biol Chem, 2003. **278**(36): p. 33774-85.
140. Yamaguchi, K., et al., *Proteomic characterization of the small subunit of Chlamydomonas reinhardtii chloroplast ribosome: identification of a novel S1 domain-containing protein and unusually large orthologs of bacterial S2, S3, and S5*. Plant Cell, 2002. **14**(11): p. 2957-74.

141. Yamaguchi, K. and A.R. Subramanian, *Proteomic identification of all plastid-specific ribosomal proteins in higher plant chloroplast 30S ribosomal subunit*. Eur J Biochem, 2003. **270**(2): p. 190-205.
142. Yamaguchi, K. and A.R. Subramanian, *The plastid ribosomal proteins. Identification of all the proteins in the 50 S subunit of an organelle ribosome (chloroplast)*. J Biol Chem, 2000. **275**(37): p. 28466-82.
143. Yamaguchi, K., K. von Knoblauch, and A.R. Subramanian, *The plastid ribosomal proteins. Identification of all the proteins in the 30 S subunit of an organelle ribosome (chloroplast)*. J Biol Chem, 2000. **275**(37): p. 28455-65.
144. Eibl, C., et al., *In vivo analysis of plastid psbA, rbcL and rpl32 UTR elements by chloroplast transformation: tobacco plastid gene expression is controlled by modulation of transcript levels and translation efficiency*. Plant J, 1999. **19**(3): p. 333-45.
145. Kuroda, H. and P. Maliga, *Complementarity of the 16S rRNA penultimate stem with sequences downstream of the AUG destabilizes the plastid mRNAs*. Nucleic acids research, 2001. **29**(4): p. 970-975.
146. Kuroda, H. and P. Maliga, *Sequences downstream of the translation initiation codon are important determinants of translation efficiency in chloroplasts*. Plant physiology, 2001. **125**(1): p. 430-436.
147. Zou, Z., C. Eibl, and H.U. Koop, *The stem-loop region of the tobacco psbA 5'UTR is an important determinant of mRNA stability and translation efficiency*. Mol Genet Genomics, 2003. **269**(3): p. 340-9.
148. Barkan, A. and M. Goldschmidt-Clermont, *Participation of nuclear genes in chloroplast gene expression*. Biochimie, 2000. **82**(6-7): p. 559-72.
149. Danon, A. and S.P. Mayfield, *Light-regulated translation of chloroplast messenger RNAs through redox potential*. Science-AAAS-Weekly Paper Edition, 1994. **266**(5191): p. 1717-1718.
150. Trebitsh, T., et al., *Translation of chloroplast psbA mRNA is modulated in the light by counteracting oxidizing and reducing activities*. Molecular and cellular biology, 2000. **20**(4): p. 1116-1123.
151. Jackson, R., *Alternative mechanisms of initiating translation of mammalian mRNAs*. Biochemical Society Transactions, 2005. **33**(6): p. 1231-1242.
152. Fernandez, J., et al., *Ribosome stalling regulates IRES-mediated translation in eukaryotes, a parallel to prokaryotic attenuation*. Molecular cell, 2005. **17**(3): p. 405-416.
153. Ruf, M. and H. Kössel, *Occurrence and spacing of ribosome recognition sites in mRNAs of chloroplasts from higher plants*. FEBS Letters, 1988. **240**(1): p. 41-44.
154. Zou, Z., *Analysis of cis-acting expression determinants of the tobacco psbA 5'UTR in vivo*. Ludwig-Maximilians-Universität München, 2001: p. Dissertation.
155. Mayfield, S.P., et al., *Translation of the psbA mRNA of Chlamydomonas reinhardtii requires a structured RNA element contained within the 5'untranslated region*. The Journal of cell biology, 1994. **127**(6): p. 1537-1545.
156. Staub, J.M. and P. Maliga, *Accumulation of D1 polypeptide in tobacco plastids is regulated via the untranslated region of the psbA mRNA*. EMBO J, 1993. **12**(2): p. 601-6.

157. Hirose, T. and M. Sugiura, *Functional Shine-Dalgarno-like sequences for translational initiation of chloroplast mRNAs*. Plant and cell physiology, 2004. **45**(1): p. 114-117.
158. Nickelsen, J., *Transcripts containing the 5' untranslated regions of the plastid genes psbA and psbB from higher plants are unstable in Chlamydomonas reinhardtii chloroplasts*. Molecular and General Genetics MGG, 1999. **262**(4-5): p. 768-771.
159. Shen, Y., A. Danon, and D.A. Christopher, *RNA binding-proteins interact specifically with the Arabidopsis chloroplast psbA mRNA 5' untranslated region in a redox-dependent manner*. Plant and Cell Physiology, 2001. **42**(10): p. 1071-1078.
160. Noordally, Z.B., et al., *Circadian control of chloroplast transcription by a nuclear-encoded timing signal*. Science, 2013. **339**(6125): p. 1316-9.
161. Cardol, P., et al., *Higher plant-like subunit composition of mitochondrial complex I from Chlamydomonas reinhardtii: 31 conserved components among eukaryotes*. Biochim Biophys Acta, 2004. **1658**(3): p. 212-24.
162. Schmitz-Linneweber, C., et al., *Heterologous, splicing-dependent RNA editing in chloroplasts: allotetraploidy provides trans-factors*. The EMBO journal, 2001. **20**(17): p. 4874-4883.
163. Alergand, T., et al., *The chloroplast protein disulfide isomerase RB60 reacts with a regulatory disulfide of the RNA-binding protein RB47*. Plant Cell Physiol, 2006. **47**(4): p. 540-8.
164. Somanchi, A., D. Barnes, and S.P. Mayfield, *A nuclear gene of Chlamydomonas reinhardtii, Tba1, encodes a putative oxidoreductase required for translation of the chloroplast psbA mRNA*. The Plant Journal, 2005. **42**(3): p. 341-352.

Appendix

Table 8: Listing of all blood samples that were used in this work. The available donor characteristics are described as well as isolated cell types, applied stimuli and applications for each sample.

blood donor ID	gender	V blood sample [ml]	Number of isolated cells/ cell types	Cell type/name	stimuli	application	remarks
1	♀	200 ml	PBMCs: 571 Mio	PBMC1	AMP	Toxicity tests	Healthy
2	♀	200 ml	PBMCs: 561,25 Mio	PBMC2	AMP	Toxicity tests	Healthy
3	♀	150 ml	PBMCs: 193,7 Mio	PBMC3	AMP	Toxicity tests	Healthy
4	♀	150 ml	PBMCs: 273,75 Mio	PBMC4	AMP, LPS, PHA	ELISA	Healthy
5	♀	150 ml	PBMCs: 340 Mio Monos: 15,4 Mio MoDCs: 11 Mio	PBMC5 DC1	AMP, LPS, PHA, Poly I:C	ELISA	Healthy
6	♂	150 ml	PBMCs: 337,5 Mio Monos: 52,75 MoDCs: 22,4 Mio	DC2	AMP, Poly I:C	ELISA	Healthy
7	♀	200 ml	PBMCs: 430 Mio Monos: 33 Mio MoDCs: 24,3 Mio	DC3	AMP, LPS, Poly I:C	ELISA	Allergic
8	♂	200 ml	PBMCs: 679 Mio Monos: 114 Mio MoDCs: 91,25 Mio	DC4	AMP, LPS, Poly I:C	ELISA	Allergic

Table 9: Applied concentrations of the designed peptides for the toxicity tests.

Conc. [$\mu\text{g/ml}$]	SP10-11 [μM]	SP13-3 [μM]	SP13-11 [μM]	SP13-14 [μM]
5	3,47	1,98	2,02	1,95
10	6,94	3,95	4,03	3,89
15	10,42	5,93	6,05	5,84
25	17,36	9,88	10,08	9,73
50	34,72	19,76	20,16	19,46
75	52,08	29,64	30,24	29,18
100	69,44	39,53	40,32	38,91

Table 10: Applied concentrations of the designed peptides for ELISA. Concentrations marked in grey color are not shown, because the severe cell-toxic effects falsified cytokine release data.

Conc. [$\mu\text{g/ml}$]	SP10-11 [μM]	SP13-3 [μM]	SP13-11 [μM]	SP13-14 [μM]
5	3,47	1,98	2,02	1,95
10	6,94	3,95	4,03	3,89
15	10,42	5,93	6,05	5,84
25	17,36	9,88	10,08	9,73
50	34,72	19,76	20,16	19,46
75	52,08			
100	69,44			

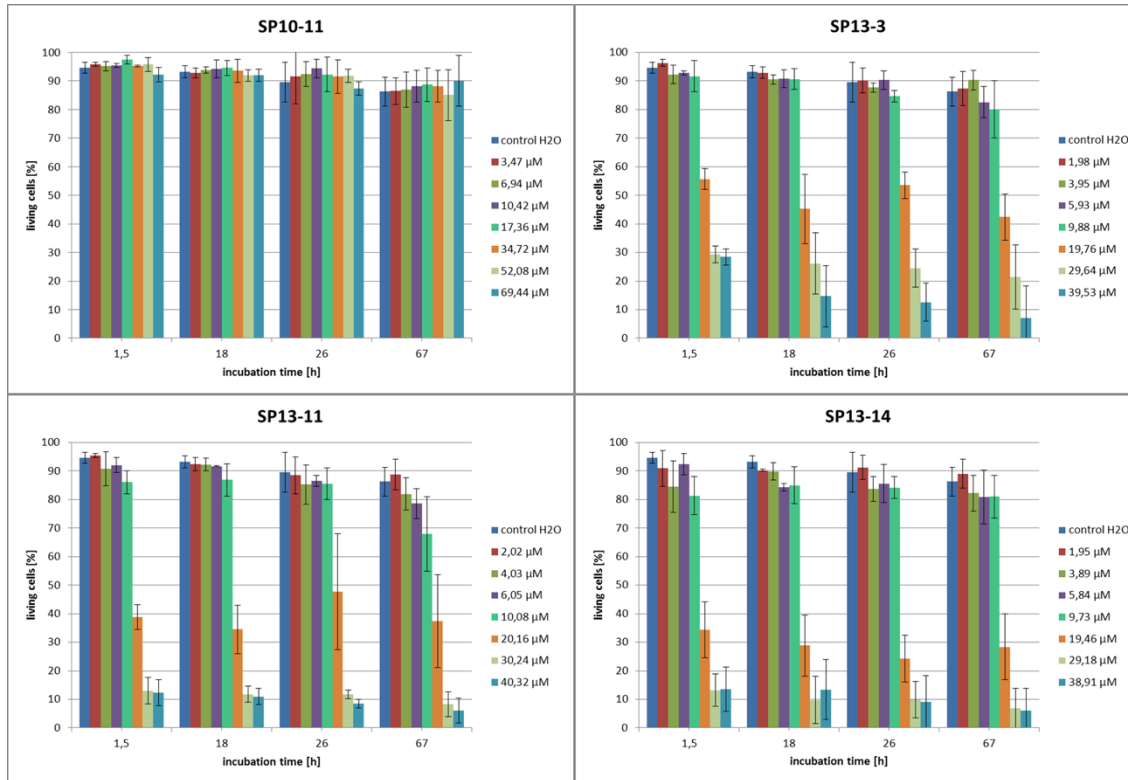


Figure 35: Determination of toxic effect of designed peptides in different concentrations on PBMCs over time. Each peptide in the specific concentration, respectively, was incubated with PBMCs for different time periods (1,5h, 18h, 26h and 67h). Quantity of viable PBMCs after incubation was determined by PI staining and flow cytometry. The controls consist of water-treated PBMC in proliferation medium. The values shown here correspond to three biological replicates with two technical replicates each. The controls consist of water-treated PBMC in complete medium. The values shown here correspond to three biological replicates with two technical replicates each.

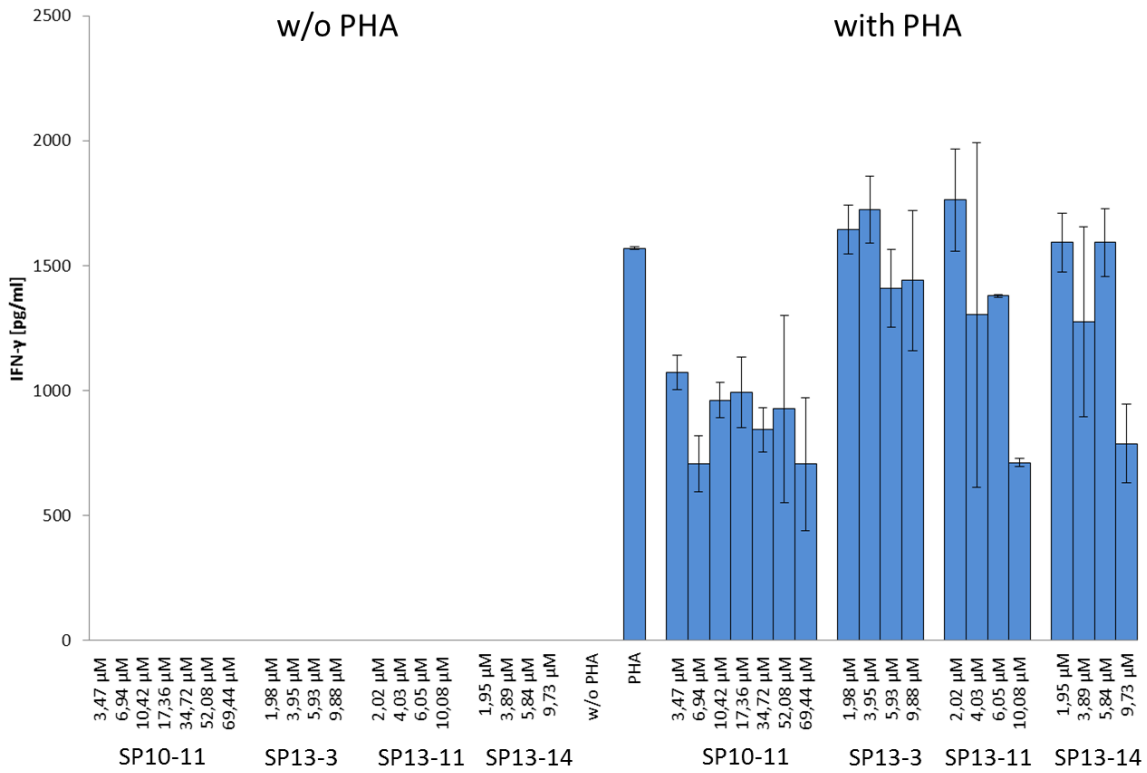


Figure 36: IFN-γ, PBMC 4, AMP + PHA stimulated.

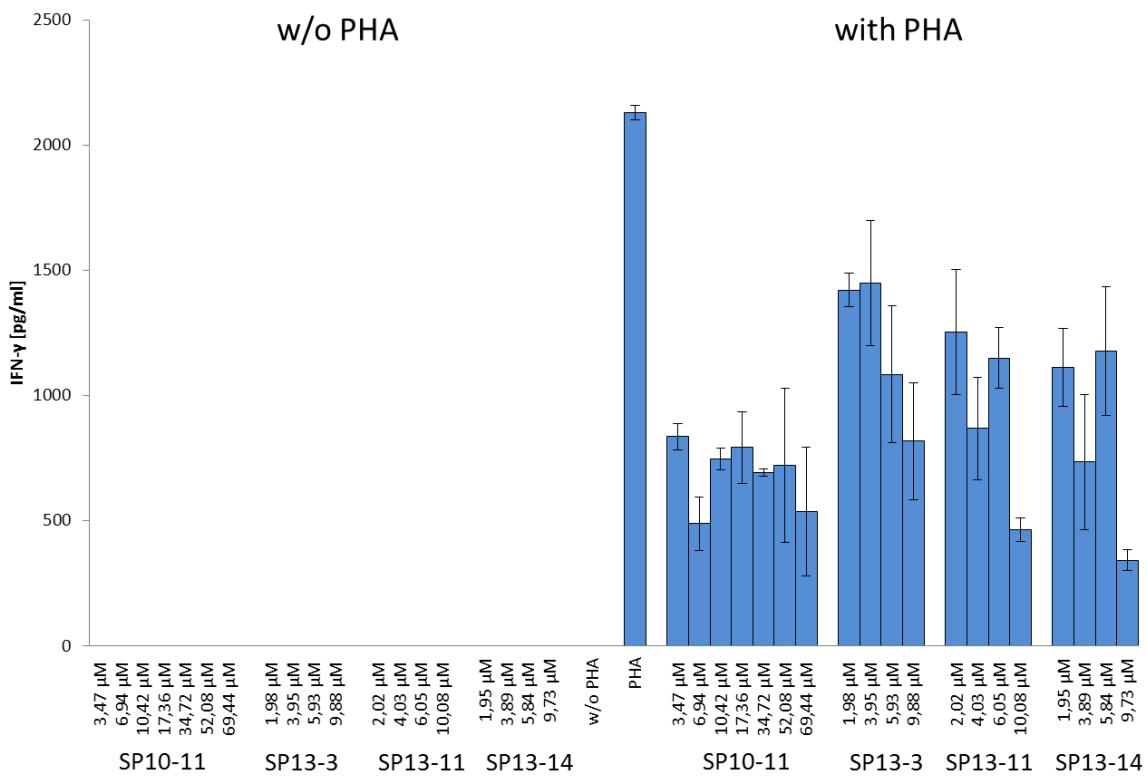


Figure 37: IFN-γ, PBMC 5, AMP + PHA stimulated.

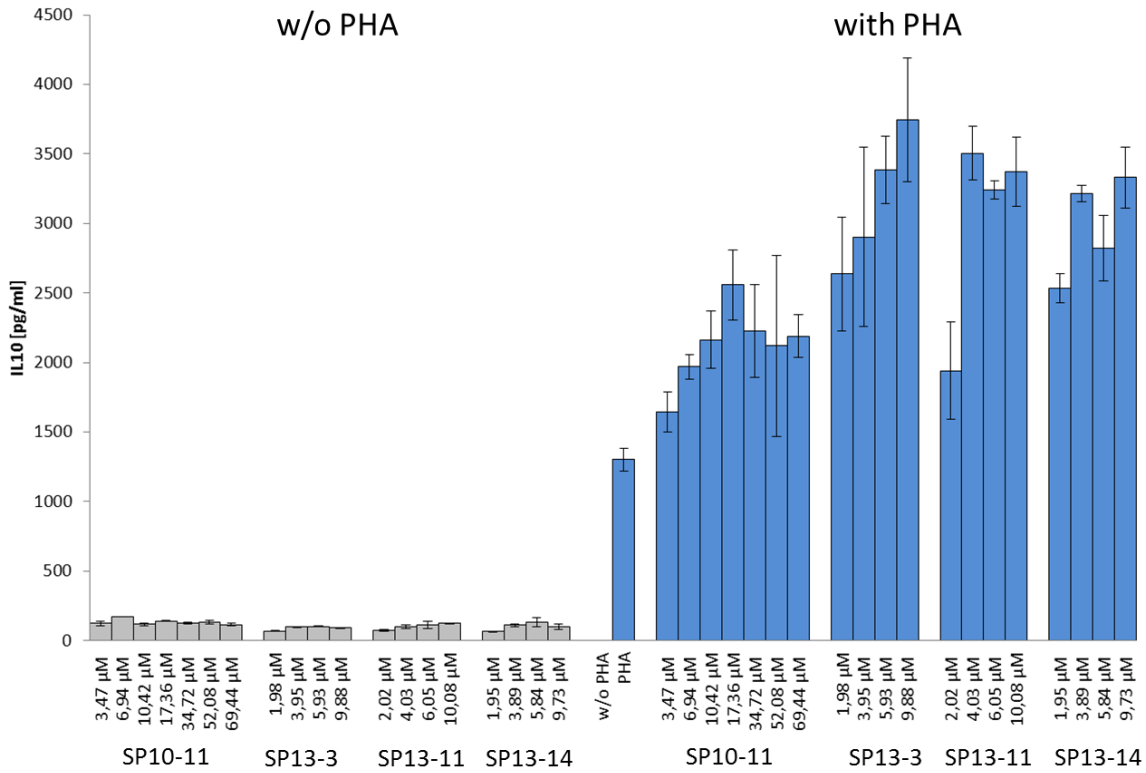


Figure 38: IL10, PBMC 4, AMP + PHA stimulated.

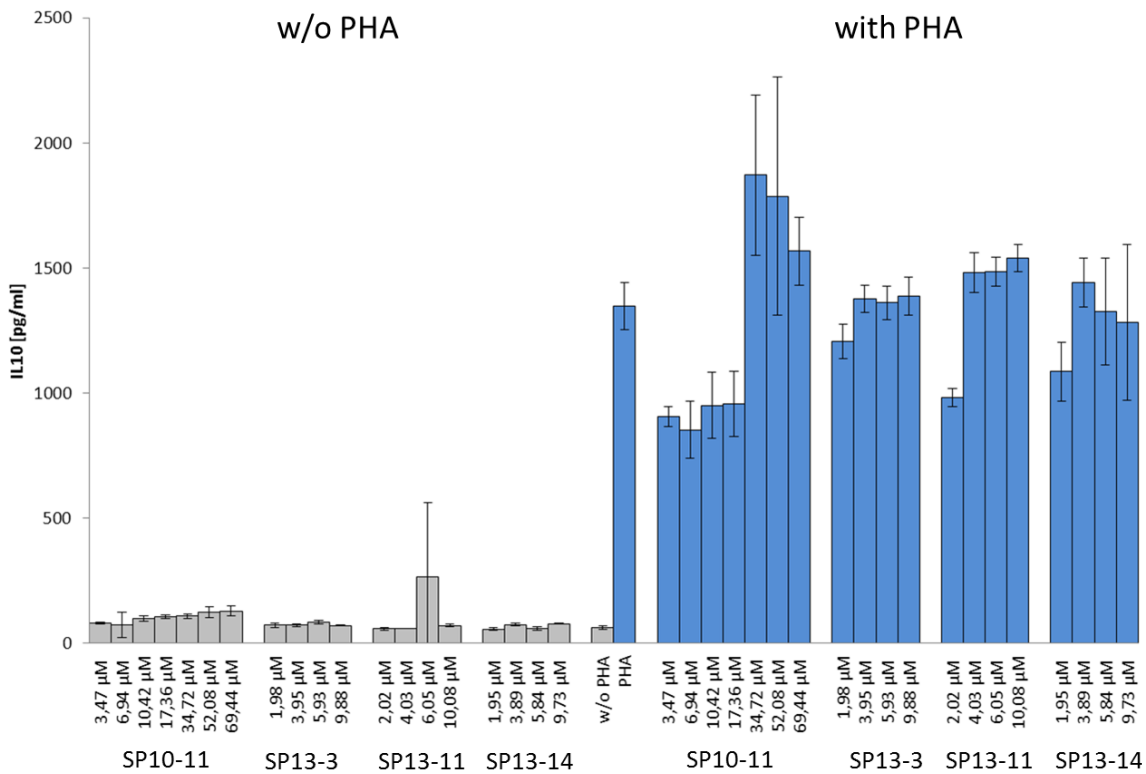


Figure 39: IL10, PBMC 5, AMP + PHA stimulated.

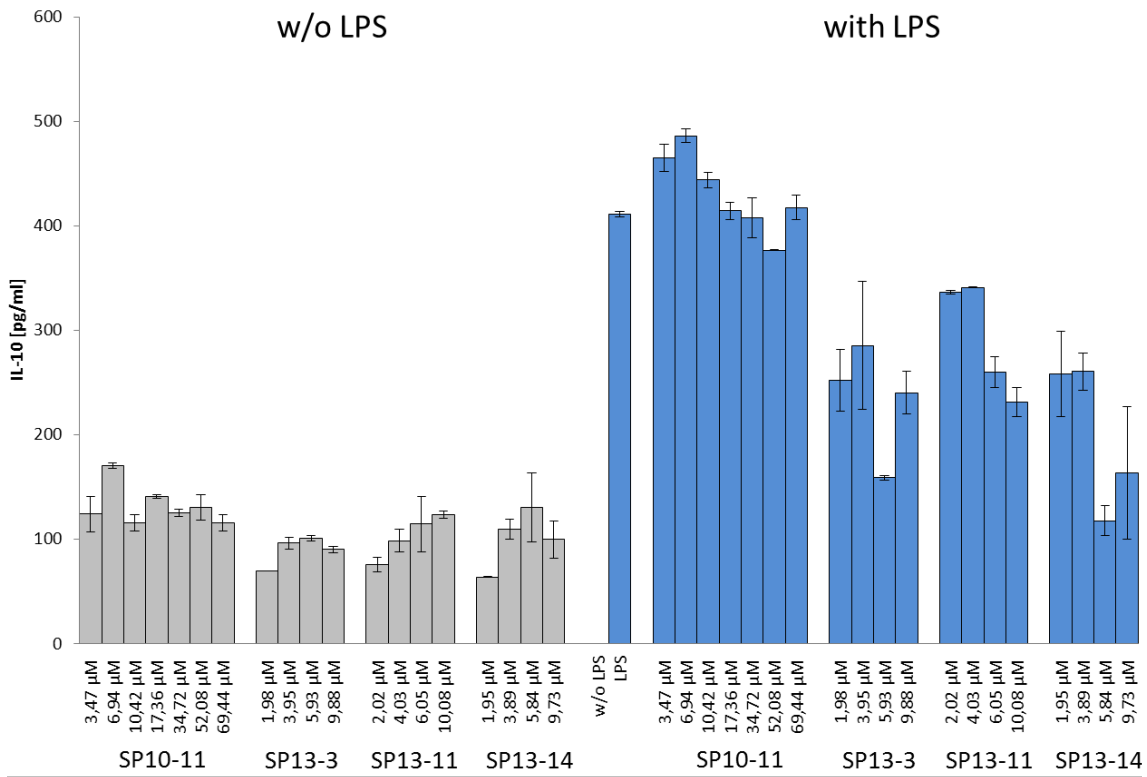


Figure 40: IL10, PBMC 4, AMP + LPS stimulated.

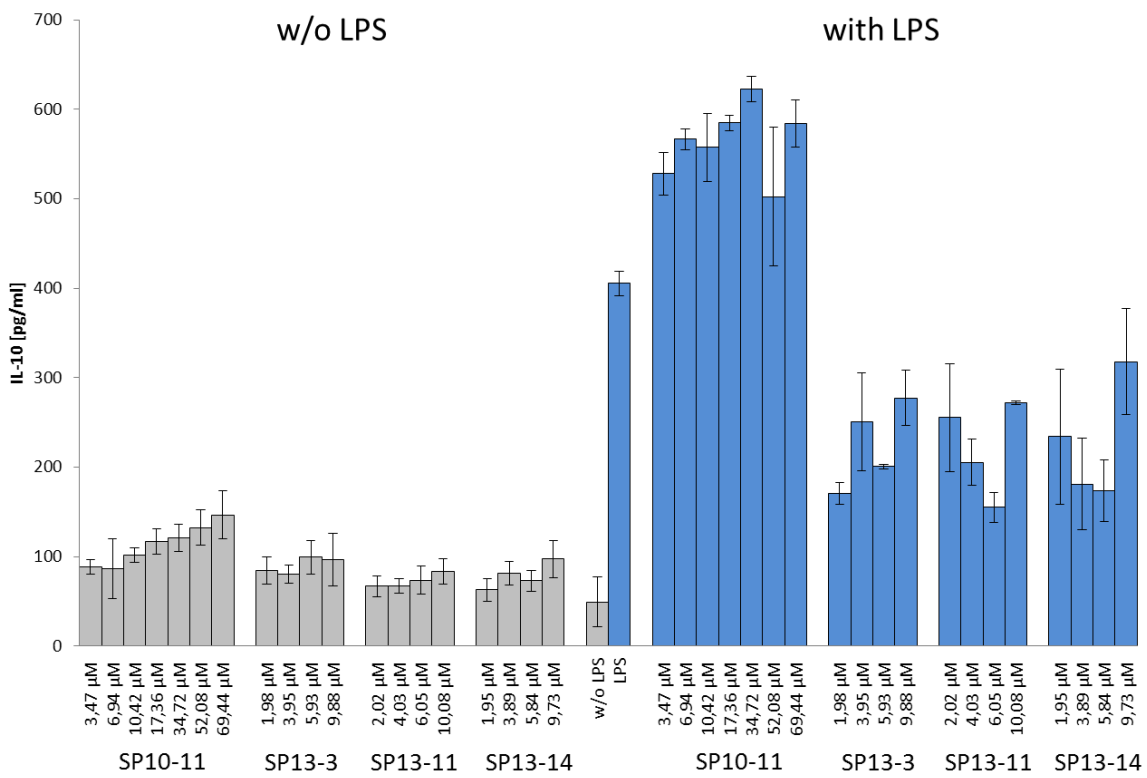


Figure 41: IL10, PBMC 5, AMP + LPS stimulated.

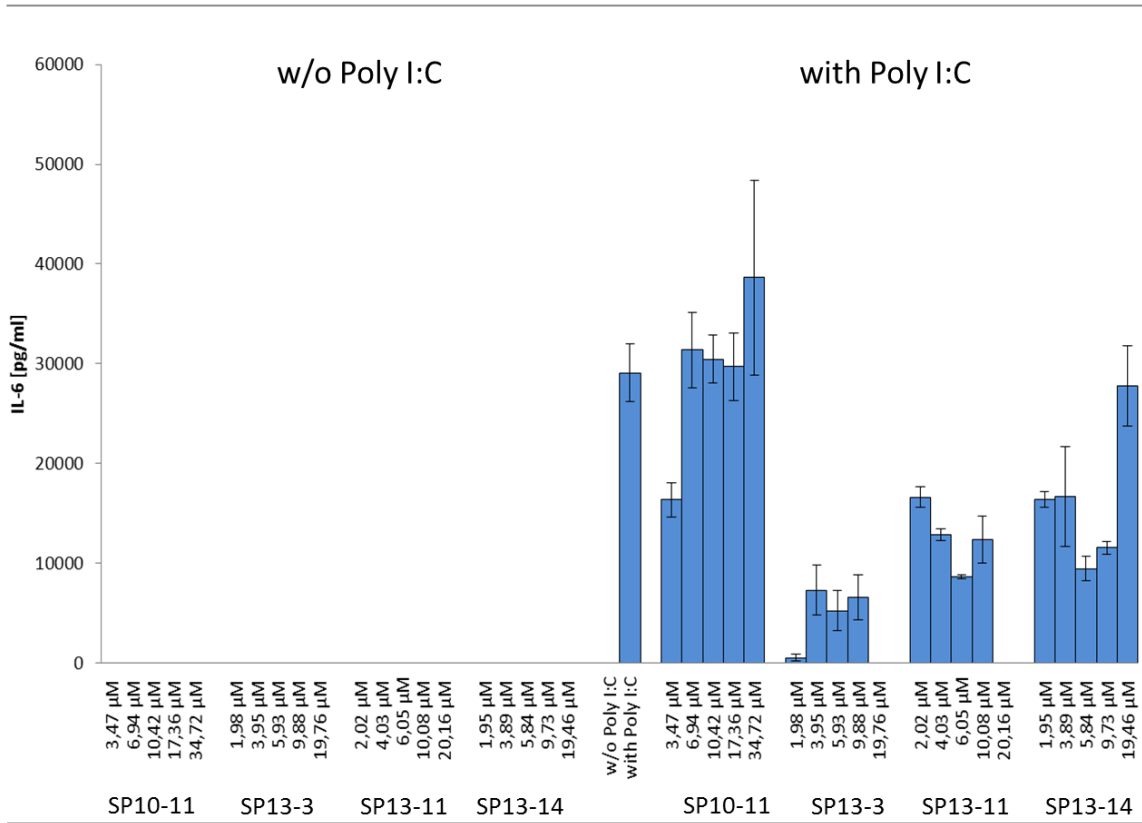


Figure 42: IL6, DC1, AMP + Poly I:C stimulated.

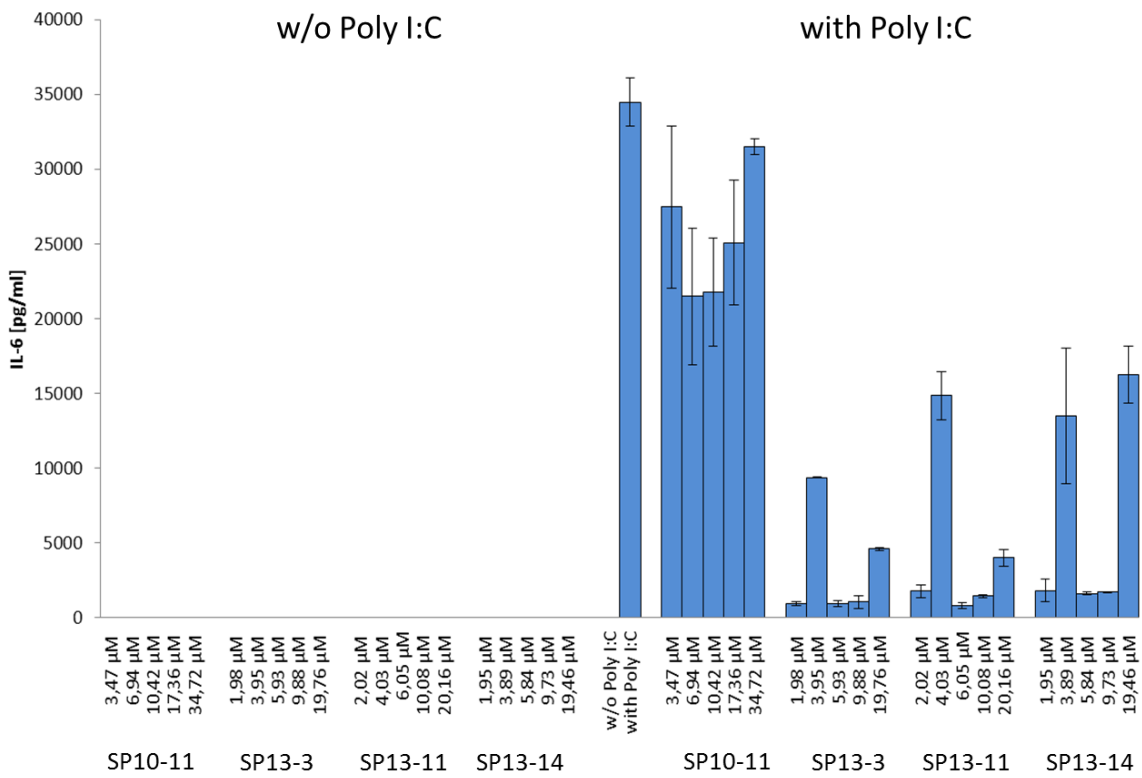


Figure 43: IL6, DC2, AMP + Poly I:C stimulated

Gccaaagaaaagtgagctattaacgcgtcctatfttaactccgaaggaggcagttggcaggcaactgccactgacgtcc
cgtaagggtaaggggacgtccactggcgccgtaaggggaaggggacgtaggtacataaatgtgctaggtactaacgt
ttgatttttggtataatatgtaccatgctttaatagaagcttgaattataaataatftttacaatftttacggagaat
taaaactttaaaaaattaacat

Figure 44: Sequence of the psbA gene promoter of *Chlamydomonas reinhartii* (PpsbA)

gccaataccgggtatataagcagtgattcaaatccagaggtaatcgactctggcaactttacgtaaggcagagtttggtttt
ttggggtagatggaaaagttgacagataagtcaccctfactgccactctacagaaccgtacatgagatttcacccatagc
gctcctcgtcaattcttgaattcattggatcctttccgcgttcgagaatcccccttctccactccgccccgaagagtaac
taggaccaatttagtcacgtttcatgtccaattgaacactgtccattttgattattctcaaaggataagattattctttacaaa
catatgcgatccaatcacgatcttatataagaagaacaaaagatctttctgatcaatccctttgccccctattctcaagaat
aaggaagatcctttcaagttgaattgttcatttggaaactgggtctctacttcatatttataatgaatatttccctctctttt
ttatattccttaagtccataggttgatcctgtagaattgacccatttctcattgaacgaaaggtacgaaataaatcagatt
gataaaagtaccatgtgaaatctcggttttnccttctcgcgatcccatcccataggtacagtgttgaatcaatagagaacctt
ntctctgtatgaatcgatatttccattccaaatcctcccgatccctccaag

Figure 45: Sequence of the rps12 flank for homologous recombination

aaggaaaatctctaatttgatcccaaatgacgggtagtgtagcttatccatgcggttatgcactcttgaataggaatccgt
ttctgaaagatcctggcttctgactttgggtgggtctccgagatccttccgatgacctatgtgaagggatctatctaaccgat
cgattgcgtaaaagcccgcgtagcaacggaaccggggaaagtatacagaaaagacagttctttctattatactagnannt
ctattatattagatattagactattatattagattagtagttagtgatcccgacttagtgagctcttctccgtgatgaactgtt
ggcaccagctcactatfttctctgtggaccgaggagaaaaggggctcggcgggaagaggagtgtaccatgagagaagc
aaggaggtcaacctttcaaatatacaacatggattctggcaatgtagttggactctcatgtcgatccgaatgaatcatccttc
cacggaggtaaatctttgctgcttaggcaagaggactggccggg

Figure 46: Sequence of the orf131 flank for homologous recombination

gtgagcaagggcgaggagctgtcaccggggtggtgccatcctggtcgagctggacggcgacgtaaacggccacaagt
tcagcgtgtccggcgaggggcgaggggcgtgccacctacggcaagctgacctgaagttcatctgcaccaccggcaagctg
cccgtgccctggccaccctcgtgaccacctgacctacggcgtgcagtgctcagccgctaccccaccacatgaagca
gcacgacttctcaagtccgcatgcccgaaggctacgtccaggagcgcaccatcttctcaaggacgacggcaactaaa
gaccgcgcccagggtgaagttcaggggcgcaccctgggtgaaccgatcgagctgaagggcacgacttcaaggaggac
ggcaacatcctggggcacaagctggagtacaactacaacgccacaacgtctatatcatggccgacaagcagaagaacgg
catcaaggtgaactcaagatccgccacaacatcgaggacggcagcgtgcagctcggcaccactaccagcagaacacc
cccctcggcgacggccccgtgctgctgcccgacaaccactacctgagcaccagtcgccccctgagcaaaagaccccaacg
agaagcgcgatcacatggtcctgctggagttcgtgaccgccggggatcactctcggcatggacgagctgtacaag

Figure 47: Sequence of the gfp marker gene

aagtaataaaacgttcgaataattgaaactgaaaaagaattcaattattcttaaattattcaattagataataattgaataat
ttaacgatttcccttcatattgatattgattagctaccaatcaatacgaatggaactcgtctcgtttctgattgatagataaaa
taatagaattaggaaatcctctatttactgaataaactttttgttgacaaaagagtaaacatcatttctattccaaggtggggag
tttcaatttccccatcgacctac

Figure 48: Sequence of the trpI31 terminator of the recombinant protein expression cassette

gccgtcgttcaatgagaatggataagaggctcgtgggattgacgtgagggggcagggatggctatatttctgggagcgaac
tccgggcgatatcactagttgtagggagggatccatggctcgtgaagcgggttcgccgaagtatcgactcaactatcagag
gtagttggcgtcatcgagcgccatctcgaaccgacgttgctggccgtacatttgtacggctccgcagtggtggcggcctga
agccacacagtgatattgattgctggttacggtgaccgtaaggcttgatgaaacaacgcggcgagctttgatcaacgaccttt
tggaaactcggttcccctggagagagcgagatttccgcgctgtagaagtcaccattgttgcacgacgacatcattccg
tggcgttatccagtaagcgcgaactgcaatttggagaatggcagcgcgaatgacattctgcaggtatcttcgagccagccac
gatcgacattgatctggctatcttctgacaaaagcaagagaacatagcgttgccttggtaggtccagcggcgggaggaactc
ttgatccggttcctgaacaggatctatttggggcgtaaatgaaacctaacgctatggaactcgcgcccgactgggctgg
cgatgagcgaatgtagtgcttacgttgcctccgatttggtagcagcgcagtaaccggcaaaatcgcgccgaaggatgtcgt
gccgactgggcaatggagcgcctgccggccagtatcagcccgctacttgaagctagacaggcttatcttgacaagaa
gaagatcgcttggcctcgcgcgcagatcagttggaagaatttgcactacgtgaaaggcgagatcactaaggtagttggca
aataactgcaggcatgcaagcttgactcaagctcgtaacgaaggtcgtgacctgctcgtgaaggtggcgacgtaattcgtt
cagcttgtaaatggctccagaactgctgctgcatgtgaagttggaaagaaattaaattcgaattgatactattgacaaacttt
aattttattttcatgatgttatgtgaatagcataaacatcgttttatttttaggtgtttaggttaataacctaaacatctttacattt
ttaaataaagtctaaagtatctttgttaaatggcctgtcttataaatacagatgtgccagaaaaataaatcttagcttttatt
ataggattatctttatgtattatatttataagtataataaaagaaatagtaacatactaaagcggatgtaactcaatcggttagagt
gcgatcc

Figure 49: Sequence of the aadA expression cassette, including 16S promotor, aadA marker gene and 3' rbcI terminator

Acknowledgment

Zunächst danke ich meinem Doktorvater Prof. Dr. Durner für die Möglichkeit am Institut für biochemische Pflanzenpathologie die Doktorarbeit anfertigen zu können sowie für die Bereitstellung der hervorragenden Arbeitsbedingungen.

Des Weiteren möchte ich mich bei meinem Zweitgutachter Prof. Dr. Scherer und der Vorsitzenden der Prüfungskommission Prof. Dr. Liebl für die Begutachtung meiner Arbeit und die Organisation des Disputationverfahrens bedanken.

Mein besonderer Dank gilt Herrn Dr. Christian Lindermayr für die Vergabe des interessanten Promotionsthemas, die fachliche Betreuung der Arbeit sowie für die kritische Durchsicht des Manuskripts. Seine Ratschläge und seine Diskussionsbereitschaft haben wesentlich zum Gelingen der vorliegenden Arbeit beigetragen.

Ferner möchte ich mich herzlichst bei allen Kooperationspartnern für die produktive Zusammenarbeit und den wissenschaftlichen Erfahrungsaustausch bedanken. Mein besondere Dank gilt hier Prof. Dr. Traidl-Hoffmann und Frau Dr. Hiller vom Zentrum für Allergie und Umwelt für die großartige Unterstützung bei den immunologischen Arbeiten sowie bei Herrn Dr. Stelljes und Herrn Stefan Kirchner vom Biozentrum der LMU für die Bereitstellung der Particle Gun und für ihre wertvollen fachlichen Anregungen und Diskussionen. Insbesondere möchte ich mich an dieser Stelle bei Prof. Dr. Koop für sein Engagement und seine hilfreichen fachlichen Ratschläge als externer Experte bei meinen Thesis Committees bedanken.

Darüber hinaus danke ich allen ehemaligen und aktuellen Kollegen bzw. Kolleginnen am Institut für die angenehme und harmonische Zusammenarbeit und wünsche ihnen für die Zukunft alles Gute und viel Erfolg.

Die wichtigste Stütze während meiner Promotion waren meine Familie, meine Freunde und mein Partner, die mich immer vorbehaltlos unterstützt haben. Ich danke vor allem dir, Christian, für deine jahrelange Motivation und den Rückhalt, den du mir gegeben hast. Ohne dich würde diese Arbeit sicherlich nicht in ihrer jetzigen Form vorliegen.

Diese Arbeit ist meiner Freundin Hedwig Engler gewidmet.

Curriculum Vitae

Name Antonie Sophie Bernhard
Address Karl-Theodor-Straße 84,
80803 Munich
Date of birth 17.03.1983
Place of birth Nördlingen, Germany

Dissertation
since 11/2010 Helmholtz Zentrum Munich (Technical University Munich)
Institute for Biochemical Plant Pathology
Title: "Approaches to plant-based production of designed antimicrobial peptides and their immunomodulatory activities."

University studies
10/2003 – 05/2009 Study of bioengineering at the Technical University Berlin,
Germany.
Degree: Dipl.-Ing. Biotechnologie (final grade 1.3)
02/2008 – 09/2008 Diploma thesis at the University Ramon Llull
Institute Quimic de Sarriá
Title: "Biological surface engineering for medical applications. Optimization of surfaces using PECVD to develop intelligent endoprosthetic bone material."

Education
09/1993 – 06/2003 Theodor-Heuss-Gymnasium, Nördlingen
Degree: "Allgemeine Hochschulreife" (final grade 1.7)

Publications (not in this work)
Zeitler B., Bernhard A., Meyer H., Michael Sattler M., Lindermayr C., Koop H.-U.,
„Production of a *de-novo* designed antimicrobial peptide in *Nicotiana benthamiana*."
Plant Mol Biol, 2013. 81(3): p. 259-72.